POLITECNICO DI MILANO
DOCTORAL PROGRAMME IN MATERIALS ENGINEERING

Modeling of the Electrostatic Interaction and Catalytic Activity of [NiFe] Hydrogenases on a Planar Electrode

Doctoral Dissertation of:
Manuel Antonio Ruiz Rodriguez

Supervisor:

Prof. Guido Raos

Tutor:
Prof. Fabio Maria Bolzoni

The Chair of the Doctoral Program:
Prof. Chiara Bertarelli

2023 – 34th cycle

Nada es imposible, solo astronómicamente improbable

Dedicatoria

El presente trabajo la dedico a mi familia, a mi madre Josefina Rodríguez Quiñones, a mi padre Manuel Ruiz Calzada, a mis hermanos Víctor Uriel Ruiz Rodríguez y José Miguel Ruiz Rodríguez, gracias por todo su apoyo.

A todas las personas que contribuyeron de una u otra forma en mi carrera académica.

Finalmente agradezco a mis profesores por brindarme sus conocimientos.

Contents

Figures

Tables

List of symbols

F = *electrostatic force*

k_e = *Coulomb constant*

q_1 = *charged species*

ε = *solvent dielectric permittivity*

ϕ_e = *electric potential*

λ_D = *Debye length*

$\phi(r)$ = *electrostatic potential.*

r = *distance*

$\vec{\nabla}$ = *gradient*

$\rho(\vec{r})$ = *charge density per unit volume*

π = *pi value*

$\sigma(\vec{r})$ = *density of a particle at any point*

$g(\vec{r})$ = *average density of the particle*

$w(\vec{r})$ = *mean force*

c_i^{∞} = *concentration of the ion to an infinite distance from the solute*

z_i = *ion valency*

$n_{\pm}$ *ion densities*

k = *Boltzmann constant*

T = *temperature*

$\lambda(\vec{r})$ = *describes the accessibility to ions at point* $\vec{r}$

q = *proton charge*

k_D = *Debye screening constant*

l_D = *Debye length*

c_j *and* $q_j = ez_j$ *are the concentrations and charges of the ions*

I = *ionic strength (salt concentration)*

Q_e = *net charge over the electrode's surface*

ΔE = interaction energy

θ_i = *tilt angle*

φ_i = *azimuthal angle*

$\phi_{reac} = \phi - \phi_{Coulomb}$

N = *normalization constant*

χ = *overall coverage of the electrode*

K = *equilibrium constant for the overall protein adsorption*

Π = *osmotic pressure*

H_{sol} = *hydrogenases in solution*

H_{surf} = *hydrogenases on the surface*

q_{vib} = *vibrational partition function*

μ^0 = *chemical potential of the proteins in the solution*

k_{ET} = *transfer of electrons*

C = *unknown factors that could affect to transfer of electrons*

β = *decay constant*

I_{tot} = total current

J_0 = *current density*

a_0 = *area occupied by one adsorbed protein*

ϕ_e = *electric potential on the electrode*

pK_a = *acid dissociation constant*

pH = *potential of Hydrogen*

n_0 = *salt concentration*

Sommario

Un gruppo di enzimi noto come idrogenasi ha la capacità di avviare una reazione redox dell'idrogeno.

$$2H^+ + 2e^- \rightleftharpoons H_2$$

Le idrogenasi possono essere utilizzate per produrre idrogeno molecolare o elettricità evitando l'uso di materiali rari come il platino nelle celle a combustibile e negli elettrolizzatori. L'incorporazione delle idrogenasi nei dispositivi elettrochimici richiede un buon orientamento che faciliti il trasferimento di elettroni dalla superficie dell'elettrodo al centro catalitico dell'enzima attraverso una serie di "cluster" di ferro-zolfo che fanno parte di questi enzimi.

Questo studio presenta un approccio computazionale per studiare la rilevanza degli orientamenti delle variabili sperimentali di pH, forza ionica e potenziale elettrico. I risultati mostrano che gli orientamenti dell'idrogenasi [NiFe] sull'elettrodo non sono significativamente influenzati da un potenziale elettrico di ±0,05 V. Al contrario, la forza ionica riduce l'energia di interazione e, di conseguenza, l'adsorbimento dell'enzima. Il principale fattore che determina l'orientamento dell'adsorbimento dell'idrogenasi sull'elettrodo è l'aumento del pH.

È stata esaminata la combinazione di due caratteristiche per determinare se un orientamento è favorevole a catalizzare la reazione redox dell'idrogeno: la probabilità e il flusso generato per questo orientamento. Questa combinazione mostra che non esistono orientamenti dominanti che controllano il trasferimento di elettroni. Tutti gli orientamenti contribuiscono in condizioni sperimentali specifiche a produrre la generazione effettiva.

Nel passo finale, è stata esaminata l'influenza che la concentrazione proteica (o del suo equivalente, la pressione osmotica) ha sulla corrente totale. La soluzione con pH=5 sembra essere leggermente migliore con

la combinazione di una densità di corrente leggermente elevata e un assorbimento complessivo leggermente migliore. Questo studio dimostra che le interazioni elettrostatiche tra idrogenasi e un elettrodo sono influenzate dal pH, dalla forza ionica e dall'orientamento della proteina.

Abstract

Hydrogenases are a group of enzymes that can catalyze the redox reaction of hydrogen.

$$2H^+ + 2e^- \rightleftharpoons H_2$$

Hydrogenases can be used for the generation of molecular hydrogen or electricity, avoiding the use of rare materials like platinum in electrolyzers and fuel cells.

The incorporation of hydrogenases in electrochemical devices requires a good orientation that facilitates the transfer of electrons from the surface of the electrode to the catalytic center of the enzyme through the array of the iron-sulfur clusters that are part of these enzymes. This study presents a computational approach to study the relevance of the orientations of the experimental variables of pH, ionic strength, and electric potential.

The obtained results indicate that an electric potential of ±0.05 V does not have a significant effect on the orientations of the [NiFe] hydrogenase on the electrode, while the ionic strength reduces the interaction energy and, for that reason, the adsorption of the enzyme. The pH rises as the most important factor determining the orientation of the adsorption of the hydrogenase on the electrode.

To evaluate if an orientation is favorable to catalyze the redox reaction of hydrogen, the combination of two characteristics was considered: the probability and the current produced for such orientation. This combination reveals that there are no dominant orientations that determine the transfer of electrons. The current generation results from a contribution of all the orientations under determinate certain conditions.

As a final step, the effect of protein concentration (or its equivalent, the osmotic pressure) on the total current was considered. The solution

with pH=5 seems to be marginally better due to the combination of a slightly high current density and slightly better overall absorption. The overall protein absorption and preferential orientations may be improved further by functionalization of the electrode or modification of the protein, to incorporate some amino acids at selected points on its surface.

This study demonstrates that electrostatic interactions between hydrogenase and an electrode are affected by pH, ionic strength, and the orientation of the protein.

CHAPTER 1

Introduction

1.1 Hydrogenases

Hydrogenases are a group of enzymes that can catalyze the redox reaction of hydrogen. In the oxidation pathway, two electrons are removed from the hydrogen molecule, producing two protons. In the reduction pathway, two electrons are added to two protons generating a molecule of hydrogen [1-3].

$$2H^+ + 2e^- \rightleftharpoons H_2$$

Hydrogenases can be found in organisms of the three dominions: Bacteria, Archaea and Eukarya, living in different environments from aerobic, anaerobic [1], to extreme conditions of temperature and pressure like hydrothermal vents [4].

The main role of these enzymes is to provide a flux of electrons and protons for the metabolic pathways of the organisms through the oxidation and reduction of hydrogen.

Some hydrogenases can be found coupled to other enzymes used in pathways of fermentation and phosphorylation, where the H_2 has the function of an energy source instead of NADH. In another metabolic pathway, hydrogenases produce hydrogen as a sub-product of reductive reactions where hydrogen is used as the final acceptor of electrons [1].

In the case of organisms of Bacteria and Archaea, hydrogenases can be found free in the cytoplasm, bound to the cellular membrane, or

in the periplasm coupled to other enzymes as part of reaction chains. In the case of Eukarya, hydrogenases can be found in specialized isolated compartments inside of the cell [1-5].

Hydrogenases can be classified into three major groups, considering the composition of their catalytic center.

The first group is called [NiFe] hydrogenases. It has a core with one atom each of nickel and iron. They are coordinated by some cysteines, one -CN, and two -CO groups [6].

There is a sub-class of the iron-nickel hydrogenases in which there is an atom of selenium in a seleno-cysteine group coordinated with the metallic core, whose presence has been considered as an important factor to improve the resistance to oxygen poisoning of this hydrogenase.

The second group is the [FeFe] hydrogenase in which the two metallic atoms are iron atoms, also has the characteristic that the core is connected to a [4Fe4S] cluster. Finally, there is a third group formed by [Fe]-only hydrogenases. These enzymes have the characteristic of having a single Fe atom in their core [1, 7].

1.2 [NiFe] hydrogenase isolated from *Desulfovibrio desulfuricans* ATCC 27774

Desulfovibrio desulfuricans ATCC 27774 is a bacterial strain belonging to the group of sulfate-reducing bacteria. This is a large and diverse group of anaerobic microorganisms that obtain the energy for their metabolism through the reduction of sulfate, using sulfide as final electron acceptor [8-14].

However, several reports have shown that sulfate-reducing bacteria can use other inorganic molecules and ions under a variety of environmental conditions like sulfite, thiosulfate, elemental sulfur and even nitrate and nitrite as final electron acceptors showing the high adaptability of these microorganisms [14, 15].

Their high metabolic flexibility enables these microorganisms to live in a big diversity of environments such as marine sediments, hydrothermal vents, freshwater sediments, anoxic sediments, or in contaminated zones such as wastewater treatment plants, oil fields, industrial discards. [14, 15].

For example: *Desulfobulbus propionicus, Desulforhopalus singaporensis, Desulfobacterium catecholicum, Desulfotomaculum thermobenzoicum, Desulfovibrio oxamicus, Desulfovibrio termidis, Desulfovibrio furfuralis, Desulfovibrio profundus, Desulfovibrio simplex* and *Desulfovibrio desulfuricans* have been reported to be able to reduce nitrate as an alternative electron acceptor [4, 11, 14-16].

The [NiFe] hydrogenase used in this study belongs to *Desulfovibrio desulfuricans* ATCC 27774. This bacterium can grow in presence of nitrate (end product: ammonium) as the previously mentioned bacteria, but also it can grow in mediums containing sulfate (end product: sulfide). Interestingly, if both nitrate and sulfate ions are present in the medium, the thermodynamically less-favorable sulfate is preferred by the bacteria. Nitrate reduction seems to occur only in the absence of sulfate and sulfite

in the medium [14, 17].

The [NiFe] hydrogenase isolated from *Desulfovibrio desulfuricans* ATCC 27774 can be found in the periplasm of the cell, associated with the periplasmic tetrahaem cytochrome c3, taking care of the first step towards recycling the chemical energy liberated during the redox reaction of hydrogen back to the cytoplasm [12].

It is a heterodimer of 89 kDa, with two subunits with molecular masses of 62 kDa and 27 kDa. It contains a series of three iron-sulfur clusters: two [4Fe4S] clusters and one [3Fe4S] cluster, denominated middle, proximal, and external clusters, respectively.

These clusters work as a wire that transports the electrons by hopping, from the exterior of the protein to the catalytic center, where the redox reaction occurs [10, 12, 14]. The Ni and Fe atoms within the catalytic core are coordinated by one -CN, two -CO groups, and 4 cysteines [8-14].

Together with this periplasmic hydrogenase it is possible to find a soluble [NiFe] hydrogenase in *Desulfovibrio desulfuricans* [18]. The crystal structure of the [NiFe] hydrogenase was obtained from the "Protein Data Bank" [19] as a PDB file (code 1e3d) [12]. This specific hydrogenase was chosen for our study also because of the good resolution in the published crystal structure (1.80 Å).

This file contains the crystalized structure of the hydrogenase in the form of a tetramer, together with the solvent molecules and ions associated with the hydrogenase at the moment of its crystallization. Thus, it was necessary to pre-process the PDB file with the "pdbeditor" software [20], in order to isolate the system to be used for the calculations. This system includes only the chains A (small subunit: 27 kDa) and B (big subunit: 62 kDa) of hydrogenase, without the water molecules associated with the enzyme. Its structure is illustrated in Figure 1.

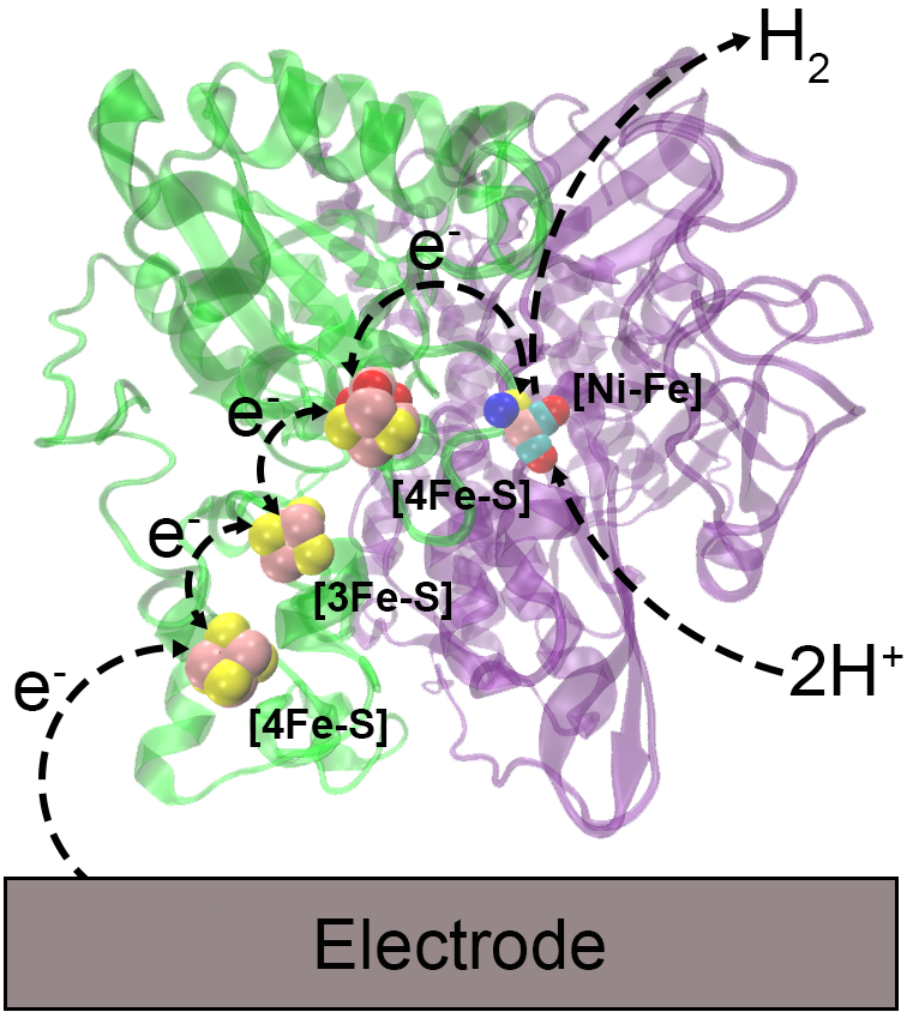

Figure 1. Model of the *Desulfovibrio desulfuricans* hydrogenase (1e3d).

The large and small subunits of the protein are depicted in purple and green, respectively. The atoms of the three iron-sulfur clusters and the catalytic center are represented as follows: sulfur (yellow), iron (pink), oxygen (red), nickel (blue), and carbon (turquoise). The external iron-sulfur 4Fe-4S cluster is the hypothetical entry point for electrons.

1.3 Hydrogenases for renewable energies

The interest in the study of hydrogenases has increased in the last decade due to the necessity of humanity to drastically reduce the use of fossil fuels as the main energetic source [3, 21].

With this priority necessity in mind, has arisen the idea of using

hydrogenases with different approaches in the field of renewable energies for the generation of hydrogen gas or electricity due its ability to catalyze the redox reaction of hydrogen [3, 22].

One of these approaches has been the adsorption of hydrogenases on the surface of electrodes used inside of electrochemical devices. The goal is to obtain a continuous flux of electrons generating electricity or using the reverse reaction to obtain electrons from electricity, and use them for the production of hydrogen. Accumulating energy in the process and making it available for its posterior release by other ways, for example in fuel cells, avoiding in this way the use of expensive metals such as platinum [23-25].

The idea of adsorbed hydrogenases on the surface of electrodes has been evaluated in a diversity of materials, like titanium [24, 26, 27], gold [4, 28, 29], silver [30], or graphite [31] with different degrees of success. Another approach has been to increase the adsorption area using porous materials, like carbon foams [31-33] or nanoparticles [28]. All these studies have reported diverse grades of hydrogen production, indicating that several factors have an important role in the reaction rate [3, 5].

One of the main factors indicated by some authors has been the orientation of the enzyme on the surface of the electrode [33-36]. The consensus is that the orientation more favorable to improve the enzymatic rate (as illustrated in Figure 1), is that one in which the distance between the external iron-sulfur cluster [4Fe-S] and the surface of the electrode is minimum. This is because these orientations can favor the transfer of electrons through the array of iron-sulfur clusters that works as a conducting wire for the transfer of electrons to the catalytic center.

The catalytic center is protected inside of a protein pocket that isolates the catalytic center from the exterior and provides a specific environment that favors the redox reaction of hydrogenase. However, this protein pocket also isolates it for the flux of electrons from the exterior, is for that reason that hydrogenases have several iron-sulfur clusters that

work has a wire for the transfer of electrons [1].

This implies that the orientation of the external iron-sulfur cluster can improve or the effectiveness of the enzyme.

1.4 Immobilization of proteins

The adsorption of proteins on charged surfaces has many technological applications, such as chromatographic separation of proteins, the design of biocompatible materials for medical uses, and food processing [1-3] [37].

The adsorption of hydrogenases on electrodes can be achieved by physical adsorption or covalent attachment. This implies that the fixation of the protein can be reversibly satisfied by the equilibrium condition, or irreversibly fixed on the electrode [38-41].

During adsorption, proteins interact with the surface through a combination of different phenomena: electrostatic forces, Van der Waals forces, hydrogen bonds, salt bridges, hydrophobic interactions, covalent bonds, etc. among other fewer known interactions [38-40]. Therefore, it is reasonable for its study to divide the adsorption of the protein in chemical and physical adsorption, depending on the main mechanism involved.

Chemical adsorption involves reactions between the protein and the surface of the electrode, mainly through covalent bonds. Its main characteristic is that once adsorbed, the protein cannot be detached from the surface. In turn, physical adsorption generally involves hydrogen bonding, Van der Waals force, hydrophobic and electrostatic interactions. Some authors have even considered that electrostatic effects are the dominant mechanism for the adsorption and orientation for immobilize proteins [41, 42]. These interactions are discussed in greater detail in the next chapter.

CHAPTER 2

2.1 Electrostatic interactions

It is possible to define the electrostatic interactions as the force between positive and negative charged objects. This force of attraction between these charged objects is dependent on the magnitude of the charges and the distance between them.

For two point-like particles, this relation is described by Coulomb's law $F = k_e(\frac{q_1 q_2}{r^2})\vec{\mu}$ in which q_1 and q_2 are two point charges, F is the vector of the electrostatic force directed from q_1 to q_2, separated by a distance r squared, $\vec{\mu}$ the direction of the force, and k_e is the Coulomb constant which takes in account the permittivity of the medium.

To apply a force, a certain amount of energy is necessary. With Coulomb's law, this energy is the electric potential energy (Coulomb's potential or Coulomb's energy), that in the case of the two point-like particles system, can be calculated with the equation:

$E_{coulomb} = k_e \frac{q_1 q_2}{r}$.

In a protein, the charged objects described by Coulomb's law are the atoms of the protein and the molecules with which the protein interacts. However, we shall see that the interaction between all the atoms cannot be computed by Coulomb's law alone, because the permittivity is not constant (water and the interior of proteins have very different permittivities) and an aqueous solution contains in general also other charges, namely the small mobile ions. In addition, the charges on the atoms of a metallic electrode are not fixed, but mobile.

Electrostatic interactions are important because they are one of the fundamental mechanisms that determine the structure, stability, binding affinity, chemical properties, and hence the biological reactivity of proteins. Also, are important for determining the stability of the protein and its folding pathway and determinate the interaction of the proteins with other molecules or objects is mainly determinate for electrostatic interactions [43, 44].

Coulomb's law is a very simple way to underline the importance of the electrostatic interactions; however, the application of these models in real life does not contemplate more factors that happen, like for example the effect of the ions in a solution in the electrostatic potential. To resolve this problem, it is necessary to adopt more sophisticate models that include more factors, in order to obtain a model that could predict the reality [45].

The solution to this problem was first tackled by Helmholtz, Gouy, Chapman and Stern in the beginning of the XX century. Their contributions are summarized mathematically by the Poisson-Boltzmann model that was used in this study. The modes proposed by these authors are differentiated between them based on the assumptions made for each model [43, 46].

2.2 Poisson-Boltzmann model

The Poisson-Boltzmann (PB) equation is a differential equation that describes the electrostatic field in ionic solutions. The equation can be used as a mathematical basis for the model of the double electric layer of Gouy-Chapman (Figure 2). This equation is important in the fields of surface science, electrochemistry and biophysics, because it can be used to model continuous dissolutions, describing the effects of the solvents on the structures of proteins, DNA, RNA and other molecules placed in solutions at different ionic strengths [43, 46-48].

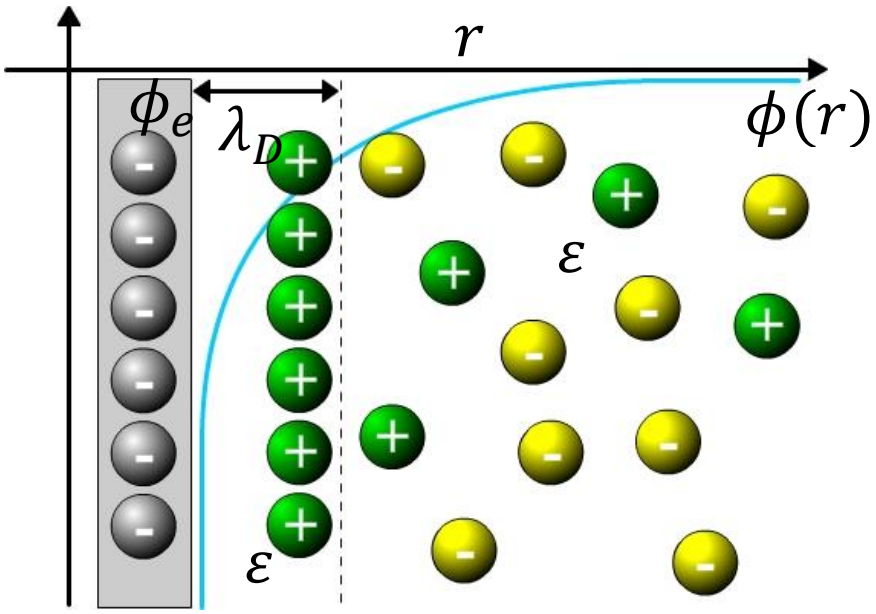

Figure 2. *Model of the electric double layer at the surface of a charged wall.*

Where: ε solvent dielectric permittivity, ϕ_e the electric potential applied to the electrode, λ_D Debye length, $\phi(r)$ is the electrostatic potential at determinate distance. The surface wall has a negative charge, the anions (−) and cations (+) are represented in spheres of color yellow and green respectably. The concentration of the ions is not uniform. The cations are attracted to the negatively charged wall, creating a layer, and its concentration decrease as the distance increase (r). The effect of the electrostatic potential, represented with a turquoise line, decreases logarithmically with the distance.

The solution of the Poisson–Boltzmann equation gives the electrostatic potential throughout the space. And when this electrostatic potential is applied with the Boltzmann distribution is possible to predict the local concentration of ions [43, 46, 49, 50].

Sometimes the equation of Poisson–Boltzmann becomes difficult to solve in complex systems. This is because, when an object is submerged in an electrolyte solution, the atoms of the solvent are in contact with the charged wall of the object. This produces that the ions of the solution reorganize themselves, forming a charged layer, the electrical double layer. This screens the surface electric field to a determinate distance, called Debye length and denoted λ_D [43, 46, 51, 52].

The electric double layer is the reason for the electrokinetic effects,

where the gradients and fluxes of different types (hydrodynamic, electrical, chemical, thermal) are influenced by the presence of charged interfaces.

To create the model of the ion distribution and electric potential profile in the electric double layer, it is necessary to combine the Poisson equation for electrostatics and the Boltzmann distribution of the ions. This model is the Poisson-Boltzmann model. It requires doing certain assumptions, that if well does not fit with the reality, they are necessary to create a robust model [43, 46, 48, 51-54].

In the model of the Poisson–Boltzmann, (figure 2) the atoms of the solute (object) are considered as individual particles with a specific dielectric constant (a typical known value for organic molecules); each particle also has assigned a charge at its position (these values are taken from the position and atomic charge). In the case of biomolecules like proteins or nucleic acids, their dielectric constants are in the range of (2-4) [43].

The dielectric value of the solute does not consider the rearrangements of polar and charged groups under the influence of external electric fields, a phenomenon that has been reported previously (see for details on models [43, 55]).

Also, the Poisson–Boltzmann equation assumes that the solvent has a local, homogeneous and isotropic dielectric permittivity that has a specific value for the conditions of the solvent (in the case of water the known value is 80 at 20 °C and 1 atm pressure).

In order to start to develop the Poisson-Boltzmann model, it is necessary first to assume a homogeneous system with a dielectric constant (ε), without charges.

The electrostatic potential of this system $\phi(r)$ is then described by the Laplace equation:

$$\overrightarrow{\nabla} \cdot \left[\vec{\nabla}\varphi(\vec{r})\right] = 0 \qquad (0)$$

In this equation, the vector ($\vec{\nabla}$) represents the gradient when it is applied to a scalar, or divergence when applied to a vector. The solution of the equation in a determinate volume depends on boundary conditions established at the moment of define the model of study.

When a charge density $\rho(\vec{r})$ is considered, its term is included in the Laplace equation leading the Poissonon equation:

$$\varepsilon \, \overrightarrow{\nabla} \cdot \left[\vec{\nabla}\varphi(\vec{r})\right] = -4\pi\rho(\vec{r}) \qquad (1)$$

This equation can be modified to another to express the general case of a non homogeneous medium to take into consideration the polarization charges developed at the dielectric boundaries (the derivation of this equation is described in Jackson [56] in [43]).

This effect is considered through the derivative of the space-dependent dielectric constant:

$$\overrightarrow{\nabla} \cdot \left[\varepsilon(\vec{r}) \, \vec{\nabla}\varphi(\vec{r})\right] = -4\pi\rho(\vec{r}) \qquad (2)$$

The charges of the solute (in our case a protein) need to be calculated and located at the atomic coordinates of the atoms of the solute (e.g. in the case of proteins this information can be obtained from the Protein Databank Structure).

In the case of solutions with ions, it is difficult to model the ionic charge distribution due to the combined effect of solute charges, dielectric distribution and the ionic distribution.

In order to deal with this difficulty, it is necessary to implement some further assumption, that lead from the Poisson to the Poisson–Boltzmann equation. First it is necessary to consider the solution as a complex system where the particles are interacting between them, the density of a particle at any point $\sigma(\vec{r})$ can be expressed in terms of relative density in absence of the interactions with other particles of the same system $\sigma_0(\vec{r})$, this can be written in the next expression:

$$\sigma(\vec{r}) = g(\vec{r})\sigma_0(\vec{r}) \tag{3}$$

where the ratio between the actual density and the average density of the particle $g(\vec{r})$ is expressed as the distribution function of that particle. A useful concept which can be derived from the distribution function is the potential of mean force $w(\vec{r})$ [43, 57] for the particle can be described with the following equation:

$$g(\vec{r}) = e^{[-w(\vec{r})]/kT} \tag{4}$$

In this equation is possible to describe the particle distribution where the “potential of mean force” (PMF) condenses the average effect of the whole system in a single particle potential. This term comes from the observation that the gradient of this potential energy, with respect to the particle coordinates, gives the mean force acting on the particle. One consequence of the “PMF” is that in ionic systems, ions will preferentially reside in regions where the average potential is high or low according to the sign of their charge.

Another utility of the potential of mean force is that it is possible to calculate the free energy along the chosen coordinate. And if the system of interest is in a solvent, then the PMF also incorporates the solvent effects in the result.

However, this sentence should be considered carefully because in systems with ions in solution, the electrostatic interactions are screened due to the influence of the solute, and they can usually be detected at a

distance of 10–20 Å [43].

This means that in a solution there is a big volume available for the ions and there is not a relevant perturbation in the distribution, and for that reason there is a tendency towards homogeneity in the system.

In order to obtain the equation for the potential, another assumption needs to be done, which consists in considering that the ionic potential of mean force is equal to the average electrostatic potential multiplied by the charge of the ion. When this assumption is included in the Poisson equation for non-homogeneous media, we obtain the Poisson–Boltzmann equation.

$$\overrightarrow{\nabla}\cdot\left[\varepsilon(\vec{r})\,\vec{\nabla}\phi(\vec{r})\right] = -4\pi\rho^{f}(\vec{r}) + 4\pi\sum_i c_i^{\infty} z_i q exp\frac{-z_i q\phi(\vec{r})}{kT}\lambda(\vec{r}) \quad (5)$$

where $\rho^{f}(\vec{r})$ includes now only molecular charges, c_i^{∞}, is the concentration of the ion to an infinite distance from the solute, z_i is the valency, k is the Boltzmann constant, T is the temperature $\lambda(\vec{r})$ describes the accessibility to ions at point $\vec{r}$ and q is the proton charge.

This equation can be linearized under the assumption that the electric potential is small:

$$\vec{\nabla}\cdot\left[\varepsilon(\vec{r})\,\vec{\nabla}\phi(\vec{r})\right] = -4\pi\rho(\vec{r}) + 4\pi\frac{\sum_i c_i^{\infty} z_i^2 q^2\phi(\vec{r})}{kT}\lambda(\vec{r}) \quad (6)$$

An important parameter is the Debye screening constant (k_D), this term describes the exponential decay of the electrostatic potential in the solvent:

$$k_D^2 = 8\,\pi\frac{\sum_i c_i^{\infty} z_i^2 q^2}{2\varepsilon kT} = \frac{1}{l_D^2} \quad (7)$$

l_D by the other side is the Debye length ($\frac{1}{k_D}$), and it is a measure of the effective thickness of the diffuse double layer, and can be seen as a

measure of the net electrostatic charge of the carrier in
and how far its electrostatic effect can persist.

In the case of the linear version of the Poisson–Boltzmann equation has the advantage that it does not lead to an inconsistency like the ones possible to found in the nonlinear version.

Let us see, for example, what happens with a solution of a 2:1 salt, and consider the average electrostatic potential, $\phi_2(\vec{r})$ and $\phi_1(\vec{r})$ computed when taking the divalent or the monovalent ion as the central, respectively.

In the nonlinear case, the reciprocity condition $z_2\phi_1(\vec{r}) = z_1\phi_2(\vec{r})$ will be difficult to reach, while the same condition is naturally met in the linear case because the potential is proportional to the source of ion valency.

If the reciprocity condition is not fit, the probability of finding a divalent ion at the distance $\vec{r}$ from a monovalent ion changes depending on which ion is used to compute the average potential, which is a mistake.

Nevertheless, considering this inconvenience, the results obtained from the linear Poisson–Boltzmann equation are close to the solution obtained from the nonlinear Poisson–Boltzmann equation, even if the linearization conditions are not fulfilled [43, 51].

Different comparisons between the linear and nonlinear models of the Poisson–Boltzmann equation have been done. And it is possible to say that there are appreciable differences between the two treatments when the magnitude of the electric potential is over 0.05 V, due to the charge density at the solute–solvent interface [43, 51].

Some modifications can be applied to the Poisson–Boltzmann equation in order to simplify it, in order to be applied to a complex model like proteins, DNA or membranes, where the shape of these

biomolecules is approximate to spheres, cylinders or planes. This is done to accelerate the calculations or make simple the model in cases where are considered several biomolecules.

2.3 Computational modeling

The model used in this study is based on the linearized version of the Poisson-Boltzmann equation. It can be used to describe the distribution of mobile ions and the electrostatic potential for one or more charged objects, such as a protein, an electrode, or their combination [43, 53].

Several software tools solve this equation numerically, including for example APBS, [58] Delphi, [55, 59] MEAD, [60] MIBPB, [61] AFMPB, [62] and TABI [63]. In this study has been selected PyGBe [49, 50, 64] due to its ability to calculate efficiently the electrostatic interaction between multiple bodies at close range.

New Python scripts were written to implement the use of PyGBe and calculate the interaction energy between the hydrogenase and the electrode. Some scripts can be found in the appendices of this document. These codes make it easier to calculate multiple protein orientations with PyGBe, which the original code cannot do.

The new script includes commands to create the protein mesh and the electrode mesh using a series of points to define the desired dimensions. Users can determine the angle and other experimental parameters in the script, simplifying the work with large amounts of data using only the initial inputs. The grades of the angle in which is desired to rotate the protein, together with the rest of the experimental parameters, can be determined by the user in the script, which makes easier the work with a big volume of data using just the initial inputs.

A first script allows us to calculate the interaction energy using PyGBe for the orientations generated previously, dividing all the orientations generated in separated nodes, accelerating in this way the

time required to obtain the results. The script also corroborates that a simulation has been accomplished successfully, in a contrary case, the simulation is run again.

The second script can be used to visualize the results from PyGBe by associating the calculated electrostatic potential values to each triangle of the protein mesh. The files generated by this script can be read and displayed with “Paraview” software [65] using a scale of colors from red to blue.

All the scripts were developed in the course of the present thesis. Also, the installation of the programs, the calculations and the subsequent analysis of the data were all performed by me (MARR).

CHAPTER 3

Methods

3.1 Goals

The main goal of this study is to calculate the electrostatic interactions between a [NiFe] hydrogenase and an electrode. Considering for such purpose, the effect of some factors previously reported has determiners for the orientation of the protein, such as pH, salinity, and electric potential.

A secondary goal is to determinate if it is possible to control the orientation of the hydrogenase on the surface of the electrode by tuning these variables, without modifying the chemistry of the electrode.

The third goal is to determinate the activity of the adsorbed enzymes as a function of the enzyme concentration, based on the assumption that there is a relationship between the adsorption equilibria and the electron transfer between the hydrogenase and the electrode.

3.2 Physical model

The mathematical model used to calculate the electrostatic interaction between the [NiFe] hydrogenase and the electrode is based on the linearized Poisson-Boltzmann equation. In order to do the calculations, the model considers the protein as a rigid object with a conformation identical to that obtained from the crystal structure obtained from the "pdb" file, collected from the protein data bank.

The model also considers that the protein and the electrode are immersed in a solvent. The solvent is considered implicitly, and consists of water with salt (NaCl) at a concentration of solution (*I*=0.15 or 0.0 M) [43, 53, 66]. The charge associated with the atoms of the protein were considered fixed points at the positions of the center of the atoms.

The interior and exterior of the protein were defined by the solvent-excluded surface (SES). This was determined by rolling a sphere with the diameter of a molecule of water around the [NiFe] hydrogenase. For the model was considered a relative permittivity (or dielectric constant) for the inside of the protein of $\varepsilon_1 = 4$, a value reported experimentally previously in several articles for proteins, while the solvent region has the relative permittivity of water ($\varepsilon_2 = 80$) [43].

In the case of the electrode, this was modeled has a flat surface with a geometry of a rectangular cuboid with dimensions 250Å, 250Å, 10 $Å^3$.

The electrode was considered as a metallic conductor and does not have an associated permittivity, but its electrostatic potential had a fixed value at all points that conform to the mesh representing its surface. The model of the interaction of the hydrogenase on the electrode is illustrated schematically in Figure 3.

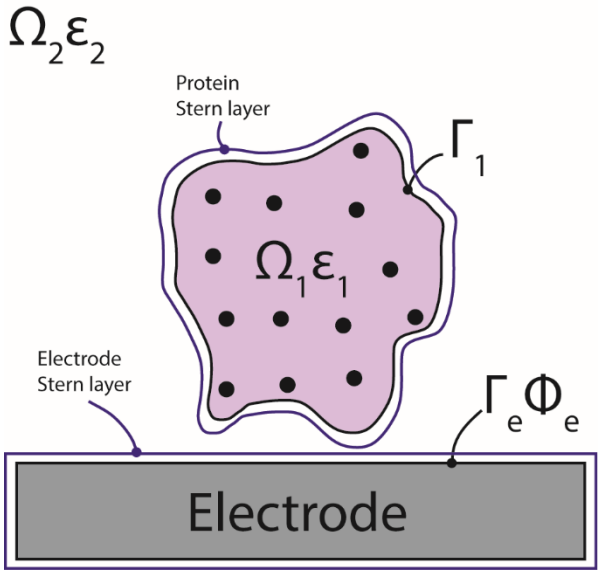

Figure 3. *Model proposed for the calculation of the hydrogenase-electrode electrostatic interaction.*

Region Ω_1 corresponds to the protein, the fixed-point charges of the atoms are represented as black points. And it is delimitated for a surface Γ_1, the protein has its own permittivity ε_1. Region Ω_2 correspond to the electrolyte solution, and it has a permittivity value of ε_2. The Surface Γ_e corresponds to the boundary of the electrode, in the electrode is applied an electric potential ϕ_e. Both the protein and the electrode are surrounded by Stern layers.

The model described in Figure 3 is expressed in a system of partial differential equations, whose solution is implemented in the software PyGBe.

3.3 PyGBe

PyGBe—pronounced pigbē—is based on a library of routines written in Python and implemented for the parallel computing platform of CUDA that uses graphical processing units (GPU's), to solve by numerical methods the linearized Poisson-Boltzmann equation. It was developed to calculate the electrostatic interaction between multiple bodies.

It uses a boundary element approach to obtain the electrostatic potential $\phi(r)$, by solving the Poisson equation inside the protein (region

Ω_1) and the linearized Poisson-Boltzmann equation in the surrounding solvent (region Ω_2):

$$\nabla^2\phi(r) = -\sum_i \frac{q_i}{\epsilon_1}\delta(r, r_i) \qquad \text{(inside } \Omega_1\text{)} \qquad (8)$$

$$\nabla^2\phi(r) = \kappa^2\phi(r) \qquad \text{(inside } \Omega_2\text{)} \qquad (9)$$

In equation (8) there is a summation on all the atomic charges of the protein, and the value of κ is the inverse of the Debye-Hückel screening length, which depends on the overall concentration of small ions dissolved in the aqueous medium:

$$\kappa^2 = \frac{2e^2}{\epsilon_2 k_B T} I \qquad (10a)$$

$$I = \frac{1}{2}\sum_j c_j z_j^2 \qquad (10b)$$

where c_j and $q_j = ez_j$ are the concentrations and charges of the ions, $k_B T$ is the thermal energy and *e* is the elementary charge. The ionic strength *I* coincides with the salt concentration, for a monovalent salt such a NaCl ($z_j = \pm 1$).

The calculations are done with a physiological solution of *I*=0.15 mol/L, at room temperature under these conditions κ has a value of $\kappa = 0.125\text{Å}^{-1}$. In the calculation where, not ionic strength was tested the condition on aqueous solution was *I*=0.0 mol/L.

Equations (8) and (9) are coupled, because $\phi(r)$ and the electric displacement $[-\epsilon_r \nabla\phi)]$ must be continuous at the interface between Ω_1 and Ω_2 (i.e., on the protein's SES).

In addition, on the electrode's surface (Γ_e) we adopted a Dirichlet boundary condition, whereby the potential takes a constant value ϕ_e:

$$\phi(r) = \phi_e \qquad \text{(on } \Gamma_e\text{)} \qquad (11)$$

while the electric displacement at the water-electrode interface (more

precisely, its component along the normal direction **n**) gives the local charge density (unit per area).

The electric potential applied to the electrode is considered constant while the electric displacement at the water-electrode interface (more precisely, its component along the normal direction **n**) gives the local charge density (unit per area).

Unlike the potential, which is constant throughout the electrode, this may depend on the position (**r**):

$$-\epsilon_2 \nabla\phi(r) \cdot n = \sigma(r) \qquad \text{(on } \Gamma_e\text{)} \qquad (12)$$

where $\sigma(r)$ is the induced surface electric charge density.

In the calculations, we included two ion-exclusion layers (denominated Stern layers within this study), respectively surrounding the protein and the electrode.

3.4 Stern layers

For the calculations, were included two ion-exclusion layers denominated Stern layers, covering the protein and the electrode. The inclusion of these layers responds to the fact that the ions at very close ranges to the surface of charged objects are repelled from the surface, eliminating their presence [49].

Previous studies have determinated that the thickness of the layer depends on the diameter of the ions, that in the case of NaCl will be approximately 2.0 Å. The solution was considered having the dielectric constant of water ($\epsilon_2 = 80$) and a local ion concentration equal to zero. The purpose of this layer is to prevent excessive accumulation of positive/negative ions in regions with very negative/positive potentials.

It is essentially an empirical correction for the assumption inherent to the Poisson-Boltzmann model of electrolyte solutions, without any short-range correlations related to the size of the ions (assumed to be point-like).

The distance between the electrode and protein surfaces was set at 4.1 Å. This accounts for the 2 Å distance for each Stern layer and an additional 0.1 Å to prevent overlap.

Below this distance, the continuum hypothesis that underlies the Poisson-Boltzmann equation might be questionable. Above this distance, the electrostatic interaction decreases monotonically (in absolute value), as shown in Figure 2.

3.5 Experimental design

The experimental model was designed considering the effects of the variables of solution pH (5, 6, 7, 8, and 9), electric potential of the electrode ϕ_e (-0.05, 0.00, and 0.05 V), and salt concentration in the solution (I=0.15 or 0.0 M).

The ranges of the different variables were determined, taking into account the limitations of the model. In the case of the pH, this was selected in the range where denaturation is not expected to occur and the hydrogenase is enzymatically functional, while the electrostatic potential of the electrode is limited by the range of reliability of the linearized Poisson-Boltzmann equation.

3.6 Assignment of atomic charges

In order to calculate the electrostatic interaction, it is necessary to obtain first the charges associated to the atoms of the protein, according to a

specific force field.

For this purpose, the “pqr” files containing the Cartesian coordinates of the atoms, their charges, and Van der Waals radii were obtained using the “pbd2pqr” software [67] using as a source of the structures of the 1e3d hydrogenase the “pdb” file obtained from the “pdb” databank.

The pbd2pqr software assigns atomic charges and radii based on the chosen force field. Currently, pbd2pqr provides parameters from CHARMM22 [68], AMBER99 [69], or PARSE [70] force fields. This step involves translating the atom and residue names found in the force field to a PQR format that matches those of the input structure file (pdb file) and assigning the appropriate parameters [67].

However, one limitation of this software is that it cannot assign atomic charges to metallic atoms (HETATM entries), which are present in the catalytic center and in the iron-sulfur clusters.

In order to obtain the atomic charges of these atoms, quantum chemical calculations on the iron-sulfur clusters and the catalytic center were conducted, extracting these groups of atoms and replacing the original chemical bonds to the amino acids of the protein for CH_3 groups.

These selections of atoms were used to calculate the CHELPG charges (CHarges from ELectrostatic Potentials using a Grid-based method). The CHELPG method is based on the calculation of the electrostatic potentials generated by the electronic densities of the atoms in a molecule. It uses a mesh or grid to evaluate these potentials and determine the partial charges of the atoms [71].

These partial charges are numerical values that represent the distribution of electron density on an atom in a molecule [71]. [72] The CHELPG charged used for the calculations were based on single-point unrestricted density function theory calculations (DFT) and were calculated using the software “ORCA” [73, 74].

A Gaussian basis set (def2-SVP) [75] was selected to do the calculations with a tight self-consistent field option, using the PBE0 [76] hybrid density functional to compute the exchange-correlation energy.

For the catalytic center we performed calculations with a total charge of 0 and spin multiplicities of 1, 3, 5, 7, and 9. For the external cluster, a total charge of 0 and multiplicities of 1, 3, 5, 7, and 9. For the medial cluster, a total charge of +2 and multiplicities of 2, 4, 6, 8, and 10. And for the proximal cluster, a total charge of -3 and multiplicities 1, 3, 5, 7, and 9.

The formation of the CHELPG charges used for the calculation in PyGBe corresponds to the calculations with the spin multiplicity with the lowest energy.

Once that all the atoms that conform the protein have their atomic charges, the software pdb2pqr was used to generate the final “pqr” files, adding the CHELPG charges calculated previously to the list of atoms of Amber force field [72] file used by pdb2pqr. The pdb2pqr program was then run using standard settings for the “propka” method for each pH tested [67].

The program pdb2pqr assigns the protonation state of the ionizable groups of the protein, depending on the value of the pH solution. This protonation state was assumed to be fixed, independently of the distance and orientation of the protein on the electrode, and does not affect the interaction between the atoms of the protein.

In principle, this assumption could be relaxed, with an increase in calculation time [39]. The total charge on the protein and the modulus of its dipole moment are reported in Table 1, for each pH value. Note that the dipole moment of an object with a non-zero charge depends on the choice of origin for its evaluation. Our values have been calculated with respect to the center of charge of the protein.

The total charge on the protein and the modulus of its dipole moment are reported in Table 1, for each pH value. The values have been calculated with respect to the center of charge of the protein.

Table 1. *Total charge on the protein and modulus of its dipole moment, at each pH value.*

The elementary charge is e *=1.602 X10^{-19} C. For the dipoles, 1* e *Å=4.803 D.*

pH	Charge (*e*)	Dipole (*e*Å)
5	15.6	1495.8
6	3.6	1497.5
7	-5.4	1500.6
8	-12.4	1494.3
9	-15.4	1504.0

3.7 Generation of model meshes

In order to calculate the electrostatic potential, PyGBe requires a mesh that represents the surface of the protein and the electrode respectably. The meshes are generated using the "Nanoshaper" software [77].

The following settings were adopted, seeking a balance between cost and numerical accuracy of the calculations: "grid scale" = 2.0, "smooth mesh" = true, "probe radius" = 1.4 and "keep water shaped cavities" = true.

The probe molecule used to create the meshes was the molecule of water with a radius of 1.4 Å. This is considered as a sphere rolling around the protein, thus generating its SES.

3.8 Electrostatic energy

Once that the atomics charges and meshes of the protein and electrode are ready, the PyGBe program was used to solve the linearized Poisson-Boltzmann equation [49, 50, 64].

The results of the calculations of PyGBe are the values of the electrostatic potential and the normal component of its gradient for each grid point of each surface represented in the mesh files. These results are used then to obtain the electrostatic component of the free energy of the system.

PyGBe considers the electrostatic component of the free energy of the system as the total energy of the system calculated. That in this study, it is conformed for the hydrogenase-electrode system.

This is calculated as the sum of Coulomb, solvation and surface contributions, according to the equation:

$$E_{total} = E_{Coulom} + E_{solvation} + E_{surface} \quad (13)$$

The Coulomb energy is calculated from the Coulomb interactions of all point charges:

$$E_{Coulomb} = \frac{1}{2}\sum_{j}^{N_q} q_j \phi_{Coulomb}(r_j) = \frac{1}{2}\sum_{j}^{N_q} \sum_{\substack{i \\ i \neq j}}^{N_q} q_j q_i \frac{1}{4\pi\varepsilon_1 \vee r_i - r_j \vee} \quad (14)$$

where ε_1 is the dielectric constant within the protein, $\phi_{Coulomb}(r_j)$ is the Coulomb potential at the position charge q_j due to the other charges q_i, and the double summation runs over all the charged atoms of the protein.

The contribution of the Coulomb energy could be expected to be large and constant, being independent of the orientation of the protein and distance from the electrode. The Coulomb energy would not have

been constant if we had included the possibility that the protonation state of the amino acids depends on the orientation of the protein.

The solvation energy is the energy contribution from the surroundings of the protein: solvent polarization, charged surfaces, possibly other proteins. It is calculated as:

$$E_{solv} = \frac{1}{2}\int_{\Omega} \rho \phi_{reac} d\Omega = \frac{1}{2}\sum_k q_k \phi_{reac}(r_k) \quad (15)$$

where ρ is the charge distribution and $\phi_{reac} = \phi - \phi_{Coulomb}$ is the electrostatic potential that arises due to the reaction of the solvent, that contains the contribution of the polarization of the solute in the solvent. Again, the summation runs over all the atomic charges of the protein. Finally, the surface energy is:

$$E_{surf} = \frac{1}{2}\int_{\Gamma_e} \phi(r)\sigma(r) d\Gamma = \phi_e Q_e \quad (16)$$

where the integral is performed over the surface of the electrode, and Q_e is the net charge on it.

The interaction energy is calculated by subtracting the values of the energy of the isolated electrode and the isolated protein from the total energy:

$$\Delta E(\theta_i \varphi_i) = E_{total}(protein@electrode) - E_{total}(protein) - E_{total}(electrode) \quad (17)$$

The values of the total energy for the protein and the electrode were calculated separately with PyGBe, using the same meshes of the combined calculation.

Negative values in the interaction energy can be interpreted as the adsorbed hydrogenase is energetically more stable than the free state of the protein.

The (θ_i, φ_i) arguments appearing on the left-hand side of Eq. (17) emphasize that this energy depends on the protein orientation, to be discussed in the next subsection.

3.9 Protein orientations and probabilities

One goal of this study was to determinate if it is possible to control the orientation of the protein on the electrode, changing the experimental variables described previously, for that reason was calculated the total energy of the protein adsorbed on the surface of the electrode at different orientations these orientations were obtained changing the inclination in the tilt angle θ $(0^o \leq \theta \leq 180^o)$ and an azimuthal angle φ $(0^o \leq \theta \leq 180^o)$ [64].

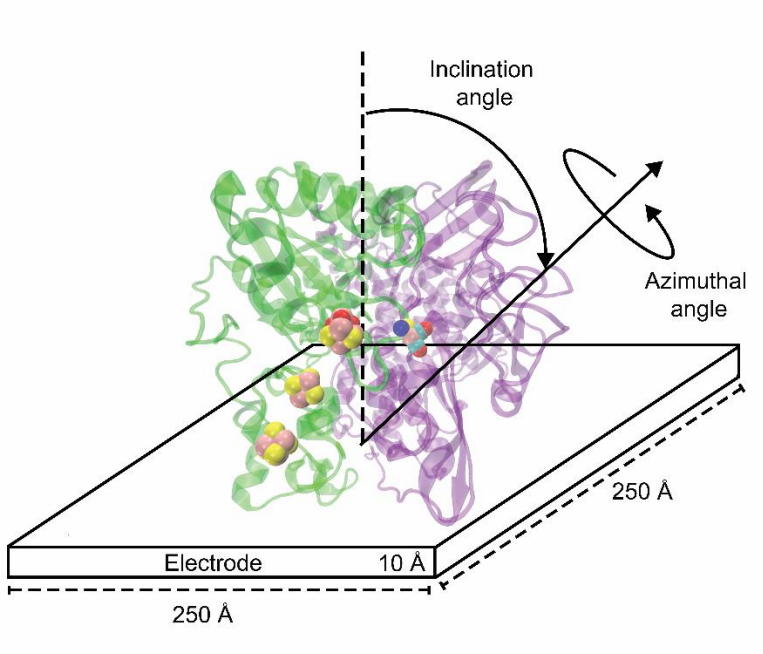

Figure 4. *Model used to test the hydrogenase-electrode electrostatic interaction. Defining the tilt θ and azimuthal angles φ.*

The orientations tested were obtained incrementing the tilt angle in even steps of 10 degrees $d\theta = 10^o$, while the changes in the azimuth angle were changing using the next expression $d\varphi = \frac{360^o}{\max[1{,}36\ \sin\theta]}$ (i.e., using only one point when $\theta = 0^o$,180° and 36 points when $\theta = 90^o$), as

is illustrated in Figure 4. With these settings, the total number of sampled orientations was M=390.

3.10 Boltzmann distribution of probabilities

Using the Boltzmann distribution for probabilities is possible to associate the orientations of the hydrogenase to its energies. Considering that the position with the lowest energy should be the one with the highest probability of occur according with the equation of the Boltzmann equilibrium distribution [57, 78, 79]:

$$P(\theta_i, \varphi_i) = \frac{1}{N} exp\left\{\frac{-E_{total}(\theta_i,\varphi_i)}{RT}\right\} \quad (18)$$

where the normalization constant *N* is given by:

$$N = \sum_{i=1}^{M} exp\left\{\frac{-E_{total}(\theta_i,\varphi_i)}{RT}\right\}. \quad (19)$$

Note that the contributions representing different orientations can be summed evenly in Eq. (17), because the differential solid angles associated with them are identical.

The interaction energies can be used in place of the total energies in equations (18) and (19), leading to the same probabilities.

3.11 Adsorption equilibria

The probabilities of Eq. (18) depend on the relative energies of the adsorbed states, but are independent of the overall adsorption energy defined by Eq. (17).

Adding or subtracting a constant value to the total energies leads to

the same probabilities, because of the normalization in Eq. (19). However, a change in the overall adsorption energy will have an effect on the degree of coverage of the electrode by the proteins, for a given protein concentration in solution.

According to the assumption of reversible equilibrium in the Poisson-Boltzmann model, the free energy determines the probability that the enzyme adopts a specific orientation on the electrode.

Considering that the probabilities of the adsorbed orientations depend on their interaction energies. It is possible to suppose that a change in the overall adsorption energy will have an effect on the degree of coverage of the electrode by the proteins, for a given protein concentration in solution. This phenomenon can be modeled using the Langmuir's theory of adsorption [57, 78, 79].

However, this mathematical model considers an ideal situation where the proteins do not interact with each other, either in solution or with the electrode. But can be used to predict the behavior the proteins adsorbed on the surface of the electrode.

Being χ the overall coverage of the electrode, defined as the fraction of its area covered with proteins ($0\chi1$). And the variable $\chi(\theta_i, \varphi_i)$ the fraction of the electrode area covered by the proteins with a specific orientation, out of *M* possibilities. These terms related with the next expression:

$$\chi = \sum_{\theta_i} \sum_{\varphi_i} \chi(\theta_i, \varphi_i) \tag{20}$$

Clearly, $\chi(\theta_i, \varphi_i)$ should be proportional to the probabilities of Eq. (18). it allows to write the next expression:

$$\chi(\theta_i, \varphi_i) = \chi \times P(\theta_i, \varphi_i) \tag{21}$$

The Langmuir adsorption equation relates χ to the osmotic pressure

Π of the protein in solution following the next expression:

$$\chi = \frac{K\Pi}{1+K\Pi} \tag{22}$$

In the expression *K* is the equilibrium constant for the overall protein adsorption. Overall coverage χ is proportional to the osmotic pressure Π (which is proportional to the protein concentration in the solution when it behaves ideally when $\Pi \ll K^{-1}$, but is saturates at 1 when $\Pi \gg K^{-1}$.

This model describes the formation of a protein monolayer on the surface of the electrode, begin K the effect of all the individual equilibria between hydrogenases in solution (H_{sol}) and hydrogenases on the surface (H_{surf}):

$$\begin{aligned} H_{sol} &\Leftrightarrow H_{surf}(\theta_1,\varphi_1) \\ H_{sol} &\Leftrightarrow H_{surf}(\theta_2,\varphi_2) \\ &\vdots \\ H_{sol} &\Leftrightarrow H_{surf}(\theta_M,\varphi_M) \end{aligned} \tag{23}$$

Each orientation has its own equilibrium constant $K(\theta_i,\varphi_i)$, which is related to its interaction energy following the next expression:

$$K(\theta_i,\varphi_i) = \frac{1}{M}\left[\frac{q_{vib}e^{\frac{\mu^0}{RT}}}{\Pi^0}\right] exp\{-\Delta E(\theta_i,\varphi_i)\} \tag{24}$$

where the terms inside of the square brackets represent the vibrational motion of the adsorbed proteins on the surface, where the inside terms are (q_{vib}) a vibrational partition function, the osmotic pressure (Π^0), and the chemical potential of the proteins in solution (μ^0), at its reference concentration.

This would be difficult, if not impossible, to calculate; therefore, it is simply assumed to be constant (independent of protein orientation).

In order to calculate the equilibrium constant $K(\theta_i,\varphi_i)$, the terms

previously described were assume them to be constant (independent of protein orientation).

The 1/*M* pre-factor in Eq. (24) is incorporated in order to include the loss in rotational entropy, which is assumed occurs when the protein passes from being free in solution to be adsorbed on the electrode.

The overall equilibrium constant described in Eq. (21) can be obtained as the summary of the individual orientation-dependent constants as expressed in the next equation:

$$K = \sum_{\theta_i} \sum_{\varphi_i} K(\theta_i, \varphi_i) \tag{25}$$

Note the similitude among Eqs. (20) and (25). All these equilibrium constants depend on pH, salinity, and electrostatic potential at the electrode.

3.12 Electron transfer rates and currents

One parameter to evaluate the catalytic efficiency of a protein orientation on the electrode is the measure of the current transfer from the electrode to the protein. Indeed, enzyme orientation on the electrode affects its catalytic efficiency, because the catalytic center could not be accessible for the electrons and protons from the exterior of the protein for the redox reaction in all its orientations [2].

Some studies have shown that electron transfer is one of the important factors in the rate-limiting step for the redox reaction. [1, 80] Is for that reason that in this study the current has been used as a parameter to measure the effectiveness of the protein orientation.

However, modeling all the factors involved in transfer electrons within the protein and between the protein and the electrode will be very complicated or impossible [81].

In order to simplify the calculations, we consider a constant value for the transfer of electrons. Considering that the main way to transfer electrons in electron hopping, while other ways like quantum mechanical tunneling are not so important. Under the supposition that the transfer of electrons studied is between the electrode and the external iron-sulfur cluster, where is expected classical hopping of electrons.

In proteins, the rate of electron transfer between two atoms decays exponentially with the distance *r* [78] following the next expression:

$$k_{ET} = Ce^{-\beta r} \tag{26}$$

Where β determinates the rate of decay in the transfer of electrons and C includes all the unknown factors that could affect the transfer of electrons such as vibrational energy and temperature according to the Marcus theory for electrons transfer [78, 81]. The distance used to calculate the current $r = r(\theta_i, \varphi_i)$ is the distance from the iron atom coordinated to histidine 187 to the surface of the electrode.

Different values for the decay constant (β) have been reported in different publications, considering the protein and the experimental conditions. In the case of the value reported by Petrenko (β = 0.45 $Å^{-1}$) this value was reported in the use of modulate the transfer of electrons in hydrogenases [82, 83].

In the case of Stein, he reports the value of β = 1.4 $Å^{-1}$, it is a very popular value used in several studies with different proteins under diverse experimental conditions. However, this value is not expected to be universal and is expected it to be dependent on the secondary structure of the protein [78].

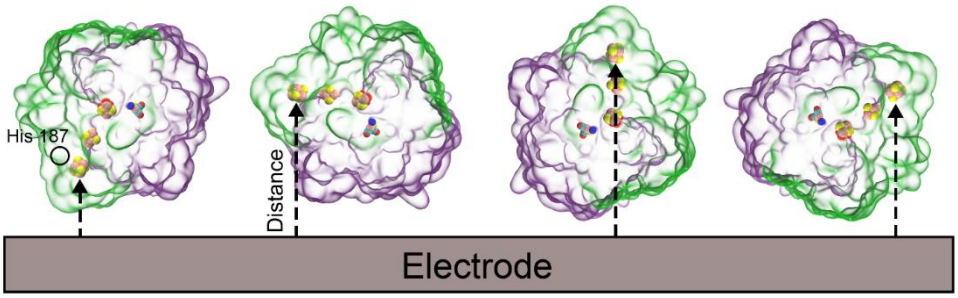

Figure 5. *Different orientations of the protein on the surface of the electrode. The external iron-sulfur cluster is the entry point for the flux of electrons to the enzyme, and its distance from the electrode has a direct impact on the rate of electron transfer. Different orientations will produce different overall electric currents.*

In order to estimate the overall hydrogen conversion rate, it is possible to use the overall electric current. Due the current is proportional to the production of hydrogen.

The protein adsorbed on a flat electrode can have different orientations with a different probability associated, multiplying their probability by their respective electron transfer rate, makes possible to calculate the total electric current by summarizing all the individual currents.

The current produced should be proportional to the area of the electrode (A) covered by the proteins (χ), which is described in the next equation:

$$I_{tot} = \chi A J_0 \tag{27}$$

where J_0 is a reference current density, independent of protein concentration and electrode area:

$$J_0 = \frac{eC}{a_0} \sum_{i=1}^{M} P(\theta_i, \varphi_i)\, exp[-\beta r(\theta_i, \varphi_i)] \tag{28}$$

In Eq. (28) it has been assumed that a_0, the area occupied by one adsorbed protein, is independent of its orientation. This is done,

considering the near spherical shape of this hydrogenase.

The previous equation can be used to describe the dependence between the electric current (hydrogen redox rate reaction) and the osmotic pressure used as a representation of the protein concentration in solution.

Both the currents and the osmotic pressures can only be given in arbitrary units (a.u.), because of the uncertainties on the prefactors used in Eqs. (17) and (21). Even considering these limitations, it is possible to calculate the effect on the current for the experimental factors selected in this study, such as the salt concentration, solution pH, and electrode potential.

These prefactors are discarded in the calculations of this document, but they may be used as adjustable parameters when fitting experimental data.

3.13 Analysis and Post-processing

In order to get a visualization of the results obtained with PyGBe, a small script in Python was written that can produce an image that represents the interaction between the protein and the electrode.

This script generates a "Visualization Toolkit" (vtk) file that could be visualized using the "Paraview" software. [65] A colorful image was created by assigning electrostatic potentials calculated for PyGBe to every triangle of the protein and electrode mesh using the "vtk" generated.

CHAPTER 4

Results and Discussion

4.1 Minimum interaction energy orientations

The results obtained in this study are summarized in the Table 2, all the calculations are explained in detail in the Figures 6 - 26. Between the most important results to evaluate the adsorption of a protein on the electrode and its availability to catalyze the redox reaction of hydrogenase we have the interaction energy and the total charge.

Each combination of experimental variables consists of: pH, electric potential ϕ_e, and concentration of salt in solution (ionic strength *I)*. The possible orientations obtained from the rotation of the protein through the theta and phi angles are 390. Considering 20 combinations of experimental variables times 390 orientations, in total 7800 calculations were done with PyGBe in this study. Several additional calculations were done in the preliminary stages of the work, for example to examine the dependence of the results on the computational mesh (the density of points used to represent the surface of the protein and the electrode) and the size of the electrode.

In Table 2 are shown the orientations with the lowest interaction energies of all these calculations. Comparing the results of these orientations it is possible to observe that, the orientation with the lowest interaction energy was obtained in the orientation 80 tilt (θ) and 131 azimuthal (φ) grades (Figure 24) under the experimental conditions of I=0.00 M, ϕ_e = 0.0 V and pH=9 with a value of -53.43 kJ mol-1. If we compare this orientation with the rest of orientation in Table 2, It is possible to consider this orientation like the best adsorbed, however this orientation is not part of the orientations that belongs to the experimental

conditions were the best total currents were obtained, for example the orientation with the highest total current was the orientation of 120 tilt (θ) and 248 azimuthal (φ) grades (Figure 8) obtained under the experimental conditions of I=0.00 M, ϕ_e = 0.0 V and pH=5

Table 2. Protein orientations (θ_{min}, φ_{min}) with the lowest energy, for each combination of pH, ϕ_e and I.
The table gives also the adsorption energy (ΔE_{min}) and the probability associated with such orientation (P_{min}), the distance from the external iron-sulfur cluster to the surface at the minimum (r_{min}) and the associated exponential, the orientation-averaged electric current (I_{total}), the total charge on the electrode and information about the closest amino acids to the electrode.

	pH	θ_{min}(°)	φ_{min}(°)	ΔE_{min} (kJ mol^{-1})	P_{min}	Charge on electrode	Closest amino acid	Charge of ten closest amino acids	r_{min} (Å)	exp(-β r_{min})	I_{total} (a.u.)
I=0.15 M, ϕ_e=-0.05 V	5	40	98	-8.15	0.031	-356.86	Lys 139	0	66.82	8.72×10^{-14}	4.58×10^{-05}
	6	80	131	-8.73	0.026	-357.45	Phe 354	-3	50.07	1.64×10^{-10}	6.64×10^{-05}
	7	80	131	-8.58	0.045	-356.00	Phe 354	-3	50.07	1.64×10^{-10}	6.31×10^{-05}
	8	170	60	-4.02	0.015	-360.02	Phe 354	2	48.14	3.91×10^{-10}	5.50×10^{-05}
	9	130	235	-9.30	0.012	-355.39	Asp 197	-2	16.28	6.58×10^{-04}	4.81×10^{-05}
I=0.15 M, , ϕ_e=0.0 V	5	60	273	-6.93	0.025	-1.35	Asp 197	0	17.26	4.23×10^{-04}	6.30×10^{-05}
	6	60	273	-5.89	0.017	-0.56	Asp 197	0	17.26	4.23×10^{-04}	5.51×10^{-05}
	7	80	131	-5.52	0.016	2.39	Phe 354	-3	50.07	1.64×10^{-10}	5.04×10^{-05}
	8	110	270	-4.78	0.011	0.32	Ala 198	-2	20.58	9.50×10^{-05}	5.27×10^{-05}
	9	80	131	-5.18	0.013	3.90	Phe 354	-3	50.07	1.64×10^{-10}	5.67×10^{-05}
I=0.15 M, , ϕ_e=+0.05 V	5	40	98	-9.54	0.198	354.42	Lys 139	0	66.82	8.72×10^{-14}	8.02×10^{-05}
	6	120	261	-9.54	0.033	355.31	Lys 194	1	18.17	2.81×10^{-04}	6.77×10^{-05}
	7	120	261	-5.80	0.021	357.05	Lys 194	0	18.17	2.81×10^{-04}	6.25×10^{-05}
	8	130	180	-7.21	0.016	361.72	Asp 480	-2	24.18	1.88×10^{-05}	5.59×10^{-05}
	9	100	44	-13.85	0.035	359.89	Thr 12	2	51.57	8.36×10^{-11}	6.51×10^{-05}
I=0.00 M, ϕ_e=0.0 V	5	120	248	-42.86	0.156	-13.26	Lys 194	4	17.13	4.49×10^{-04}	1.31×10^{-04}
	6	120	261	-13.12	0.061	-3.50	Lys 194	1	18.17	2.81×10^{-04}	8.58×10^{-05}
	7	80	131	-17.03	0.082	5.46	Phe 354	-3	50.07	1.64×10^{-10}	4.25×10^{-05}
	8	80	131	-36.32	0.068	11.54	Phe 354	-3	50.07	1.64×10^{-10}	2.01×10^{-05}
	9	80	131	-53.43	0.133	14.16	Phe 354	-3	50.07	1.64×10^{-10}	1.08×10^{-05}

This is because a good orientation for the transfer of electrons is not necessary a good orientation for the adsorption of the protein. Also, it is necessary consider that the total current is result of the contribution of all the possible orientations for a determinate combination of experimental variables.

In order to structure the presentation of findings and enhance readability for the reader, the document initially outlines the impact of the experimental factors, such as ionic strength, electric potential, and pH, on interaction energy. Subsequently, it delves into another section to examine the outcomes related to total current and the influence of protein adsorption on total current.

The results obtained in this research, if well in most of the calculations were not obtained favorable results for the adsorption for the protein. The author considers important report them for future consulting. The results of each combination of experimental variables in figures divided in panels, showing the results as a two-dimensional heatmaps as a function of the tilt (θ) and azimuthal (φ) angles.

The results illustrate the absorption energies [panel (a)], the Boltzmann probabilities [panel (b)], the probability*current [panel (c)], and the orientation with the highest probability of occurrence [panel (d)].

The results of the currents of all the experimental combinations are shown in Figure 6. Note that the results of this figure are identical for all the calculations, this is because the electron transfer rate, as explained in equation (26) depends on the electrode-cluster distance, and the orientations tested are the same for all the calculations. Is for that reason that this panel is presented only in the Figure 6 and deleted to avoid repetition in the subsequent figures.

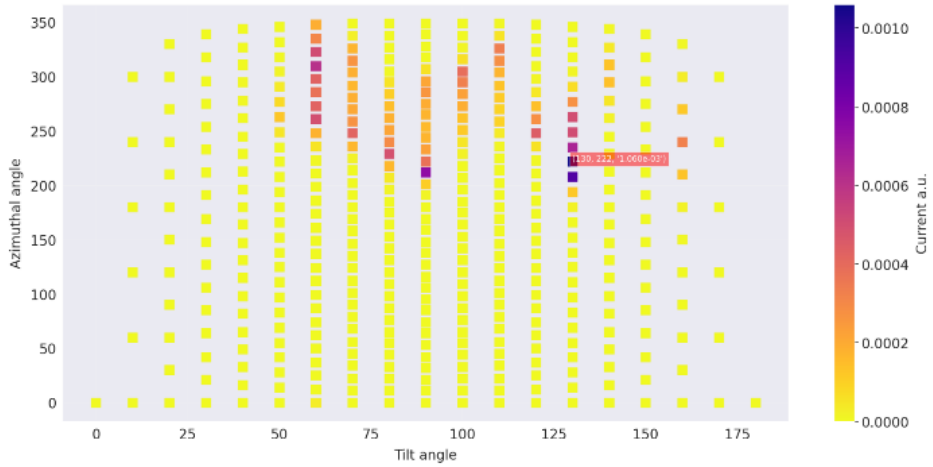

Figure 6. *Heatmap of the electron transfer rate (current, measured in arbitrary units).*

The heatmap of the electron transfer rate shows that the orientation with the highest current is the orientation (θ=130°, φ=222°). This happens because this is the orientation where the external iron-sulfur cluster is closest to the surface of the electrode. Together with this orientation, there are another six among the closest orientations in the columns 120°-130° of the tilt angle.

In the heatmap, it is possible to appreciate a shape of "S" with the orientations colored with current values over 0.0004 (in arbitrary units). This is originated because these ordinations are in the face of the protein where the external iron-sulfur cluster is located.

4.1.1 Results of the computational simulation with the combination of variables of pH=5, electric potential 0.0 V, ionic strength 0.15 M (code: 1e3d_5_0.0_salt)

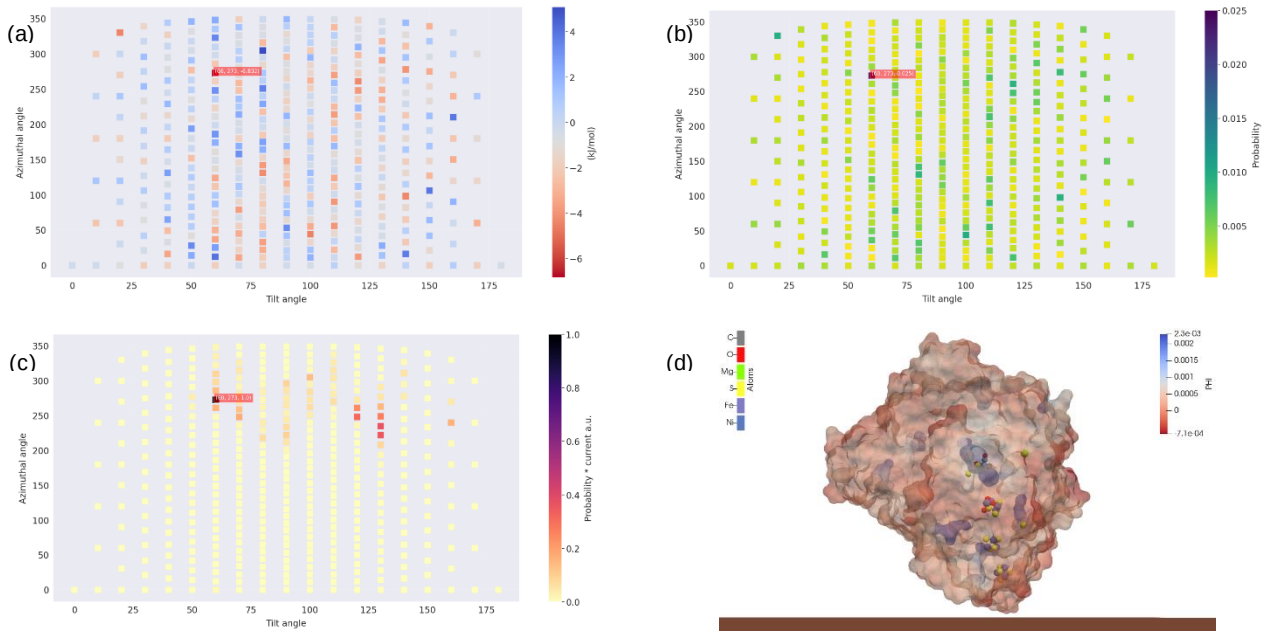

Figure 7. *Heatmaps of the results of the combination of variables of pH=5, 0.15 M of NaCl, 0.0 V of electric potential applied on the electrode.*

The image is divided in interaction energies [panel (a)], the Boltzmann probabilities [panel (b)], and the electron transfer rates [panel (c)]. Panel (d) in the figure, displays the orientation with the lowest interaction energy obtained. In the panel is possible to observe the surface of the hydrogenase (1e3d) colored with the values of the electrostatic potential calculated by PyGBe, and the atoms of the catalytic center and the iron-sulfur cluster, colored with the next pattern: gray (carbon), red (oxygen), green (magnesium), yellow (sulfur), purple (iron), and navy blue (nickel).

In Figure 7, the panel (a) shows a uniform distribution in the values of the interaction energy, this indicates that there is not a dominant orientation in which the protein prefers to be adsorbed. This result is confirmed for the distribution of the Boltzmann probabilities panel (b), in this case the orientation with the lowest energy (60 θ, 273 φ), is the orientation with the highest probability of occur, however its probability is very low (0.025).

In this orientation, the amino acid Asp 197 was the closest to the

surface of the electrode, and the distance from the iron atom bonded to cysteine of the external iron-sulfur cluster was 17.26 Å.

With the combination of probabilities and currents, shown in panel (c) it is possible to indicate the contribution to the total current of each orientation. This is important because if one orientation is good for the transfer of electrons and has a very low probability, it will have a very low contribution to the total current.

In panel (c) is possible to appreciate that there is a small group of orientations in the column of 60 tilt angle with high contribution to the total current. However, the orientation with the highest probability of occur with the combinations of experimental variables panel (d) is not between these orientations.

4.1.2 Results of the computational simulation with the combination of variables of pH=5, electric potential 0.0 V, ionic strength 0.0 M (Code: 1e3d_5_0.0_water)

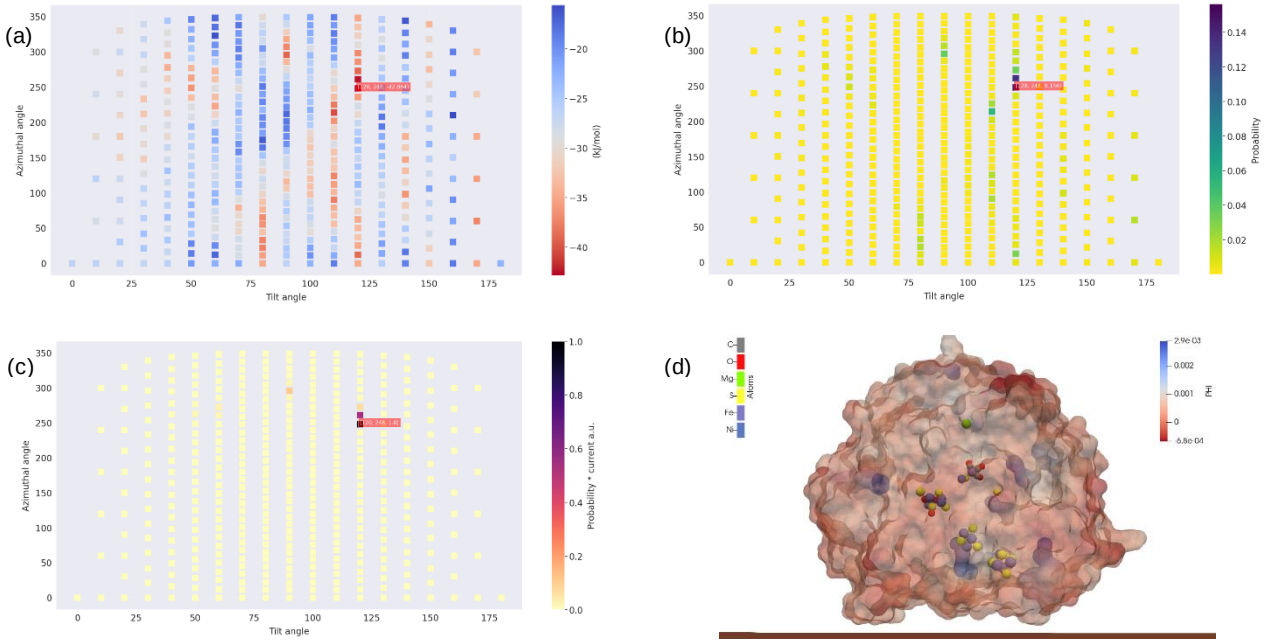

Figure 8. *Heatmaps of the results of the combination of variables of pH=5, 0.0 M of NaCl, 0.0 V of electric potential applied on the electrode.*

The image is divided in interaction energies [panel (a)], the Boltzmann probabilities [panel (b)], and the electron transfer rates [panel (c)]. Panel (d) in the figure, displays the orientation with the lowest interaction energy obtained. In the panel is possible to observe the surface of the hydrogenase (1e3d) colored with the values of the electrostatic potential calculated by PyGBe, and the atoms of the catalytic center and the iron-sulfur cluster, colored with the next pattern: gray (carbon), red (oxygen), green (magnesium), yellow (sulfur), purple (iron), and navy blue (nickel).

In this combination of experimental factors Figure 8, there was not an orientation dominating the interaction energy (panel a) and Boltzmann probabilities (panel b) for that reason the distribution for probabilities was uniform, however in the column of 60 of tilt angle is possible to observe a group of orientations with higher probabilities, this column is the same for the heatmap of the combination of probabilities and current (panel c), the orientation with the highest probability of occur is shown in (panel d), (120 θ, 248 φ) with a probability of 0.156.

In this orientation, the amino acid Lys 194 was the closest amino acid to the surface of the electrode and the distance from the iron atom bonded to cysteine of the external iron-sulfur cluster to the electrode was 17.13 Å.

4.1.3 Results of the computational simulation with the combination of variables of pH=5, electric potential 0.05 V, ionic strength 0.15 M (Code: 1e3d_5_0.05_salt)

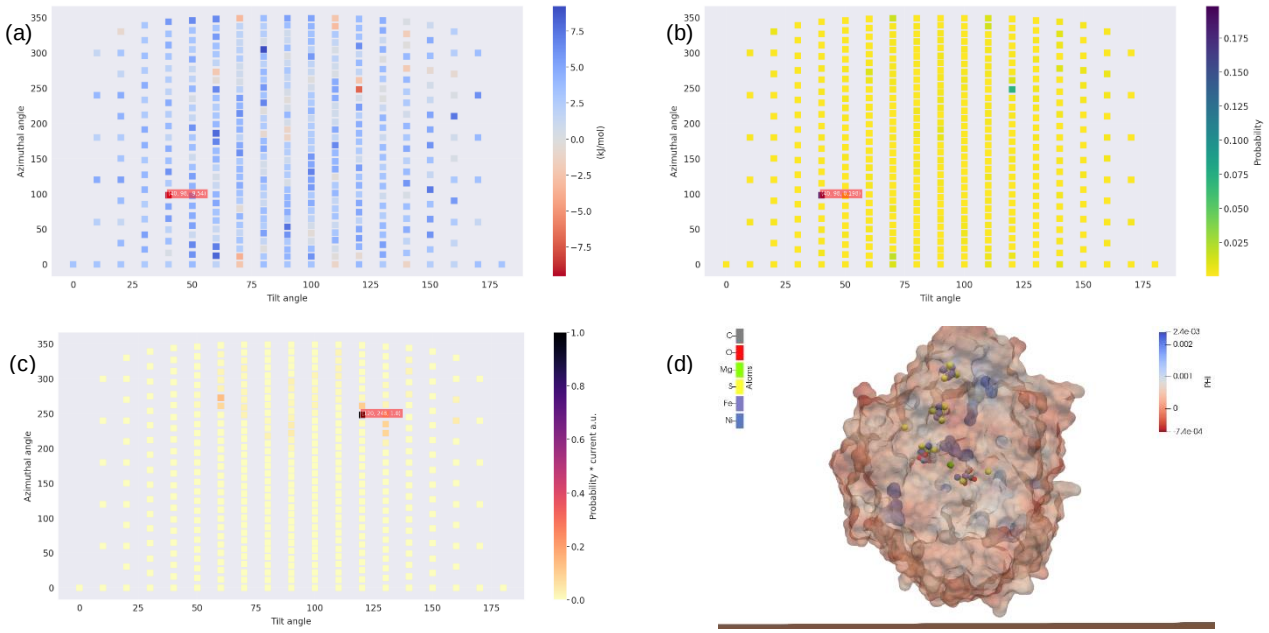

Figure 9. *Heatmaps of the results of the combination of variables of pH=5, 0.15 M of NaCl, 0.5 V of electric potential applied on the electrode.*

The image is divided in interaction energies [panel (a)], the Boltzmann probabilities [panel (b)], and the electron transfer rates [panel (c)]. Panel (d) in the figure, displays the orientation with the lowest interaction energy obtained. In the panel is possible to observe the surface of the hydrogenase (1e3d) colored with the values of the electrostatic potential calculated by PyGBe, and the atoms of the catalytic center and the iron-sulfur cluster, colored with the next pattern: gray (carbon), red (oxygen), green (magnesium), yellow (sulfur), purple (iron), and navy blue (nickel).

With Figure 9, again there was not a dominant orientation and the distribution of the interaction energies (panel a) was uniform, this has an impact in the Boltzmann probabilities (panel b) where there was not a dominant orientation, the heatmap of total current (panel c) shows the orientation (120 θ, 248 φ) as the one that more contributes to the current, however this orientation (panel d) place the external iron-sulfur cluster very far from the electrode.

The orientation with the highest probability (40 θ, 90 φ) had a value

of 0.198, in this orientation the amino acid Lys 139 was the closest amino acid to the surface of the electrode and the distance from the iron atom bonded to cysteine of the external iron-sulfur cluster to the electrode was 66.82 Å.

4.1.4 Results of the computational simulation with the combination of variables of pH=5, electric potential -0.05 V, ionic strength 0.15 M (Code: 1e3d_5_-0.05_salt)

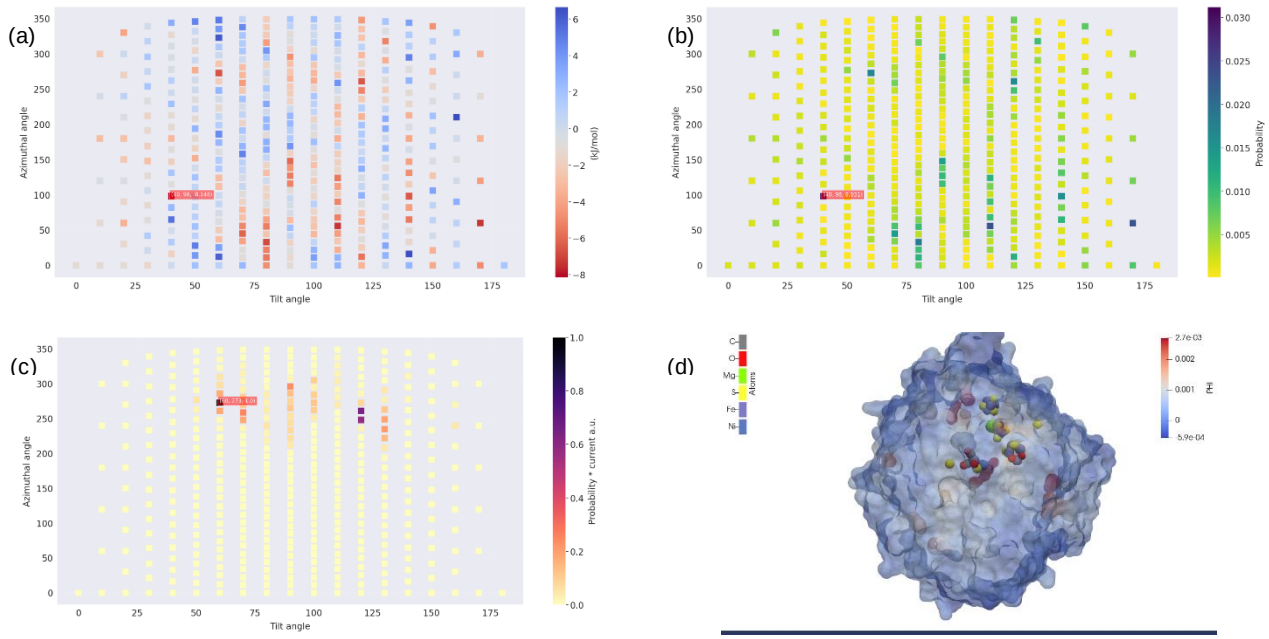

Figure 10. *Heatmaps of the results of the combination of variables of pH=5, 0.15 M of NaCl, -0.05 V of electric potential applied on the electrode.*

The image is divided in interaction energies [panel (a)], the Boltzmann probabilities [panel (b)], and the electron transfer rates [panel (c)]. Panel (d) in the figure, displays the orientation with the lowest interaction energy obtained. In the panel is possible to observe the surface of the hydrogenase (1e3d) colored with the values of the electrostatic potential calculated by PyGBe, and the atoms of the catalytic center and the iron-sulfur cluster, colored with the next pattern: gray (carbon), red (oxygen), green (magnesium), yellow (sulfur), purple (iron), and navy blue (nickel).

Here Figure 10, again there was not a dominant orientation and the distribution of the interaction energies (panel a) was uniform, this has an impact in the Boltzmann probabilities (panel b) where there was not a dominant orientation, the heatmap of current (panel c) shows that the orientation (60 θ, 273 φ) as the one that more contributes to the total current, however this orientation (panel d) place the external iron-sulfur cluster very far from the electrode.

The Boltzmann probability associated to the orientation (40 θ, 98 φ)

is 0.031, in this orientation the amino acid Lys 139 was the closest amino acid to the surface of the electrode, and the distance from the iron atom bonded to cysteine of the external iron-sulfur cluster was 66.82 Å.

4.1.5 Results of the computational simulation with the combination of variables of pH=6, electric potential 0.0 V, ionic strength 0.0 M (Code: 1e3d_6_0.0_salt)

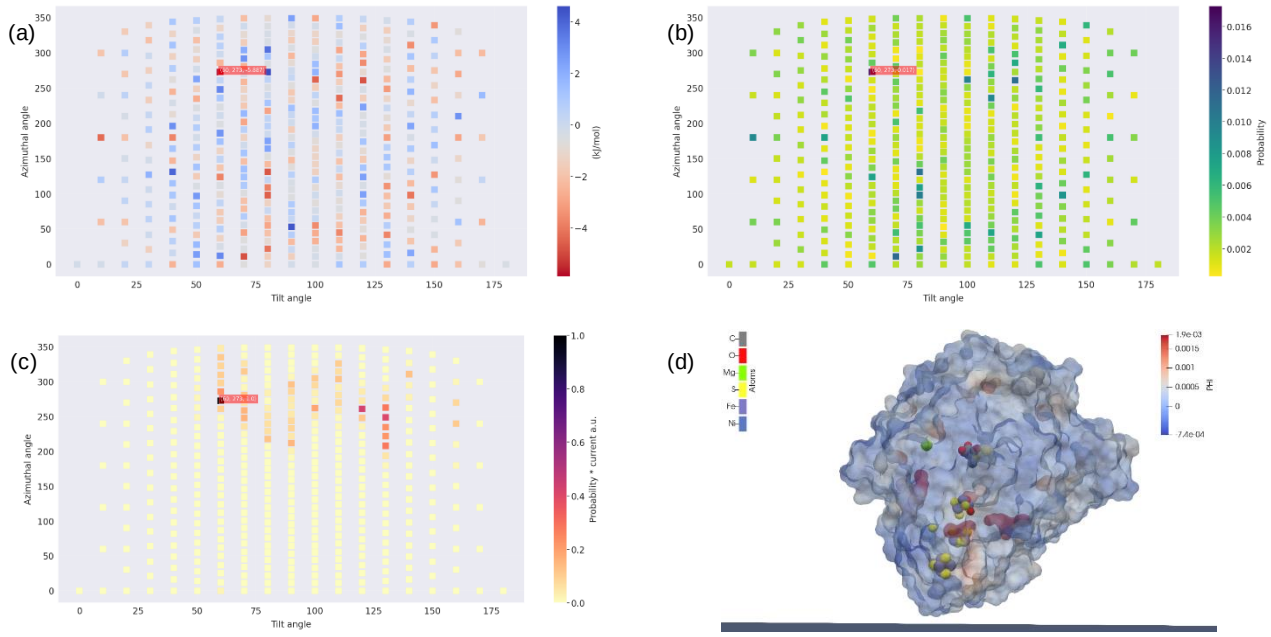

Figure 11. *Heatmaps of the results of the combination of variables of pH=6, 0.15 M of NaCl, 0.0 V of electric potential applied on the electrode.*

The image is divided in interaction energies [panel (a)], the Boltzmann probabilities [panel (b)], and the electron transfer rates [panel (c)]. Panel (d) in the figure, displays the orientation with the lowest interaction energy obtained. In the panel is possible to observe the surface of the hydrogenase (1e3d) colored with the values of the electrostatic potential calculated by PyGBe, and the atoms of the catalytic center and the iron-sulfur cluster, colored with the next pattern: gray (carbon), red (oxygen), green (magnesium), yellow (sulfur), purple (iron), and navy blue (nickel).

For this combination of experimental variables in Figure 11, the distribution of the interaction energies (panel a) and the Boltzmann probabilities (panel b) were homogenous, without an orientation dominating over the rest. The combination of current and probabilities (panel c) shows that in the column of the tilt angle 60 there is an orientation with high contribution to the total current, this orientation (panel d) has the external iron-sulfur cluster close to the surface of the electrode favoring the transfer of electrons.

The Boltzmann probability associated to the orientation (60 θ, 273 φ) is 0.017, in this orientation the amino acid Asp 197 was the closest amino acid to the surface of the electrode and the distance from the iron atoms bonded to cysteine of the external iron-sulfur cluster to the electrode was 17.26 Å.

4.1.6 Results of the computational simulation with the combination of variables of pH=6, electric potential 0.0 V, ionic strength 0.0 M (Code: 1e3d_6_0.0_water)

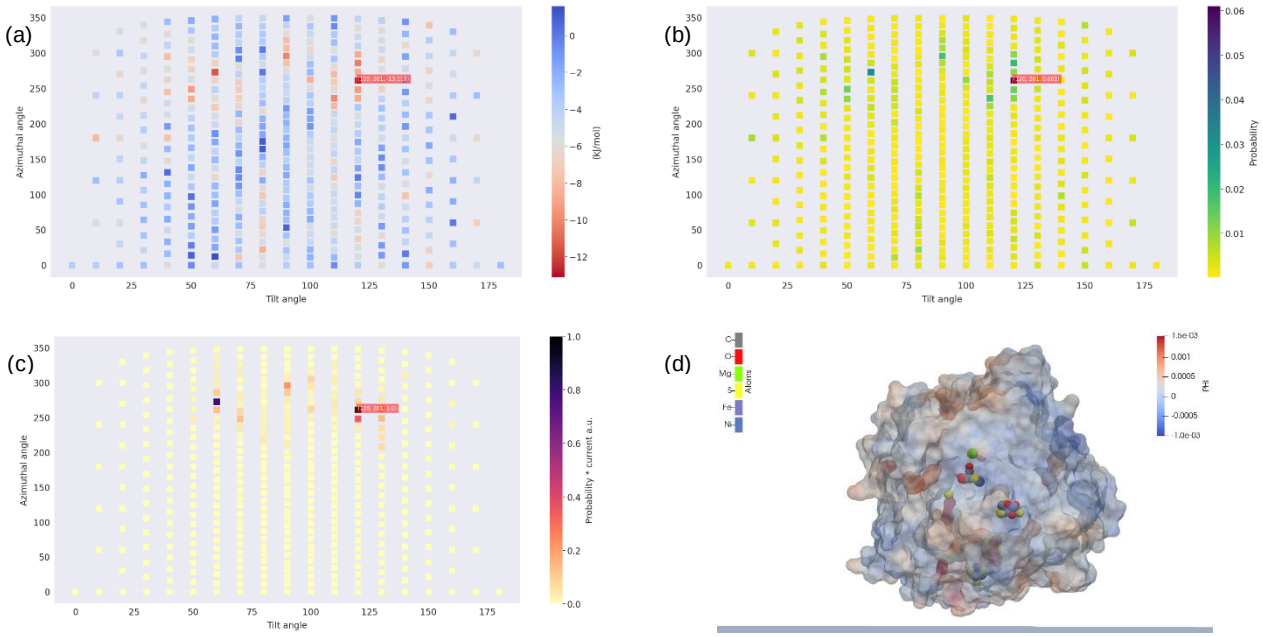

Figure 12. *Heatmaps of the results of the combination of variables of pH=6, 0.0 M of NaCl, 0.0 V of electric potential applied on the electrode.*

The image is divided in interaction energies [panel (a)], the Boltzmann probabilities [panel (b)], and the electron transfer rates [panel (c)]. Panel (d) in the figure, displays the orientation with the lowest interaction energy obtained. In the panel is possible to observe the surface of the hydrogenase (1e3d) colored with the values of the electrostatic potential calculated by PyGBe, and the atoms of the catalytic center and the iron-sulfur cluster, colored with the next pattern: gray (carbon), red (oxygen), green (magnesium), yellow (sulfur), purple (iron), and navy blue (nickel).

For this combination of experimental variables in Figure 12, there is homogeneity in the interaction energies (panel a), however is possible to appreciate a group of orientations in the column 120 (tilt angle) where the interaction energy is lower than in the rest

of the orientations, the same column presents the orientation with higher probability (panel b), in the combination of probabilities and current (panel c), there were two groups in the column 60 and in the column and 120 (tilt angle). The panel (d) shows the orientation with the lowest value of interaction energy. It has a good orientation to favor the transfer of

electrons.

The Boltzmann probability associated to the orientation (120 θ, 261 φ) is 0.061, in this orientation the amino acid Lys 194 was the closest amino acid to the surface of the electrode and the distance from the iron atom bonded to cysteine of the external iron-sulfur cluster to the electrode was 18.17 Å.

4.1.7 Results of the computational simulation with the combination of variables of pH=6, electric potential 0.05 V, ionic strength 0.15 M (Code: 1e3d_6_0.05_salt)

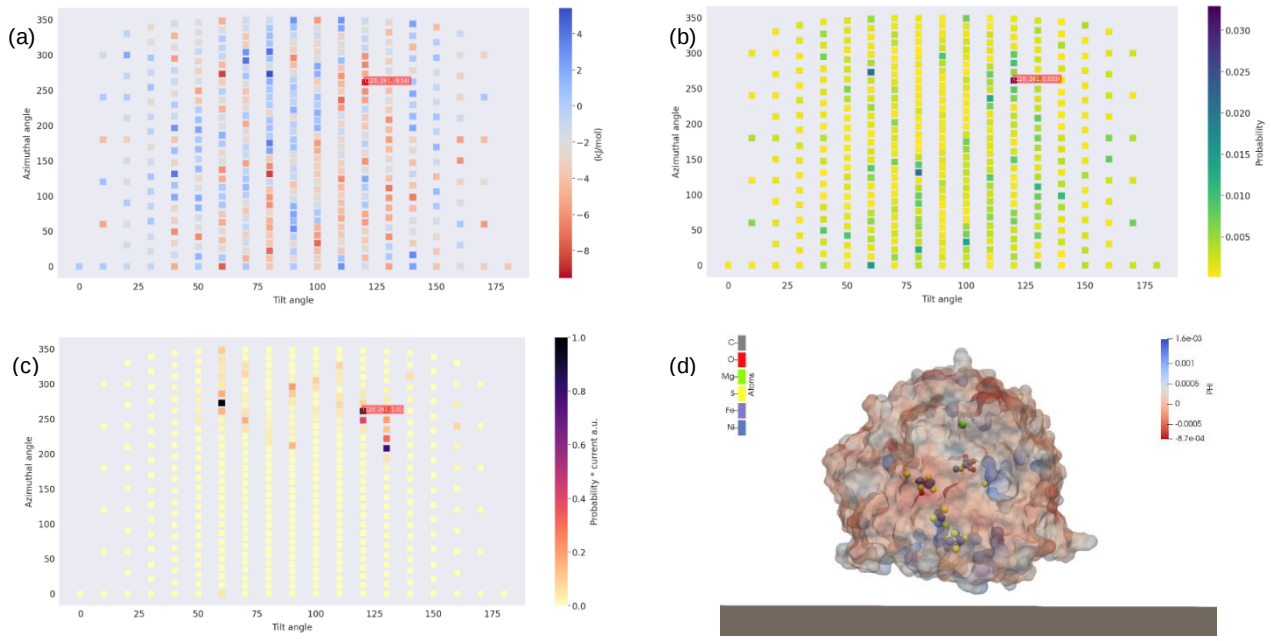

Figure 13. *Heatmaps of the results of the combination of variables of pH=6, 0.15 M of NaCl, 0.05 V of electric potential applied on the electrode.*

The image is divided in interaction energies [panel (a)], the Boltzmann probabilities [panel (b)], and the electron transfer rates [panel (c)]. Panel (d) in the figure, displays the orientation with the lowest interaction energy obtained. In the panel is possible to observe the surface of the hydrogenase (1e3d) colored with the values of the electrostatic potential calculated by PyGBe, and the atoms of the catalytic center and the iron-sulfur cluster, colored with the next pattern: gray (carbon), red (oxygen), green (magnesium), yellow (sulfur), purple (iron), and navy blue (nickel).

In this experimental combination (Figure 13) the heatmap plots shows homogeneity in the interaction energy (panel a) and the Boltzmann probabilities (panel b), the orientation with the lowest energy (120 θ, 261 φ) had a high contribution in the heatmap of probability*current (panel c), this orientation had an orientation that could favor the electrons transfer (panel d).

The Boltzmann probability associated to this orientation (120 θ,

261 φ) is 0.033, in these orientations the amino acid Lys 194 was the closest amino acid to the surface of the electrode and the distance from the iron atom bonded to cysteine of the external iron-sulfur cluster to the electrode was 18.17 Å.

4.1.8 Results of the computational simulation with the combination of variables of pH=6, electric potential -0.05 V, ionic strength 0.15 M (Code: 1e3d_6_-0.05_salt)

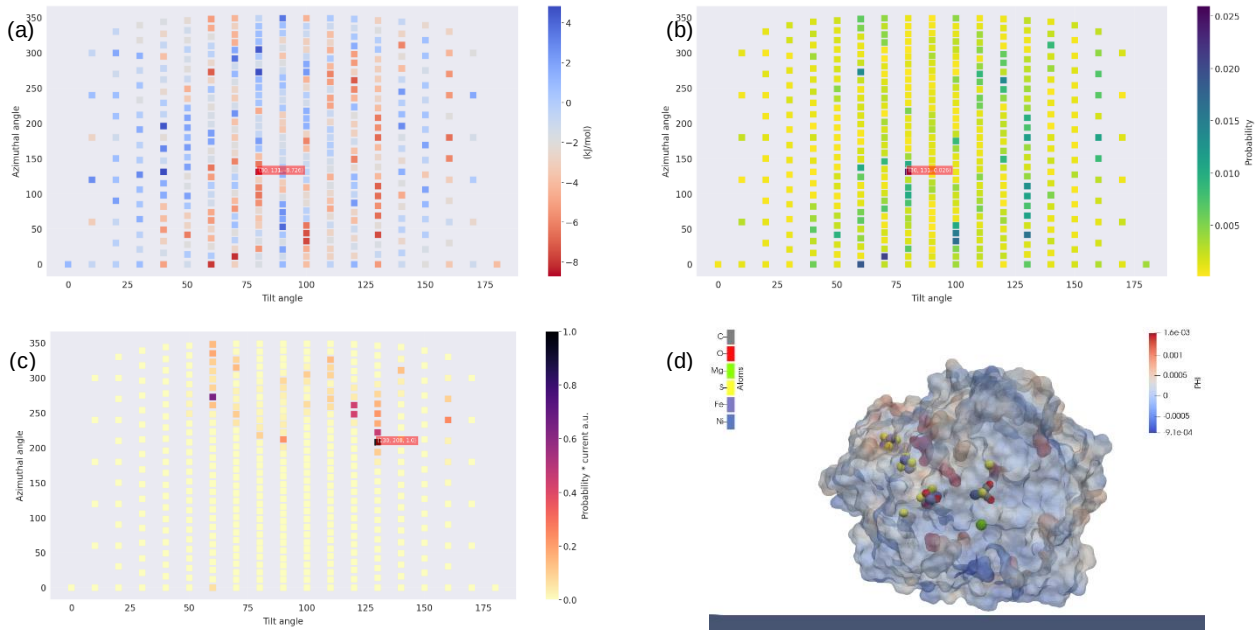

***Figure 14**. Heatmaps of the results of the combination of variables of pH=6, 0.15 M of NaCl, -0.05 V of electric potential applied on the electrode.*

The image is divided in interaction energies [panel (a)], the Boltzmann probabilities [panel (b)], and the electron transfer rates [panel (c)]. Panel (d) in the figure, displays the orientation with the lowest interaction energy obtained. In the panel is possible to observe the surface of the hydrogenase (1e3d) colored with the values of the electrostatic potential calculated by PyGBe, and the atoms of the catalytic center and the iron-sulfur cluster, colored with the next pattern: gray (carbon), red (oxygen), green (magnesium), yellow (sulfur), purple (iron), and navy blue (nickel).

In Figure 14 is illustrated a combination of experimental variables that shows a homogeneity in the interaction energies (panel a) and Boltzmann probabilities (panel b), however it is possible to appreciate a diagonal line ascending between the columns of 50 and 125 tilt angle with orientations with low energies and relative high probabilities. In panel (c), the combination of probability and current shows a group of orientations that contributes more that the rest of the orientations in the column 130 of the tilt angle, however these orientations have the external iron-sulfur cluster

far from the electrode making difficult the transfer of electrons. The orientation with the highest probability of occurrence (90 θ, 131 φ) had a probability of 0.033 and is shown in panel (d) this orientation is favorable for the transfer of electrons.

In this orientation the amino acid Lys 194 was the closest amino acid to the surface of the electrode and the distance from the iron atom bonded to cysteine of the external iron-sulfur cluster and the electrode was 18.17 Å.

4.1.9 Results of the computational simulation with the combination of variables of pH=7, electric potential 0.0 V, ionic strength 0.15 M (Code: 1e3d_7_0.0_salt)

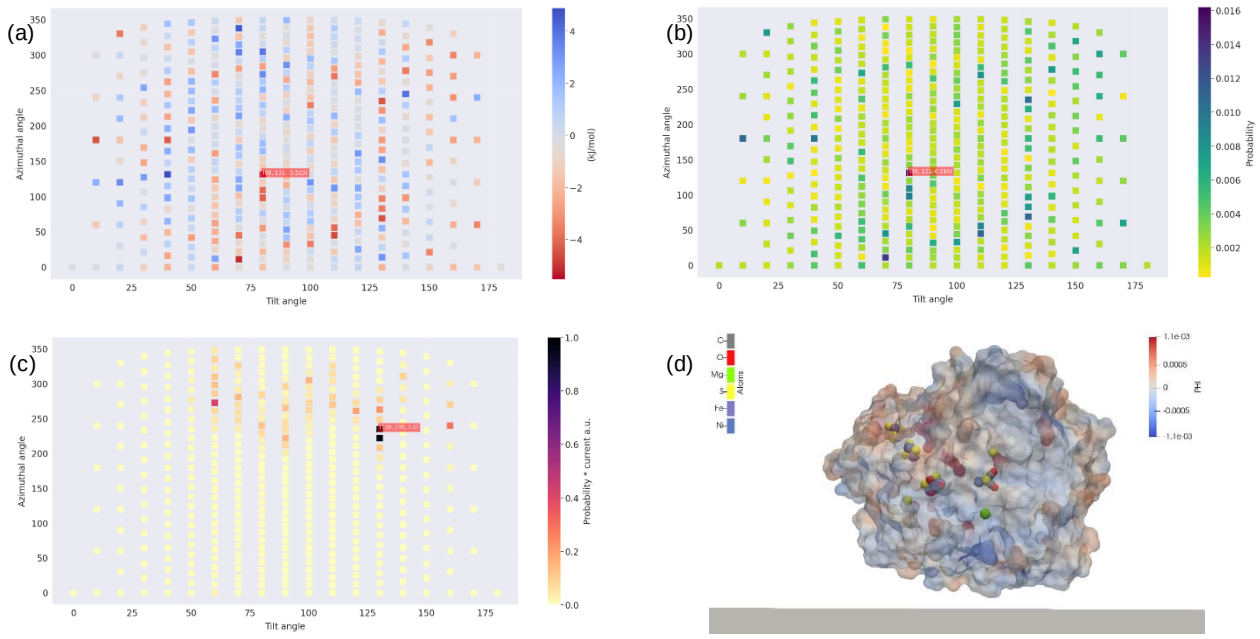

Figure 15. *Heatmaps of the results of the combination of variables of pH=7, 0.15 M of NaCl, 0.0 V of electric potential applied on the electrode.*

The image is divided in interaction energies [panel (a)], the Boltzmann probabilities [panel (b)], and the electron transfer rates [panel (c)]. Panel (d) in the figure, displays the orientation with the lowest interaction energy obtained. In the panel is possible to observe the surface of the hydrogenase (1e3d) colored with the values of the electrostatic potential calculated by PyGBe, and the atoms of the catalytic center and the iron-sulfur cluster, colored with the next pattern: gray (carbon), red (oxygen), green (magnesium), yellow (sulfur), purple (iron), and navy blue (nickel).

In Figure 15, the heatmap plots of the interaction energy (panel a) and Boltzmann distributions (panel b) show homogeneity, but it is possible to appreciate a diagonal line in the orientations with low interaction energy and high probabilities between the columns 60 and 130 (tilt angle). In fact, two orientations have a high contribution to the total current, which is appreciated in the heatmap of probability*current (panel c). The orientation with the lowest interaction energy (panel d) had a not favorable position for electron transfer.

The Boltzmann probability associated to this orientation (80 θ, 133 φ) is 0.016, in this orientation the amino acid Phe 354 was the closest amino acid to the surface of the electrode and the distance from the iron atom bonded to cysteine of the external iron-sulfur cluster to the electrode was 50.07 Å.

4.1.10 Results of the computational simulation with the combination of variables of pH=7, electric potential 0.0 V, ionic strength 0.0 M (Code: 1e3d_7_0.0_water)

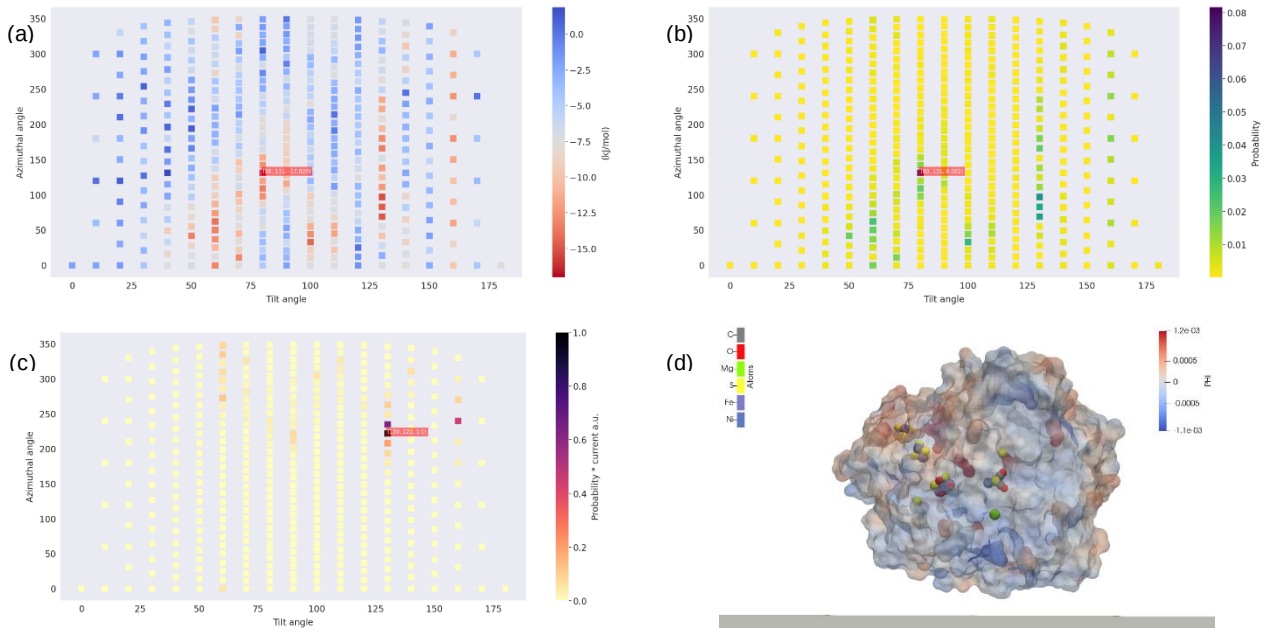

Figure 16. *Heatmaps of the results of the combination of variables of pH=7, 0.0 M of NaCl, 0.0 V of electric potential applied on the electrode.*

The image is divided in interaction energies [panel (a)], the Boltzmann probabilities [panel (b)], and the electron transfer rates [panel (c)]. Panel (d) in the figure, displays the orientation with the lowest interaction energy obtained. In the panel is possible to observe the surface of the hydrogenase (1e3d) colored with the values of the electrostatic potential calculated by PyGBe, and the atoms of the catalytic center and the iron-sulfur cluster, colored with the next pattern: gray (carbon), red (oxygen), green (magnesium), yellow (sulfur), purple (iron), and navy blue (nickel).

In Figure 16, the heatmaps of the interaction energies (panel a) and the Boltzmann probabilities (panel b) is possible to appreciate two groups of orientations ascending diagonally, the first one between the columns 50 to 80 and between 100 to 140 (tilt angles). The orientations that more contribute to the total current (panel c) were located in the column 130. However, the orientation with the lowest energy (panel d) does not favor the transfer of electrons.

The probability associated to this orientation (80 θ, 131 φ) is 0.016,

in this orientation the amino acid Phe 354 was the closest amino acid to the surface of the electrode and the distance from the iron atom bonded to cysteine of the external iron-sulfur cluster to the electrode was 50.07 Å.

4.1.11 Results of the computational simulation with the combination of variables of pH=7, electric potential 0.05 V, ionic strength 0.15 M (Code: 1e3d_7_0.05_salt)

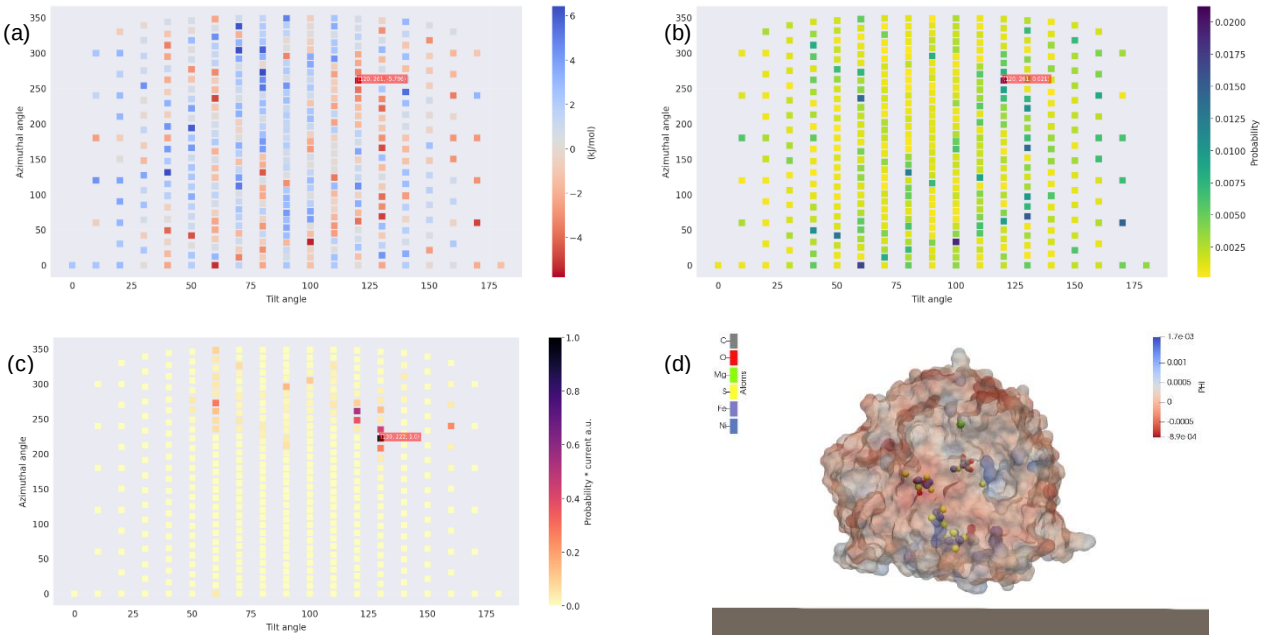

Figure 17. *Heatmaps of the results of the combination of variables of pH=7, 0.15 M of NaCl, 0.05 V of electric potential applied on the electrode.*

The image is divided in interaction energies [panel (a)], the Boltzmann probabilities [panel (b)], and the electron transfer rates [panel (c)]. Panel (d) in the figure, displays the orientation with the lowest interaction energy obtained. In the panel is possible to observe the surface of the hydrogenase (1e3d) colored with the values of the electrostatic potential calculated by PyGBe, and the atoms of the catalytic center and the iron-sulfur cluster, colored with the next pattern: gray (carbon), red (oxygen), green (magnesium), yellow (sulfur), purple (iron), and navy blue (nickel).

In Figure 17, there is homogeneity in the results of interaction energy (panel a) and Boltzmann distribution (panel b). However, it is possible to appreciate a group of orientations with relatively high probabilities between the columns 120 and 130 (tilt angle). In this last column, it is possible to find the orientation that more contribute to the total current (panel c), and is the orientation with highest probability (panel d) of occur, this orientation has a good orientation to favor the electron transfer.

The Boltzmann probability associated to this orientation (80 θ, 131 φ) is 0.021, in this orientation the amino acid Lys 194 was the closest amino acid to the surface of the electrode and the distance from the iron atom bonded to cysteine of the external iron-sulfur cluster to the electrode was 18.17 Å.

4.1.12 Results of the computational simulation with the combination of variables of pH=7, electric potential -0.05 V, ionic strength 0.15 M (Code: 1e3d_7_-0.05_salt)

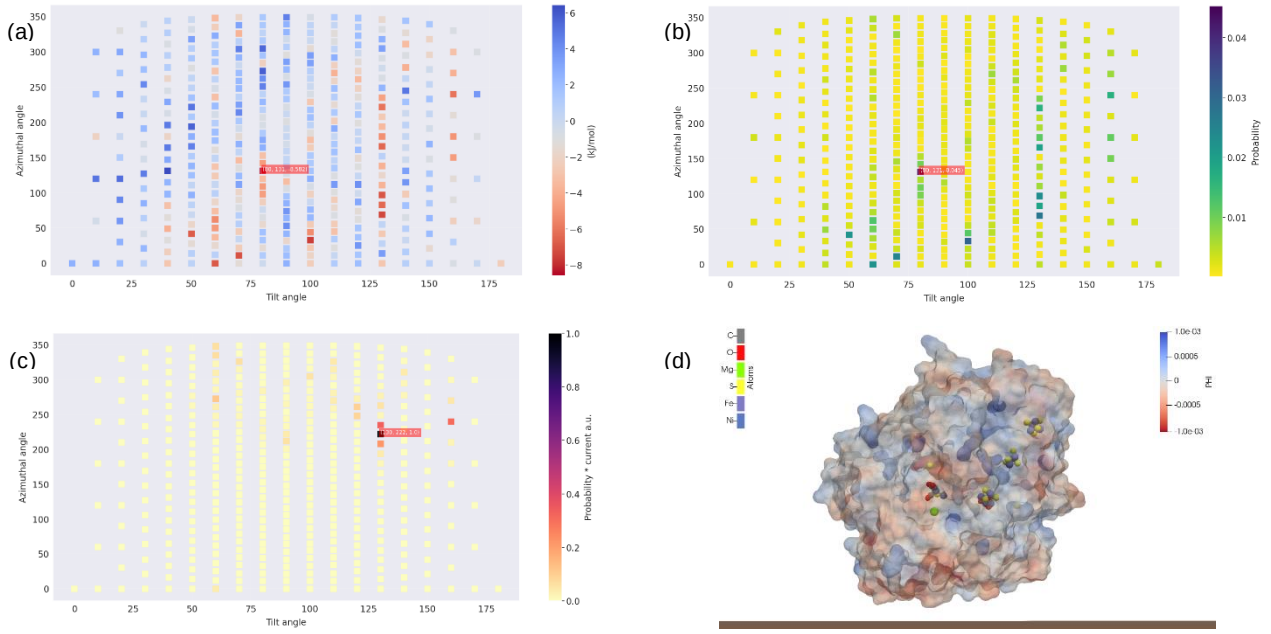

Figure 18. *Heatmaps of the results of the combination of variables of pH=7, 0.15 M of NaCl, -0.05 V of electric potential applied on the electrode.*

The image is divided in interaction energies [panel (a)], the Boltzmann probabilities [panel (b)], and the electron transfer rates [panel (c)]. Panel (d) in the figure, displays the orientation with the lowest interaction energy obtained. In the panel is possible to observe the surface of the hydrogenase (1e3d) colored with the values of the electrostatic potential calculated by PyGBe, and the atoms of the catalytic center and the iron-sulfur cluster, colored with the next pattern: gray (carbon), red (oxygen), green (magnesium), yellow (sulfur), purple (iron), and navy blue (nickel).

Figure 18 shows the results of this combination of experimental variables, is presented homogeneity in the results of interaction energy (panel a) and Boltzmann probabilities (panel b). However, there is a group of orientations forming a diagonal ascending line between the columns 50 - 140 (tilt angle). In the column 130 are placed the orientations that more contributes to the total current (panel c). The orientation most probable to occur (panel d), place the external iron-sulfur cluster in a position not favorable for transfer electrons.

The Boltzmann probability associated to this orientation (80 θ, 131 φ) is 0.045, in these orientations the amino acid Phe 354 was the closest amino acid to the surface of the electrode and the distance from the iron atoms bonded to cysteine of the external iron-sulfur cluster to the electrode was 50.07 Å.

4.1.13 Results of the computational simulation with the combination of variables of pH=8, electric potential 0.0 V, ionic strength 0.15 M (Code: 1e3d_8_0.0_salt)

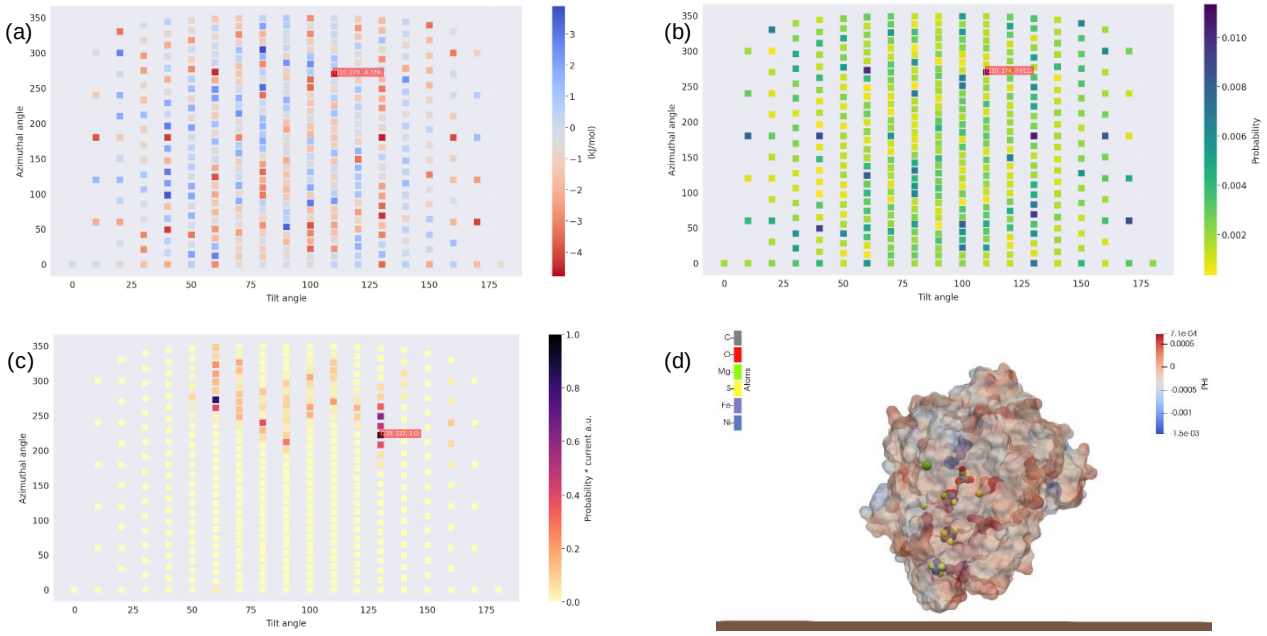

Figure 19. *Heatmaps of the results of the combination of variables of pH=8, 0.15 M of NaCl, 0.0 V of electric potential applied on the electrode.*

The image is divided in interaction energies [panel (a)], the Boltzmann probabilities [panel (b)], and the electron transfer rates [panel (c)]. Panel (d) in the figure, displays the orientation with the lowest interaction energy obtained. In the panel is possible to observe the surface of the hydrogenase (1e3d) colored with the values of the electrostatic potential calculated by PyGBe, and the atoms of the catalytic center and the iron-sulfur cluster, colored with the next pattern: gray (carbon), red (oxygen), green (magnesium), yellow (sulfur), purple (iron), and navy blue (nickel).

In this Figure (19) for the combination of experimental variables, the results of interaction energies (panel a) and Boltzmann probabilities (panel b) have a homogeneous distribution, without any pattern appreciable. However, there is a group of orientations in the column 130, that have a high contribution in the total current (panel c), in this group is the orientation with the lowest energy (panel d) with an orientation that favor the transfer of electrons.

The Boltzmann probability associated to this orientation (110 θ,

270 φ) is 0.011, in this orientation the amino acid Ala 198 was the closest amino acid to the surface of the electrode and the distance from the iron atom bonded to cysteine of the external iron-sulfur cluster to the electrode was 20.58 Å.

4.1.14 Results of the computational simulation with the combination of variables of pH=8, electric potential 0.0 V, ionic strength 0.0 M (Code: 1e3d_8_0.0_water)

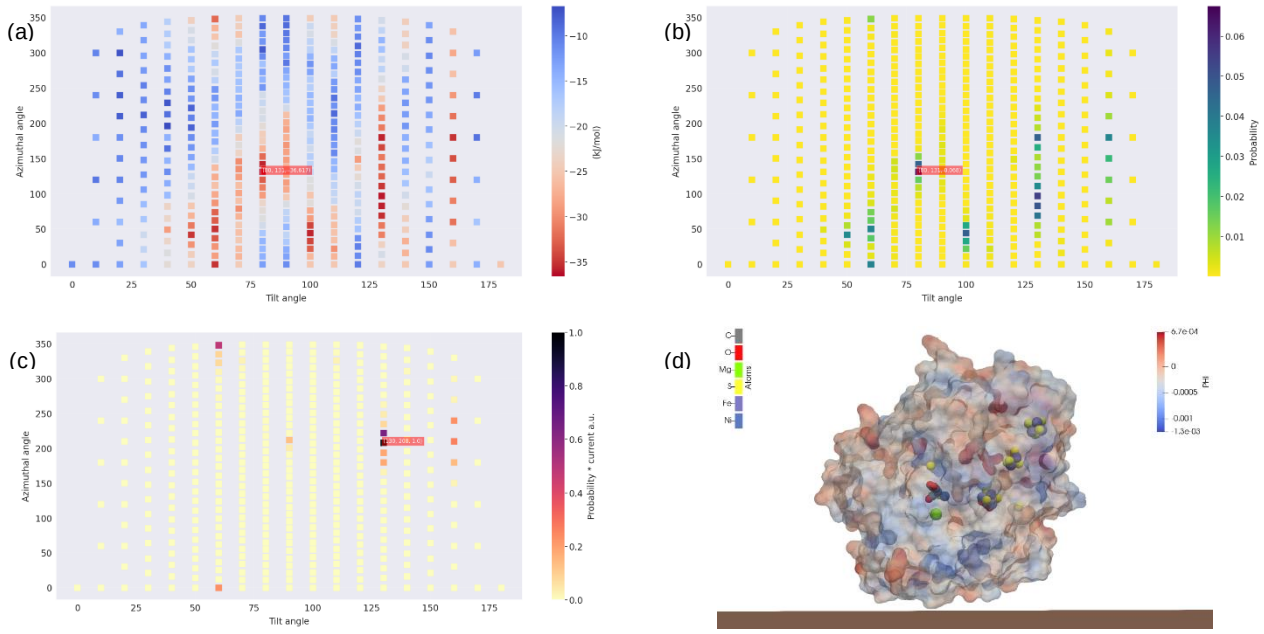

Figure 20. *Heatmaps of the results of the combination of variables of pH=8, 0.0 M of NaCl, 0.0 V of electric potential applied on the electrode.*

The image is divided in interaction energies [panel (a)], the Boltzmann probabilities [panel (b)], and the electron transfer rates [panel (c)]. Panel (d) in the figure, displays the orientation with the lowest interaction energy obtained. In the panel is possible to observe the surface of the hydrogenase (1e3d) colored with the values of the electrostatic potential calculated by PyGBe, and the atoms of the catalytic center and the iron-sulfur cluster, colored with the next pattern: gray (carbon), red (oxygen), green (magnesium), yellow (sulfur), purple (iron), and navy blue (nickel).

In this Figure 20, for the combination of experimental variables, it is possible to observe patterns in the results of interactions energies (panel a) and Boltzmann distributions (panel b), two groups of orientations are formed between the columns of 40-90 and 100 -130 (tilt angle). However, the probabilities associated with these orientations, if well appreciable, are not very high. The orientation that more contribute to the total current (panel d) was in the column of 130, but the orientation with higher probability of occur (panel d) did not happen in this angle, and the position of external iron-sulfur cluster do not favor the transfer of electrons.

The Boltzmann probability associated to this orientation (80 θ, 131 φ) is 0.068, in this orientation the amino acid Phe 354 was the closest amino acid to the surface of the electrode and the distance from the iron atom bonded to cysteine of the external iron-sulfur cluster to the electrode was 50.07 Å.

4.1.15 Results of the computational simulation with the combination of variables of pH=8, electric potential 0.05 V, ionic strength 0.15 M (Code: 1e3d_8_0.05_salt)

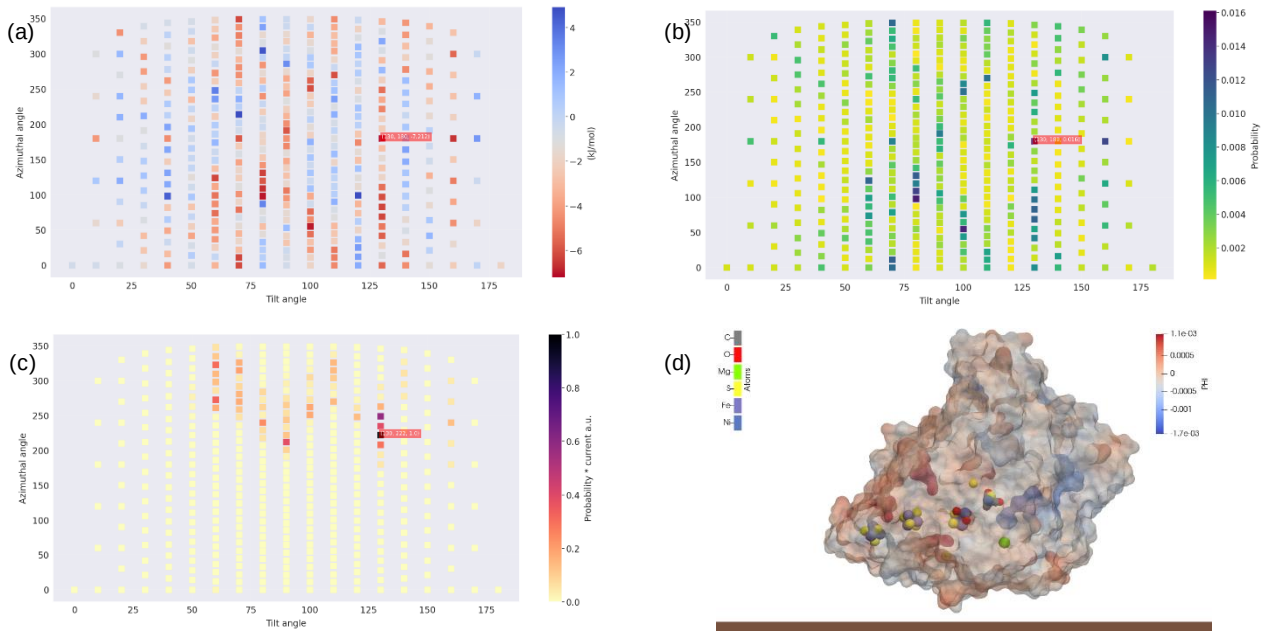

Figure 21. *Heatmaps of the results of the combination of variables of pH=8, 0.15 M of NaCl, 0.05 V of electric potential applied on the electrode.*

The image is divided in interaction energies [panel (a)], the Boltzmann probabilities [panel (b)], and the electron transfer rates [panel (c)]. Panel (d) in the figure, displays the orientation with the lowest interaction energy obtained. In the panel is possible to observe the surface of the hydrogenase (1e3d) colored with the values of the electrostatic potential calculated by PyGBe, and the atoms of the catalytic center and the iron-sulfur cluster, colored with the next pattern: gray (carbon), red (oxygen), green (magnesium), yellow (sulfur), purple (iron), and navy blue (nickel).

This combination of experimental variables in Figure 21 shows uniformity in the results of interaction energy (panel a) and Boltzmann probabilities (panel b), the heatmap of probabilities*current (panel c), the column 130 have a group of orientations that contribute to the total current, the orientation with the higher probability (panel d) have the irons-sulfur clusters aligned parallel to the surface of the electrode which could not favor the transfer of electrons.

The Boltzmann probability associated to this orientation (130 θ, 180 φ) is 0.016, in this orientation the amino acid Asp 480 was the closest amino acid to the surface of the electrode and the distance from the iron atom bonded to cysteine of the external iron-sulfur cluster to the electrode was 24.18 Å.

4.1.16 Results of the computational simulation with the combination of variables of pH=8, electric potential -0.05 V, ionic strength 0.15 M (Code: 1e3d_8_-0.05_salt)

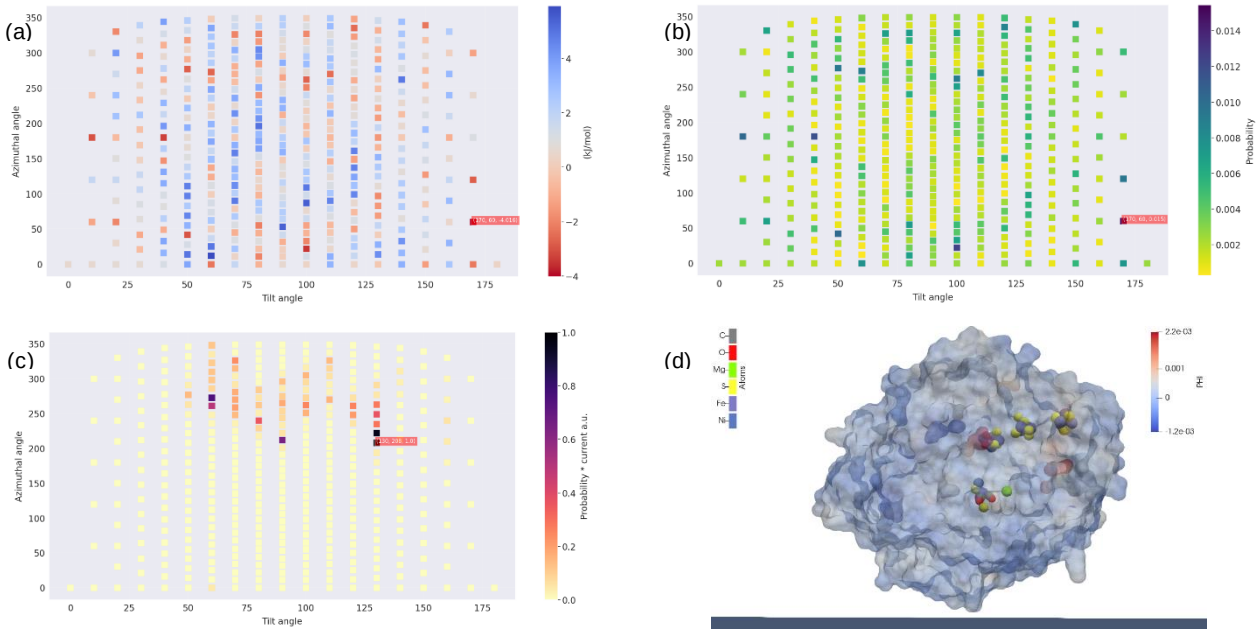

Figure 22. *Heatmaps of the results of the combination of variables of pH=8, 0.15 M of NaCl, -0.05 V of electric potential applied on the electrode.*

The image is divided in interaction energies [panel (a)], the Boltzmann probabilities [panel (b)], and the electron transfer rates [panel (c)]. Panel (d) in the figure, displays the orientation with the lowest interaction energy obtained. In the panel is possible to observe the surface of the hydrogenase (1e3d) colored with the values of the electrostatic potential calculated by PyGBe, and the atoms of the catalytic center and the iron-sulfur cluster, colored with the next pattern: gray (carbon), red (oxygen), green (magnesium), yellow (sulfur), purple (iron), and navy blue (nickel).

With this combination of experimental variables in Figure 22 there is homogeneity in the results of interaction energy (panel a) and Boltzmann probabilities (panel b), the orientations that contributes more to the total current (panel c) are more present in the column 130, however the most probable orientation to occur (panel d) has the iron-sulfur clusters placed horizontal regarding the surface of electrode, and the orientation is not favorable for transfer electrons.

The Boltzmann probability associated to this orientation (170 θ, 60 φ)

is 0.015, in this orientation the amino acid Phe 354 was the closest amino acid to the surface of the electrode and the distance from the iron atom bonded to cysteine of the external iron-sulfur cluster to the electrode was 48.14 Å.

4.1.17 Results of the computational simulation with the combination of variables of pH=9, electric potential 0.0 V, ionic strength 0.15 M (Code: 1e3d_9_0.0_salt)

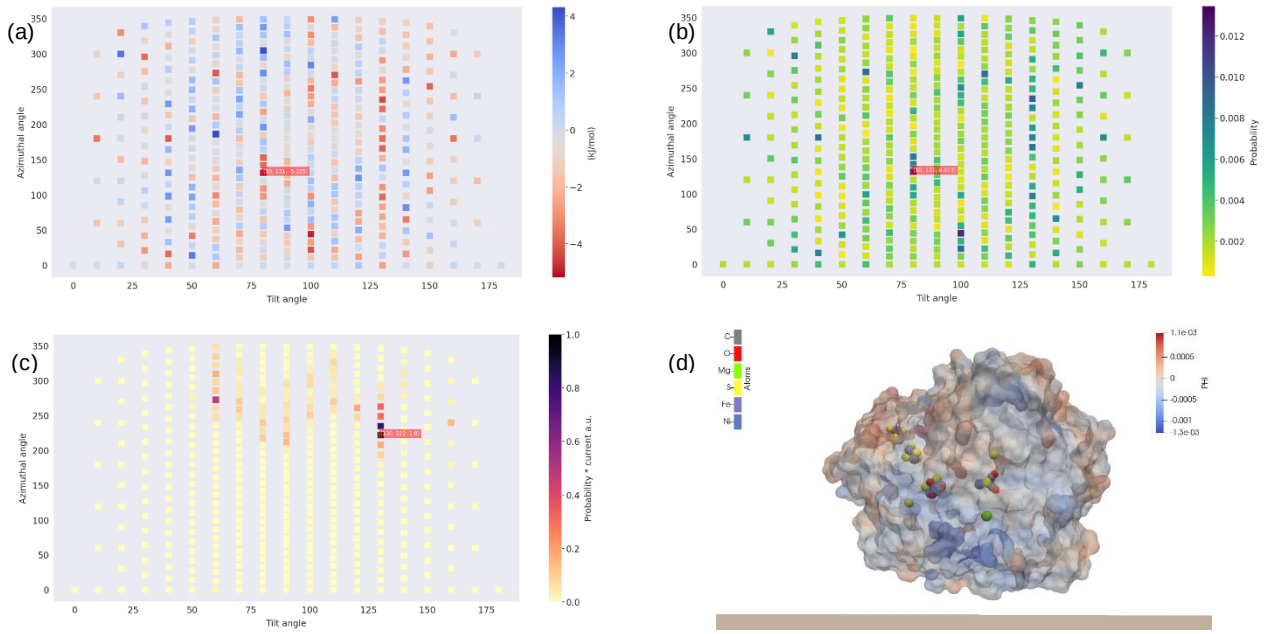

Figure 23. *Heatmaps of the results of the combination of variables of pH=9, 0.15 M of NaCl, 0.0 V of electric potential applied on the electrode.*

The image is divided in interaction energies [panel (a)], the Boltzmann probabilities [panel (b)], and the electron transfer rates [panel (c)]. Panel (d) in the figure, displays the orientation with the lowest interaction energy obtained. In the panel is possible to observe the surface of the hydrogenase (1e3d) colored with the values of the electrostatic potential calculated by PyGBe, and the atoms of the catalytic center and the iron-sulfur cluster, colored with the next pattern: gray (carbon), red (oxygen), green (magnesium), yellow (sulfur), purple (iron), and navy blue (nickel).

The results of these combinations of variables in Figure 23 shows homogeneity in the heatmap lots of interaction energy (panel a) and Boltzmann probabilities (panel b), without dominant orientations. The total current (panel c) is determinate for a group of orientations in the column 130 (tilt angle), the orientation most probable to occur (panel d) is not favorable for the transfer of electrons.

The Boltzmann probability associated to the orientation with the highest probability (80 θ, 131 φ) is 0.013, in this orientation the amino

acid Phe 354 was the closest amino acid to the surface of the electrode and the distance from the iron atom bonded to cysteine of the external iron-sulfur cluster to the electrode was 50.07 Å.

4.1.18 Results of the computational simulation with the combination of variables of pH=9, electric potential 0.0 V, ionic strength 0.0 M (Code: 1e3d_9_0.0_water)

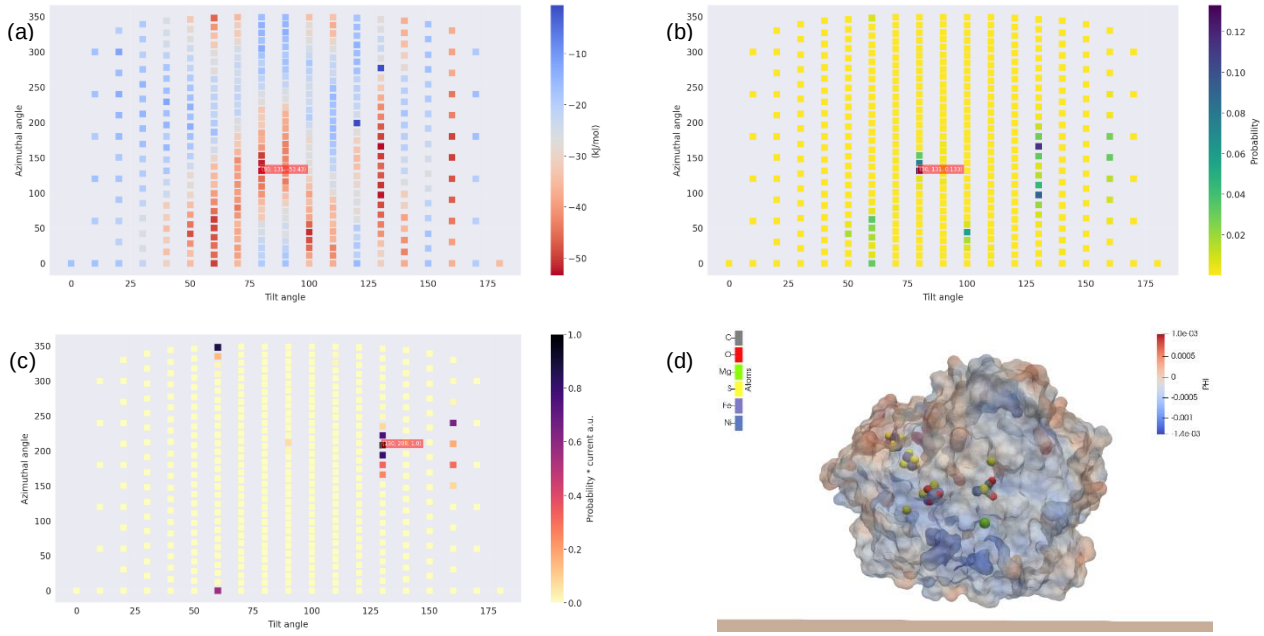

Figure 24. *Heatmaps of the results of the combination of variables of pH=9, 0.0 M of NaCl, 0.0 V of electric potential applied on the electrode.*

The image is divided in interaction energies [panel (a)], the Boltzmann probabilities [panel (b)], and the electron transfer rates [panel (c)]. Panel (d) in the figure, displays the orientation with the lowest interaction energy obtained. In the panel is possible to observe the surface of the hydrogenase (1e3d) colored with the values of the electrostatic potential calculated by PyGBe, and the atoms of the catalytic center and the iron-sulfur cluster, colored with the next pattern: gray (carbon), red (oxygen), green (magnesium), yellow (sulfur), purple (iron), and navy blue (nickel).

These combinations of experimental variables in Figure 24 have a patter in the distribution of the results in the interaction energies (panel a) and the Boltzmann probabilities (panel b), there are two groups between the columns 40-90 y 100-140 of the tilt angle, these orientations have relative high probabilities compared to the rest of the orientations, the group of orientation in the column 140 also have a noticeable contribution to the total current (panel c), however the orientation most probable to occur (panel d) has not favored position for electrons transfer.

The Boltzmann probability associated to this orientation (80 θ, 131 φ) is 0.133, in this orientation the amino acid Phe 354 was the closest amino acid to the surface of the electrode and the distance from the iron atom bonded to cysteine of the external iron-sulfur cluster to the electrode was 50.07 Å.

4.1.19 Results of the computational simulation with the combination of variables of pH=9, electric potential 0.05 V, ionic strength 0.15 M (Code: 1e3d_9_0.05_salt)

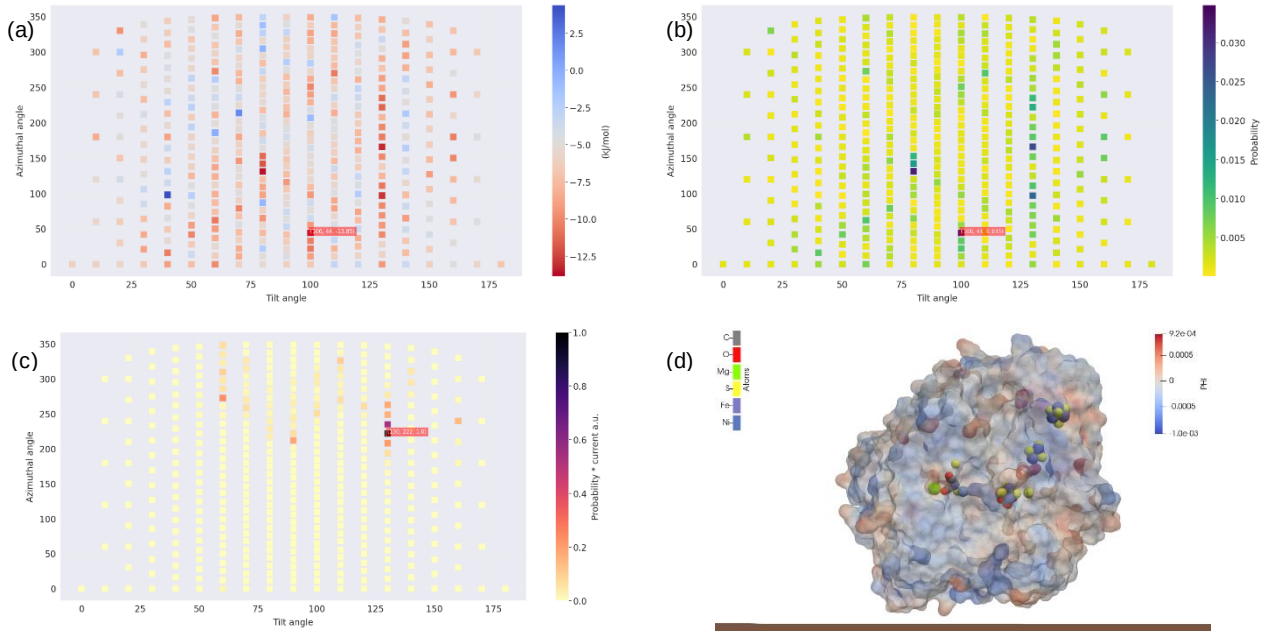

Figure 25. *Heatmaps of the results of the combination of variables of pH=9, 0.15 M of NaCl, 0.05 V of electric potential applied on the electrode.*

The image is divided in interaction energies [panel (a)], the Boltzmann probabilities [panel (b)], and the electron transfer rates [panel (c)]. Panel (d) in the figure, displays the orientation with the lowest interaction energy obtained. In the panel is possible to observe the surface of the hydrogenase (1e3d) colored with the values of the electrostatic potential calculated by PyGBe, and the atoms of the catalytic center and the iron-sulfur cluster, colored with the next pattern: gray (carbon), red (oxygen), green (magnesium), yellow (sulfur), purple (iron), and navy blue (nickel).

Here in Figure 25 there is homogeneity in the heatmap plots of the interaction energies (panel a) and Boltzmann probabilities (panel b), and there are not dominant orientations, with the total current (panel c) the orientations with more contribution are in the column 130 (tilt angle), this is because the orientations in these angles have a position close to the surface of the electrode. The orientations with the highest probability (panel d) have a not favorable orientations for electron transfer.

The Boltzmann probability associated with the highest probability

orientation (100 θ, 44 φ) is 0.035, in this orientation the amino acid Thr12 was the closest amino acid to the surface of the electrode and the distance from the iron atom bonded to cysteine of the external iron-sulfur cluster to the electrode was 51.57 Å.

4.1.20 Results of the computational simulation with the combination of variables of pH=9, electric potential -0.05 V, ionic strength 0.15 M (Code: 1e3d_9_-0.05_salt)

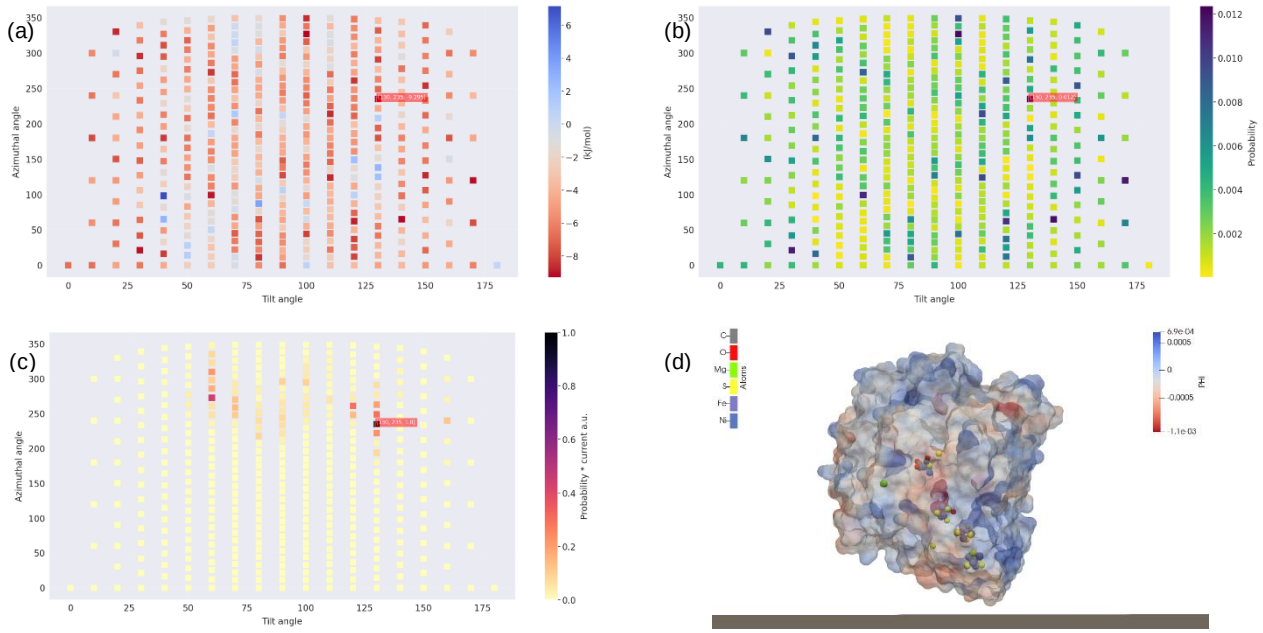

Figure 26. *Heatmaps of the results of the combination of variables of pH=9, 0.15 M of NaCl, -0.05 V of electric potential applied on the electrode.*

The image is divided in interaction energies [panel (a)], the Boltzmann probabilities [panel (b)], and the electron transfer rates [panel (c)]. Panel (d) in the figure, displays the orientation with the lowest interaction energy obtained. In the panel is possible to observe the surface of the hydrogenase (1e3d) colored with the values of the electrostatic potential calculated by PyGBe, and the atoms of the catalytic center and the iron-sulfur cluster, colored with the next pattern: gray (carbon), red (oxygen), green (magnesium), yellow (sulfur), purple (iron), and navy blue (nickel).

This combination of experimental factors in Figure 26 do not shows a dominant orientation in the interaction energies (panel a) and Boltzmann probabilities (panel b), the orientations that more contributes to the total current (panel c) are on the column 130 (tilt angle), the orientation with the highest probability (panel d) have an orientation that favor the electron transfer.

The Boltzmann probability associated to this orientation (130 θ, 235 φ) is 0.012, in this orientation the amino acid Asp 197 was the

closest amino acid to the surface of the electrode and the distance from the iron atoms bonded to cysteine of the external iron-sulfur cluster to the electrode was 16.28 Å.

4.1.21 Results of the orientations with the lowest interaction energies

The results of the orientations with the lowest interaction energies and their probabilities associated are summarized in Table 2. According to equations (10) and (11), the probabilities are normalized by summing over all θ and φ angles (for given pH, ϕ_e and *I*).

It is possible to say that a negative value in the interaction energy indicates that the protein is adsorbed on the surface of the electrode in a stable state.

According to the results shown in Table 2 the ionic strength appears to be the most important variable that determinate the adsorption of the protein on the surface of the electrode. This is mostly lower than 10 kJ mol^{-1} in the presence of salt (with only one exception, for ϕ_e=+0.05V at pH=9), but it ranges between 13 and 53 kJ mol^{-1} in the salt-free cases.

In order to structure the presentation of findings and enhance readability for the reader, the document initially outlines the impact of the experimental factors, such as ionic strength, electric potential, and pH, on interaction energy. Subsequently, it delves into another section to examine the outcomes related to total current and the influence of protein adsorption on total current.

4.1 Ionic strength effect

Comparing the orientations by its ionic strength, it is possible to separate them in two groups 0.15 M and 0.0 M of NaCl concentration the comparison between the groups Table 2 shows that the presence of salt in the solution decrees the interaction energy

The effect of the ionic strength on the interaction energies can be explained due to the screening effect of the dissolved ions on electrostatic interactions. In general, the salt-free solutions are the ones that produce the strongest absorption of the hydrogenase. Some studies have reported similar behavior, where the amount of adsorbed proteins on charged surfaces decreases as the ionic strength increases [42, 84-88].

Small concentrations of salt could be necessary in order to have a functional hydrogen electrolyzer with electrodes covered with adsorbed hydrogenases. Due to work under salt-free or salt-poor conditions could reduce the electrical conductivity of the solution and the flux of electrons to the enzyme.

However, some conditions where is possible to obtain a good adsorption could not be appropriate for a functional protein, because conditions such as salt-free or salt-poor conditions could reduce the electrical conductivity of the solution, affecting the catalytic activity of the enzyme and the stability of the protein. Nonetheless, even if the salt free case could be not realistic from the physiology point of view, it is interesting because it sets an upper limit to the strength and to the spatial range of the electrostatic interactions that could be expected.

4.2 Electric potential effect

Three groups of electric potential of 0.05, 0.0 and -0.05 V were modeled for the experimental conditions. Comparing the results in Table 2 reveals that while the interaction energy is generally unaffected by the presence of an electric potential, the orientation of the protein was affected by the sign of the applied electric potential, suggesting that the orientation of the protein may be controlled by the applied electric potential.

Before discussion our results of the effect of the electrode's potential, we summarize some key concepts and findings from the literature.

It has been claimed that when the electrostatic interaction is the main factor that determines the adsorption of a protein on a charged surface, two mechanisms can be responsible for such interaction and may affect or modulate it. The first one is charge regulation (CR). This mechanism consists in that the charge of the protein changes due to the influence of the charges on the surface. The second mechanism is the charge patches (CP). In this case, the protein is oriented toward a charged surface due to a concentration of amino acids with opposite sign to the charge of the surface.

In the charge regulation mechanism, the presence of a charged surface induces a charge of opposite sign on the protein by displacing the charge of all the amino acids of the protein, and in this way favoring its adsorption [39, 89, 90].

In the mechanism of charge patches, some regions of the proteins have amino acids with the same charge. These charged zones can allow the attachment of a protein to a surface with an opposite sign [39].

Placing the protein near a highly charged surface will modify the pKa of the amino acids close to it, whereby the protein tends to maximize the number of oppositely charged amino acids next to the surface [89, 90].

The dipole moment has been used to explain the orientation of the protein on a surface. However, the dipole is a very rough descriptor of the electrostatic properties of a protein. Charged patches are also related to the distribution of the protein and can give a more precise description and explanation of the orientation of a protein on a surface [38].

The charge regulation mechanism has been predicted theoretically and confirmed experimentally [86, 87] in different systems, and it is responsible for the change of pKa of free amino acids when they are in solution to a very different value when they are inside of a protein [88, 91]. However, it is necessary to note that our PyGBe calculations do not include charge regulation. The charges of the aminoacids are fixed (at a certain pH) and they do not depend on the orientation/position with respect to the surface.

Electrostatic interactions can favor the absorption of proteins at their isoelectric points when they are placed on charged surfaces, even if the protein by itself does not have a net charge in a solution.

On a charged surface, a protein will preferentially be adsorbed with its dipole moment orthogonal to the surface. However, the dipole moment only provides a raw approximation of the orientation of the protein.

This suggests that the position of an adsorbed protein on a charged surface will be oriented towards the charges of the opposite sign. In fact, the electrostatic interaction between the protein and a conducting surface can be predicted using the dipole moment of the protein in solution (without the actual electrode), possibly indicating the hypothetical orientation through molecular dynamics simulations [38].

However, other studies have shown that protein adsorption can happen in modified surfaces even if the charges of the protein and the surface have the same sign. These cases demonstrate that the orientation of the protein can be determined by the presence of groups of amino acids “patches” that interact with the surface of the electrode, favoring some orientations over others [84-86, 92, 93].

A detailed analysis of the absorption for the protein is discussed in the work of Boubeta *et al.* [39], they reported the interaction of Lysozyme (IEP: 11.2) with a negatively charged surface. Under these conditions, the protein had an orientation with minimal energy.

In this orientation, the amino acids Arg114, Arg125, Arg128, Arg5, and Lys1 of the Lysozyme were the closest amino acids to the surface of the electrode and were almost fully dissociated, for that reason these were the amino acids that more contribute the surface attraction.

Other amino acids that were almost fully dissociated were Arg45 and Arg112, but they were far from the surface.

It is necessary to mention that during the protein adsorption on negatively charged surfaces, the charge of the surface inhibits the dissociation of the negative amino acids and enhances the ionization of positive amino acids.

The charge regulation mechanism can increase the net charge of a protein, which favor the protein adsorption. However, to understand the effect of the charge regulation, it is necessary to consider the effect of the charged surface and its interactions with the amino acids that conforms the protein.

Notably Lys33 in Lysozyme, is very close to the surface of the electrode and its degree of ionization for pH = IEP change from weak dissociation at (f = 0.09) in solution, to strong dissociated (f = 0.72) under the influence of the charged surface.

Another interesting studies with which is possible to compare the results of this work are those obtained from molecular dynamic computational simulations in the literature, which modeled the adsorption of Lysozyme on negatively charged surfaces at pH 7 [94, 95] and 8 [96].

According to their results, regarding the effect of the potential applied on the electrode, it is possible to assume that the adsorption of the protein will be favored on a surface with an opposite signal to the net charge of the protein.

However, this assumption could fall in an over simplification mistake because several studies have shown that even surfaces with the same signal of the charges of the protein can be adsorbed, due between several other factors to a concentration of amino acids with the opposite charge in specific areas of the protein (i.e., by CP-type mechanism) [84-86, 93, 97].

Indeed, it was found in the results of table 2 that the electrostatic potential on the electrode affects the minimum-energy orientation of the protein, but it does not produce a large change in the overall adsorption energy.

These results obtained show that the changes are difficult to interpret, because there is not an observable pattern in all the cases.

For example, at the pH=8 the orientation (θ_{min},φ_{min}) angles appear systematic when the potential changes from -0.05 V to +0.05 V, indicating a re-orientation of the protein due to the potential.

The energy change $|\Delta E_{min}|$ changes by a relatively small amount, from 5 to 7 kJ mol^{-1}. Considering that the protein has a change of -12.4e and the overall charge on the electrode changes from -360e to +361e, which could made expect to have bigger difference in energies.

One possible explanation for this observation is given for the charge on the electrode is actually distributed, being roughly proportional to its size and the electrode compared to the size of the protein is too big implying a large overall charge, but this does not automatically translate into a strong local interaction.

It is possible to use the case when the total charge on the electrode is ϕ_e=0.00 V, as a function of pH and ionic strength. In this case as the protein is placed at a distance from the electrode, the total charge tends to zero.

It could be expected that when the protein approaches the electrode, it induces a negative charge on the surface of the electrode. When the total charge of the protein is positive, for example, in conditions where the environment has acidic pH, in this case when the electrode is negative, the protein will be positively charged (at basic pH, see Table 1).

It is possible that this effect will be strongest in salt-free cases due to that the induced charge on the electrode compensates almost exactly the total charge of the protein (about $\pm$15 at pH=5 and 8), resulting in an electrically neutral electrode-protein complex.

However, it was not possible to include the contribution of the CR mechanism in our calculations, because the model used in PyGBe assumes that the atomic charges of the atoms of the protein are fixed and do not change dynamically changing depending of its orientation and distance from the electrode.

Nonetheless, even if was not possible to calculate the contribution of the CP mechanism to the total energy, it was considered its effect.

For each orientation, the closest amino acid to the electrode surface was identified and the total charge for the ten closest amino acids was calculated.

The data of the charge of the amino acids is given in Table 2. One recurring orientation θ=80° and φ=131° has the amino acid Phe 354 closest to the surface of the electrode. An amino acid that has the characteristic of be electrically neutral and non-polar. However, if we consider the group of the 10 closest amino acids, we find a value of -3*e*,

at any pH≥6, for this group. This could explain the recurrence of this particular orientation within the table (7 instances out of 24).

A second orientation with a large charge of the patch (+4*e*) is observed pH=5 in pure water (Figure 8). In this case the closest amino acid is a positively charged Lys 194, and the absorption energy is relatively large (-42 kJ/mol).

Interestingly, this is the closest amino acid also at pH=6, with a slightly different orientation. However, now the overall charge of the patch is only +1 (that of Lys itself), and consequently the value of the absorption energy is significantly smaller (-13 kJ/mol).

Despite, at pH=6 (Figure 12), it was found the same amino acid with a similar orientation, but the overall charge of the ten closest amino acids was only +1 and consequently the value of the absorption energy was significantly smaller (-13 kJ/mol).

It is necessary to mention that the presence of the amino acid Lys close to the electrode occurs also in other orientations of Table 2, suggesting that this amino acid could be important for achieving a good absorption on the electrode.

The probabilities of the minimum-energy orientations are summarized in Table 2, the probabilities associated to obtain these orientations are in general low with values less than 0.1. These results suggest that is not possible to obtain stable orientation adsorbed on the surface of the electrode, the heatmaps of the probabilities for the combination of factors also indicate that there is not another group of orientations dominating the probabilities suggesting that there is an equilibrium between all the orientations and they are slightly different in energy.

There are only three entries in the Table 2 where P_{min}>0.1. Two of them occur in the salt-free cases, where the ten closest amino acids have

a big charge that could favor a strong adsorption. The third case occurs in the saline solution at pH=5 (Figure 9), with a positive electrode potential. The net charge of the ten closest amino acids is zero, but the closest amino acid is again Lys.

4.3 pH effect

In the case of the pH effect, 5 pHs were tested, comparing the results of interaction energy between all the pHs tested in Table 2. it is showing a separation between two groups of predominant orientations in acid and basic pH, while the pH=7 tends to have the same orientations that those obtained at pH acids.

Regarding the effect of the pH, it has been reported previously that the protein adsorption is maximum at pHs close to the isoelectric point (IEP) of the protein [85, 97, 98].

It is possible that the results reported for these publications could be due the role of non-electrostatics forces (e.g., Van der Waals) hydrophobic interactions, covalent bonds, etc. which could lead to the protein being adsorbed even in unfavorable electrostatic interactions [42, 99, 100].

These non-electrostatic forces could be included approximately by a solvent-accessible surface area (SASA) model [101].
Furthermore, in numerous reports, protein adsorption displays at maximum at pHs near the isoelectric point (IEP) of the protein. [85, 97, 98] In principle, these observations can be ascribed to the role of non-electrostatics forces, which will lead to protein adsorption even in the presence of unfavorable electrostatic interactions [85, 97, 98].

Nevertheless, this conclusion does not account for numerous experiments where protein adsorption decreases with increasing ionic strength [84-88]. This correlation between the adsorption of the proteins

with the ionic strength suggests that electrostatic interactions favor adsorption even for proteins without net charge or with proteins with a charge of the same sign as the surface.

The calculations done for the hydrogenase 1e3d assume a rigid model for the protein; this has the consequence of consider a near-spherical nature of our hydrogenase, and disseminates the possible deformation of the protein as this approach to the surface of the electrode, with the possible consequence of lost catalytic activity [80, 102].

Thus, it is possible that an overall enhancement or reduction of the protein-electrode interaction would leave the equilibrium distribution essentially unchanged.

In our calculations, the potentials applied to the electrode were -0.05, 0.0 and 0.05V. Potentials are relatively low and were selected with the goal of simulate the conditions of an operative fuel cell. At this point, it is necessary to mention that applying higher voltages can destroy proteins by physical denaturation or by chemical reaction with radicals formed at the electrodes [36, 103-106].

However, the effect of high voltages is not included in our results and is beyond of the scope of this study.

Another aspect to consider it is that the protonation state of an amino acid depends not only of the pH of the solution but also of the chemical environment of the amino acid, the presence of charged groups and the local dielectric properties [91, 107].

Placing the protein near a highly charged surface will modify the pKa of the amino acids which will be affected by the charge of the surface and the local charge of the amino acids close to the surface [89, 90].

One of the main disadvantages of modeling the charge in proteins under the influence of pH, is that most of the models consider the charge of the monoacids constant, thus neglecting the charge residual effect.

Besides the calculation of the adsorption free energies is still complicated due to the constant change in the charges and the statistical sampling of the free energy landscape that should be implemented to modulate this effect [39, 108].

4.4 Orientational distributions

In this section it is discussed the orientations of the protein on the electrode in its effect in their catalytic activity, on which depends the rate of electron transfer from the electrode to the external iron-sulfur cluster.

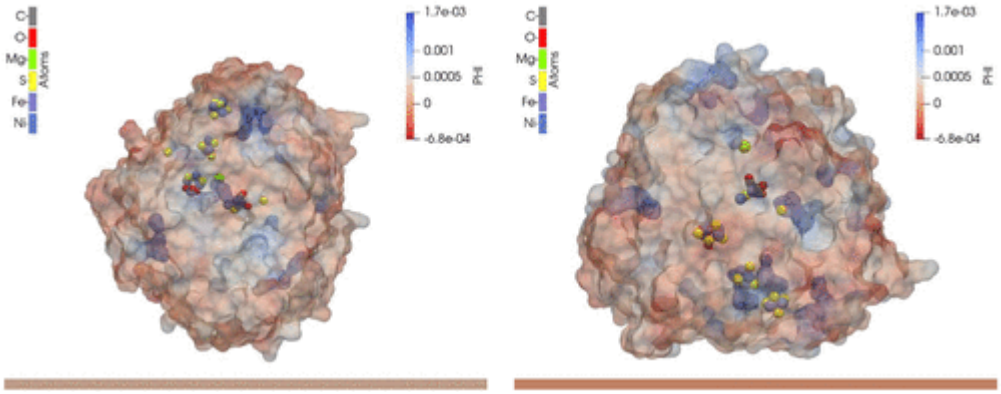

Figure 27. *Electrostatic potentials of the 1e3d hydrogenase with two different orientations.*

Left: θ =40° and φ =98°, when ϕ_e =0.05 V, I=0.15 M and pH=5. Right: θ =120° and φ =248°, when ϕ_e =0.0 V, I=0.0 M and pH=5.

Two orientations are shown in Figure 27, as an example of orientations with different rates transfer of electrons. In each orientation the position of the external iron-sulfur cluster is far from the electrode on the left-hand side of the figure and is close in the right-side, having a direct effect in the rate of electron transfer.

These distances are reported in Table 2, in the r_{min} column. The shortest distance of all is 16.28 Å, obtained under the conditions of salt solution of pH=9 with a negative potential (θ=130º and φ=235º).

However, a specific orientation is not representative of the whole system, because they represent a small proportion of all the adsorbed orientations.

The orientations of Figure 26 have P_{min}=0.198 and 0.156, respectively. In all cases, more than 80% of the proteins would adopt an orientation different from that one with the minimum energy. There is a thermal and dynamical equilibrium between a multitude of orientations, each with a different catalytic activity.

The rate of electron transfer is directly impacted by protein orientations, which is determined by the distance between the external iron-sulfur cluster and the electrode surface.

The final results for the reference current densities (J_0) are reported in the last-but-one column of Table 2. even considering the difference in the values of energy between all the orientations there are not big difference in the current densities (J_0).

The highest and the lowest values of the current density are present in the salt-free solutions, and they differ by one order of magnitude.

According to the Marcus theory, the transfer of electrons between an electron acceptor and an electron donor is a function of the potential difference between the electron acceptor and the electron donor, given as the Gibbs free energy of activation (DG), and of the reorganization energy [39, 109]. Based on this theory, the maximum distance of electron tunneling between donor and acceptor was estimated to be 20 Å [39, 91, 107, 110].

The transfer of electrons between two interacting proteins can be done in distances of 20 Å. Bigger distances have been observed cases where the electrons can travel longer distances trough the conserved aromatic residues of the amino acids of the protein [39, 111].

4.4 Absorption equilibria and currents

The influence of protein concentration on the electrode was simulated, considering osmotic pressure. According to the Langmuir model, protein adsorbs onto the electrode surface, forming a homogeneous monolayer with a limited number of equally spaced attachment sites.

The adsorption of the protein is determinate only for the interaction between the surface of the electrode and the protein, neglecting the interaction between the proteins. This is expressed in [see Eq. (22)]. A consequence of this model is that affects the electrode coverage (χ) through the overall equilibrium constant *K* [see Eq. (22)]. In this way, the value of *K* may be dominated by a few strongly adsorbed orientations.

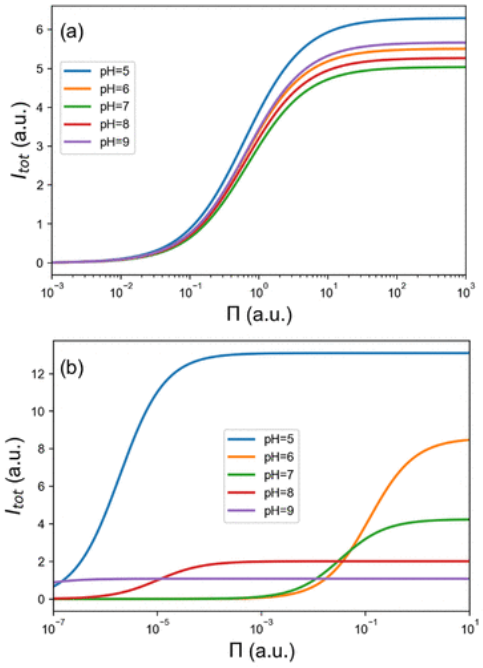

Figure 28. *Dependence of current at different pH and protein osmotic pressure, at zero electrode potential. (a) salty solutions, I=0.15 M; (b) salt-free solutions, I=0.00 M.*

There is little difference between the results at different pH, confirming our earlier conclusions (Figure 28). The solution at pH=5 seems to be marginally better, because of the combination of a slightly higher J_0 (determining the saturation value of the current at large protein concentrations) and a slightly higher K (determining the position of the inflection point in the Langmuir isotherms).

The pH=5 solution yields superior results, possibly due to a higher J_0 and K combination, indicating a larger proportion of proteins adsorbed with a favorable orientation.

The plots show that there is a dependence on the pH for the results obtained in the salt-free solutions, where the cases at pH=8 and 9 are characterized by strong absorption (large *K*), but the values of J_0 are low, which indicates that the proteins are adsorbed in an unfavorable orientation for electron transfer.

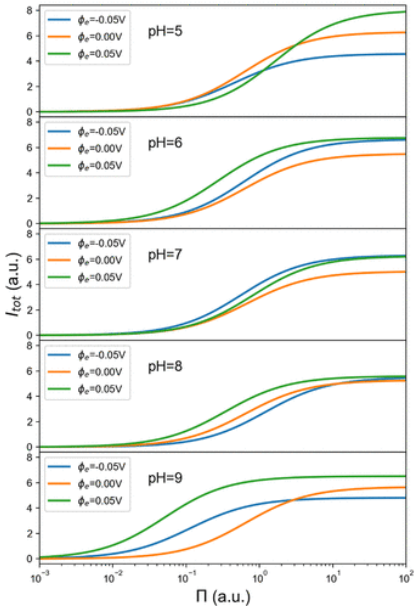

Figure 29. *Effect of modulating the electrode potential. Range of applicability of the linearized Poisson-Boltzmann equation (-0.05 V ≤ ϕ_e ≤ 0.05 V), for saline solutions with I=0.15 M.*

The most visible effect of the electrode potential on the total current can be appreciated at the pH=8 and pH=9, when to the electrode was applied an electric potential. For example, a negatively charged protein (obtained at pH=9) has a much greater affinity for the electrode at positive potential, and the affinity of the protein is decreasing when the electrode is negative, but it is before that the electrode has a zero potential.

This could not have been not expected on the basis of the charge and dipole of the protein. At a positively charged protein (pH=5), absorption in theory should be more favorable with a negative potential, but the sensitivity of the equilibrium constant show in Figure 29 indicates that is much lower in this case.

This sensitivity of the reference current density could be ascribed to the change in the distribution of the protein orientations.

The moduli of the protein charge and dipole moment are similar in these two cases (Table 1) however, this effect of the electrode potential could not follow the basis of the descriptors of the protein charge distributions.

Finally, it is necessary to mention that the Langmuir model neglects protein-protein interactions, and it is a very theoretical model that does not count other types of interactions could affect that adsorption of the protein or the possible formation of multilayer structures or aggregates of proteins. Phenomena that have been observed in several studies in diverse proteins, especially at high applied voltages (of the order of ± 1 V), affecting even the integrity of the proteins [112].

Could be expected that, in order to achieve high catalysis efficiency, enzymes must be oriented with the active site in the opposite side to the surface in order to allow the access of the substrate. In the case of electron transfer, it is the contrary, because electron transfer depends on the distance between the electrode and the catalytic center.

CHAPTER 5

Conclusions

The study examines the adsorption of a hydrogenase on a planar conducting electrode, analyzing the total energy of Poisson-Boltzmann interactions in relation to pH, salinity, and applied electric potential.

One of the main goals was to explore the possibility of control of orientations of the adsorbed proteins using the electrostatic interactions. Even if they are not the only way to adsorbed proteins, they have a dominant role in the adsorption of proteins.

According to the results, the adsorption of the enzyme on the electrode depends mainly on the pH of the solution, followed by the salinity and the electrostatic potential of the electrode. The results show that the latter does not affect too much the adsorption energy of the protein, but it has a clear effect on the orientation of the protein.

The orientation with the lowest total energies was obtained when there was a presence of charged patches on the surface of the protein, and the presence of these patches depends on the solution pH. Is observed that interaction is largest in salt-free solutions, where electrostatic interactions are not screened by the presence of counter-ions.

The total current which measures the overall rate of the redox reaction of all the adsorbed proteins, has its maximum value when there is a positive synergy between the Boltzmann probabilities of the orientations, their electron transfer rates, and the strength of the protein absorption on the electrode surface.

In our results, it was not possible to find situations dominated by a single protein orientation, and it is for that reason that the overall current depends on a whole population of absorbed orientations.

One recurrent particularity is the presence of a Lys residue close to the surface of the electrode in a number of minimum-energy orientations. It could be interesting to pursue further this observation and determine the role of Lys residues in the adsorption of the protein and if it is possible to increase it by introducing more Lys residues on the exterior of the protein, at favorable positions with respect to the [3Fe4S] external cluster.

These results are according to similar results obtained with molecular dynamics on ribonuclease A were electrostatic interactions were affected by pH and ionic strength, and apart from the orientational effect, the magnitude of the double-layer contribution in affects the calculations of the total energy of the protein-surface interaction [37].

Some of the future goals in the study of the applications of hydrogenases in renewable energies, imply the application of these models to other hydrogenases, starting with the thermo and oxygen tolerant, and the extension from non-linear solutions to the full Poisson-Boltzmann equation, including also charge regulation effects, larger values of the electrode potential and hydrophobic effects by a SASA model.

Another interesting extension of this study is the generation of starting orientations for molecular dynamics simulations, seeking more specific orientations, including more factors in the models like non-electrostatic interactions and the deformation of the protein at the moment of be in contact with the surface of the electrode.

Indeed, some flexibility is known to be necessary for the functionality of an enzyme, for example, to assist the diffusion of the substrates to and away from the catalytic site.

The molecular dynamics results could also be used as a new input for further Poisson-Boltzmann based analyzes of electrostatic effects and free energies [101], and to improve the models for electron transfer including other factors like hopping or quantum tunneling electron transfer [82, 113].

Another interesting incorporation of the model is the re-orientational motion of the enzyme, which can be induced for the voltage of the electrode [36, 99, 114]. Complemented with a micro hydrodynamic description of the surrounding fluid [115].

Of course, the implementation of such parameters to the model should be cross-checked by experiments, including ones based on modern *in situ* operand spectroscopies that could give some new information about local interactions at the protein-electrode interface [116, 117].

Finally, I can say that the present study has demonstrated the usefulness of computational approaches to study the adsorption of proteins on electrodes using models based in the linearized Poisson-Boltzmann equation.

Bibliography

1. Lubitz, W., et al., *Hydrogenases.* Chem Rev, 2014. **114**(8): p. 4081-148.
2. Lojou, E., *Hydrogenases as catalysts for fuel cells: Strategies for efficient immobilization at electrode interfaces.* Electrochimica Acta, 2011. **56**(28): p. 10385-10397.
3. Vincent, K.A., A. Parkin, and F.A. Armstrong, *Investigating and exploiting the electrocatalytic properties of hydrogenases.* Chemical reviews, 2007. **107**(10): p. 4366-4413.
4. Luo, X., et al., *Immobilization of the hyperthermophilic hydrogenase from Aquifex aeolicus bacterium onto gold and carbon nanotube electrodes for efficient H2 oxidation.* J Biol Inorg Chem, 2009. **14**(8): p. 1275-88.
5. Jugder, B.-E., et al., *Fundamentals and electrochemical applications of [Ni–Fe]-uptake hydrogenases.* RSC Advances, 2013. **3**(22).
6. Breglia, R., et al., *Theoretical insights into [NiFe]-hydrogenases oxidation resulting in a slowly reactivating inactive state.* J Biol Inorg Chem, 2017. **22**(1): p. 137-151.
7. Siegbahn, P.E., J.W. Tye, and M.B. Hall, *Computational studies of [NiFe] and [FeFe] hydrogenases.* Chemical reviews, 2007. **107**(10): p. 4414-4435.
8. Abreu, I.A., et al., *A novel iron centre in the split-Soret cytochrome c from Desulfovibrio desulfuricans ATCC 27774.* JBIC Journal of Biological Inorganic Chemistry, 2003. **8**: p. 360-370.
9. Costa, C., et al., *Formate dehydrogenase from Desulfovibrio desulfuricans ATCC 27774: isolation and spectroscopic characterization of the active sites (heme, iron-sulfur centers and molybdenum).* JBIC Journal of Biological Inorganic Chemistry, 1997. **2**: p. 198-208.
10. da Silva, S.M., I. Pacheco, and I.A.C. Pereira, *Electron transfer between periplasmic formate dehydrogenase and cytochromes c in Desulfovibrio desulfuricans ATCC 27774.* JBIC Journal of Biological Inorganic Chemistry, 2012. **17**: p. 831-838.
11. Lobo, S.A., et al., *The anaerobe Desulfovibrio desulfuricans ATCC 27774 grows at nearly atmospheric oxygen levels.* FEBS letters, 2007. **581**(3): p. 433-436.
12. Matias, P.M., et al., *[NiFe] hydrogenase from Desulfovibrio desulfuricans ATCC 27774: gene sequencing, three-dimensional structure determination and refinement at 1.8 A and modelling studies of its interaction with the tetrahaem cytochrome c3.* J Biol Inorg Chem, 2001. **6**(1): p. 63-81.
13. Pires, R.H., et al., *A novel membrane-bound respiratory complex from Desulfovibrio desulfuricans ATCC 27774.* Biochimica et Biophysica Acta (BBA)-Bioenergetics, 2003. **1605**(1-3): p. 67-82.
14. Sousa, J.R., et al., *Understanding the response of Desulfovibrio desulfuricans ATCC 27774 to the electron acceptors nitrate and sulfate-biosynthetic costs modulate substrate selection.* Biochimica et Biophysica Acta (BBA)-Proteins and Proteomics, 2017. **1865**(11): p. 1455-1469.
15. Muyzer, G. and A.J. Stams, *The ecology and biotechnology of sulphate-reducing bacteria.* Nature reviews microbiology, 2008. **6**(6): p. 441-454.
16. Devereux, R., et al., *Diversity and origin of Desulfovibrio species: phylogenetic definition of a family.* Journal of Bacteriology, 1990. **172**(7): p. 3609-3619.
17. Marietou, A., L. Griffiths, and J. Cole, *Preferential reduction of the thermodynamically less favorable electron acceptor, sulfate, by a nitrate-reducing strain of the sulfate-reducing bacterium Desulfovibrio desulfuricans 27774.* Journal of bacteriology, 2009. **191**(3): p. 882-889.
18. RIEDER, R., R. CAMMACK, and D.O. HALL, *Purification and properties of the soluble hydrogenase from Desulfovibrio desulfuricans (strain Norway 4).* European journal of biochemistry, 1984. **145**(3): p. 637-645.

19. Berman, H.M., et al., *The protein data bank.* Nucleic acids research, 2000. **28**(1): p. 235-242.
20. Lee, J. and S.H. Kim, *PDB Editor: a user-friendly Java-based Protein Data Bank file editor with a GUI.* Acta Crystallogr D Biol Crystallogr, 2009. **65**(Pt 4): p. 399-402.
21. Krasna, A.I., E. Riklis, and D. Rittenberg, *The purification and properties of the hydrogenase of Desulfovibrio desulfuricans.* Journal of Biological Chemistry, 1960. **235**(9): p. 2717-2720.
22. Glick, B.R., W.G. Martin, and S.M. Martin, *Purification and properties of the periplasmic hydrogenase from Desulfovibrio desulfuricans.* Canadian Journal of Microbiology, 1980. **26**(10): p. 1214-1223.
23. Karyakin, A.A., et al., *Hydrogenase electrodes for fuel cells.* Biochem Soc Trans, 2005. **33**(Pt 1): p. 73-5.
24. Lee, C.Y., et al., *Photoelectrochemical H2 evolution with a hydrogenase immobilized on a TiO2-protected silicon electrode.* Angewandte Chemie International Edition, 2016. **55**(20): p. 5971-5974.
25. Xiao, X., et al., *Tackling the Challenges of Enzymatic (Bio)Fuel Cells.* Chem Rev, 2019. **119**(16): p. 9509-9558.
26. Mersch, D., et al., *Wiring of Photosystem II to Hydrogenase for Photoelectrochemical Water Splitting.* J Am Chem Soc, 2015. **137**(26): p. 8541-9.
27. Morra, S., et al., *Direct electrochemistry of an [FeFe]-hydrogenase on a TiO2 electrode.* Chem Commun (Camb), 2011. **47**(38): p. 10566-8.
28. Monsalve, K., et al., *Hydrogen bioelectrooxidation on gold nanoparticle-based electrodes modified by Aquifex aeolicus hydrogenase: Application to hydrogen/oxygen enzymatic biofuel cells.* Bioelectrochemistry, 2015. **106**(Pt A): p. 47-55.
29. Rüdiger, O., et al., *Enzymatic Anodes for Hydrogen Fuel Cells based on Covalent Attachment of Ni-Fe Hydrogenases and Direct Electron Transfer to SAM-Modified Gold Electrodes.* Electroanalysis, 2010. **22**(7-8): p. 776-783.
30. Gutierrez-Sanz, O., et al., *H2 -Fueled ATP Synthesis on an Electrode: Mimicking Cellular Respiration.* Angew Chem Int Ed Engl, 2016. **55**(21): p. 6216-20.
31. Quinson, J., et al., *Comparison of carbon materials as electrodes for enzyme electrocatalysis: hydrogenase as a case study.* Faraday Discuss, 2014. **172**: p. 473-96.
32. Liu, J., et al., *Immobilization of hydrogenase on carbon nanotube polyelectrolytes as heterogeneous catalysts for electrocatalytic interconversion of protons and hydrogen.* Journal of Nanoparticle Research, 2016. **18**(8).
33. Mazurenko, I., et al., *Impact of substrate diffusion and enzyme distribution in 3D-porous electrodes: a combined electrochemical and modelling study of a thermostable H 2/O 2 enzymatic fuel cell.* Energy & Environmental Science, 2017. **10**(9): p. 1966-1982.
34. Rüdiger, O., et al., *Oriented immobilization of desulfovibrio gi gas hydrogenase onto carbon electrodes by covalent bonds for nonmediated oxidation of H2.* Journal of the American Chemical Society, 2005. **127**(46): p. 16008-16009.
35. Gutierrez-Sanchez, C., et al., *Oriented immobilization of a membrane-bound hydrogenase onto an electrode for direct electron transfer.* Langmuir, 2011. **27**(10): p. 6449-57.
36. Heidary, N., et al., *Orientation-Controlled Electrocatalytic Efficiency of an Adsorbed Oxygen-Tolerant Hydrogenase.* PLoS One, 2015. **10**(11): p. e0143101.
37. Yoon, B.J. and A.M. Lenhoff, *Computation of the electrostatic interaction energy between a protein and a charged surface.* The Journal of Physical Chemistry, 1992. **96**(7): p. 3130-3134.
38. Oteri, F., et al., *The weak, fluctuating, dipole moment of membrane-bound hydrogenase from Aquifex aeolicus accounts for its adaptability to charged electrodes.* Phys Chem Chem Phys, 2014. **16**(23): p. 11318-22.
39. Boubeta, F.M., G. Soler-Illia, and M. Tagliazucchi, *Electrostatically Driven Protein Adsorption: Charge Patches versus Charge Regulation.* Langmuir, 2018. **34**(51): p. 15727-15738.

40. Tsori, Y., *Bistable colloidal orientation in polar liquid near a charged wall.* Journal of colloid and interface science, 2020. **559**: p. 45-50.
41. Urzúa, S.A., et al., *Predicting the orientation of adsorbed proteins steered with electric fields using a simple electrostatic model.* The Journal of Physical Chemistry B, 2022. **126**(28): p. 5231-5240.
42. Norde, W., *My voyage of discovery to proteins in flatland... and beyond.* Colloids and surfaces. B, Biointerfaces, 2007. **61**(1): p. 1-9.
43. Fogolari, F., A. Brigo, and H. Molinari, *The Poisson-Boltzmann equation for biomolecular electrostatics: a tool for structural biology.* J Mol Recognit, 2002. **15**(6): p. 377-92.
44. Mirny, L. and E. Shakhnovich, *Protein folding theory: from lattice to all-atom models.* Annual review of biophysics and biomolecular structure, 2001. **30**(1): p. 361-396.
45. Sharp, K.A. and B. Honig, *Electrostatic interactions in macromolecules: theory and applications.* Annual review of biophysics and biophysical chemistry, 1990. **19**(1): p. 301-332.
46. Herrero, C. and L. Joly, *Poisson-boltzmann formulary.* arXiv preprint arXiv:2105.00720, 2021.
47. Li, C., et al., *Progress in developing Poisson-Boltzmann equation solvers.* Mol Based Math Biol, 2013. **1**.
48. Hsu, J.-P. and B.-T. Liu, *Solution to the linearized Poisson–Boltzmann equation for a spheroidal surface under a general surface condition.* Journal of colloid and interface science, 1996. **183**(1): p. 214-222.
49. Cooper, C.D., J.P. Bardhan, and L.A. Barba, *A biomolecular electrostatics solver using Python, GPUs and boundary elements that can handle solvent-filled cavities and Stern layers.* Comput Phys Commun, 2014. **185**(3): p. 720-729.
50. Cooper, C.D. and L.A. Barba, *Poisson–Boltzmann model for protein–surface electrostatic interactions and grid-convergence study using the PyGBe code.* Computer Physics Communications, 2016. **202**: p. 23-32.
51. Fogolari, F., et al., *Biomolecular electrostatics with the linearized Poisson-Boltzmann equation.* Biophysical journal, 1999. **76**(1): p. 1-16.
52. Baker, N.A., *Improving implicit solvent simulations: a Poisson-centric view.* Curr Opin Struct Biol, 2005. **15**(2): p. 137-43.
53. Honig, B. and A. Nicholls, *Classical electrostatics in biology and chemistry.* Science, 1995. **268**(5214): p. 1144-1149.
54. Hsu, J.-P. and B.-T. Liu, *Exact solution to the linearized Poisson–Boltzmann equation for spheroidal surfaces.* Journal of colloid and interface science, 1996. **178**(2): p. 785-788.
55. Gilson, M.K., K.A. Sharp, and B.H. Honig, *Calculating the electrostatic potential of molecules in solution: method and error assessment.* Journal of computational chemistry, 1988. **9**(4): p. 327-335.
56. Jackson, J.D., *Classical electrodynamics*. 1999: John Eiley & Sons, Inc.
57. Hill, T.L., *An introduction to statistical thermodynamics*. 1986: Courier Corporation.
58. Baker, N.A., et al., *Electrostatics of nanosystems: application to microtubules and the ribosome.* Proceedings of the National Academy of Sciences, 2001. **98**(18): p. 10037-10041.
59. Rocchia, W., E. Alexov, and B. Honig, *Extending the applicability of the nonlinear Poisson− Boltzmann equation: multiple dielectric constants and multivalent ions.* The Journal of Physical Chemistry B, 2001. **105**(28): p. 6507-6514.
60. Bashford, D. *An object-oriented programming suite for electrostatic effects in biological molecules An experience report on the MEAD project*. in *Scientific Computing in Object-Oriented Parallel Environments: First International Conference, ISCOPE 97 Marina del Rey, California, USA December 8–11, 1997 Proceedings 1*. 1997. Springer.
61. Geng, W., S. Yu, and G. Wei, *Treatment of charge singularities in implicit solvent models.* J Chem Phys, 2007. **127**(11): p. 114106.

62. Lu, B., et al., *Order N algorithm for computation of electrostatic interactions in biomolecular systems.* Proceedings of the National Academy of Sciences, 2006. **103**(51): p. 19314-19319.
63. Geng, W. and R. Krasny, *A treecode-accelerated boundary integral Poisson–Boltzmann solver for electrostatics of solvated biomolecules.* Journal of Computational Physics, 2013. **247**: p. 62-78.
64. Cooper, C.D., N.C. Clementi, and L.A. Barba, *Probing protein orientation near charged nanosurfaces for simulation-assisted biosensor design.* J Chem Phys, 2015. **143**(12): p. 124709.
65. Ahrens, J., et al., *36-paraview: An end-user tool for large-data visualization.* The visualization handbook, 2005. **717**: p. 50038-1.
66. Ren, P., et al., *Biomolecular electrostatics and solvation: a computational perspective.* Quarterly reviews of biophysics, 2012. **45**(4): p. 427-491.
67. Dolinsky, T.J., et al., *PDB2PQR: an automated pipeline for the setup of Poisson-Boltzmann electrostatics calculations.* Nucleic Acids Res, 2004. **32**(Web Server issue): p. W665-7.
68. MacKerell Jr, A.D., et al., *All-atom empirical potential for molecular modeling and dynamics studies of proteins.* The journal of physical chemistry B, 1998. **102**(18): p. 3586-3616.
69. Wang, J., P. Cieplak, and P.A. Kollman, *How well does a restrained electrostatic potential (RESP) model perform in calculating conformational energies of organic and biological molecules?* Journal of computational chemistry, 2000. **21**(12): p. 1049-1074.
70. Sitkoff, D., K.A. Sharp, and B. Honig, *Accurate calculation of hydration free energies using macroscopic solvent models.* The Journal of Physical Chemistry, 1994. **98**(7): p. 1978-1988.
71. Breneman, C.M. and K.B. Wiberg, *Determining atom-centered monopoles from molecular electrostatic potentials. The need for high sampling density in formamide conformational analysis.* Journal of Computational Chemistry, 1990. **11**(3): p. 361-373.
72. Hornak, V., et al., *Comparison of multiple Amber force fields and development of improved protein backbone parameters.* Proteins, 2006. **65**(3): p. 712-25.
73. Neese, F., *The ORCA program system.* WIREs Computational Molecular Science, 2011. **2**(1): p. 73-78.
74. Neese, F., *Software update: the ORCA program system, version 4.0.* WIREs Computational Molecular Science, 2017. **8**(1).
75. Weigend, F. and R. Ahlrichs, *Balanced basis sets of split valence, triple zeta valence and quadruple zeta valence quality for H to Rn: Design and assessment of accuracy.* Phys Chem Chem Phys, 2005. **7**(18): p. 3297-305.
76. Adamo, C. and V. Barone, *Toward reliable density functional methods without adjustable parameters: The PBE0 model.* The Journal of chemical physics, 1999. **110**(13): p. 6158-6170.
77. Decherchi, S. and W. Rocchia, *A general and robust ray-casting-based algorithm for triangulating surfaces at the nanoscale.* PLoS One, 2013. **8**(4): p. e59744.
78. Atkins, P., P.W. Atkins, and J. de Paula, *Atkins' physical chemistry*. 2014: Oxford university press.
79. Ken Dill, S.B., *Molecular Driving Forces: Statistical Thermodynamics in Biology, Chemistry, Physics, and Nanoscience (2nd ed.).* 2010: Garland Science.
80. Hitaishi, V., et al., *Controlling Redox Enzyme Orientation at Planar Electrodes.* Catalysts, 2018. **8**(5).
81. Winkler, J.R. and H.B. Gray, *Electron flow through metalloproteins.* Chem Rev, 2014. **114**(7): p. 3369-80.
82. Petrenko, A. and M. Stein, *Rates and Routes of Electron Transfer of [NiFe]-Hydrogenase in an Enzymatic Fuel Cell.* J Phys Chem B, 2015. **119**(43): p. 13870-82.
83. Petrenko, A. and M. Stein, *Distal [FeS]-Cluster Coordination in [NiFe]-Hydrogenase Facilitates Intermolecular Electron Transfer.* Int J Mol Sci, 2017. **18**(1).

84. Wittemann, A. and M. Ballauff, *Interaction of proteins with linear polyelectrolytes and spherical polyelectrolyte brushes in aqueous solution.* Phys Chem Chem Phys, 2006. **8**(45): p. 5269-75.
85. Bremer, M.G., et al., *Electrostatic interactions between immunoglobulin (IgG) molecules and a charged sorbent.* Colloids and surfaces A: Physicochemical and engineering aspects, 2004. **250**(1-3): p. 29-42.
86. Chen, K., et al., *Electrostatic selectivity in protein-nanoparticle interactions.* Biomacromolecules, 2011. **12**(7): p. 2552-61.
87. Henzler, K., et al., *Adsorption of β-lactoglobulin on spherical polyelectrolyte brushes: direct proof of counterion release by isothermal titration calorimetry.* Journal of the American Chemical Society, 2010. **132**(9): p. 3159-3163.
88. Galisteo, F. and W. Norde, *Adsorption of lysozyme and α-lactalbumin on poly (styrenesulphonate) latices 1. Adsorption and desorption behaviour.* Colloids and Surfaces B: Biointerfaces, 1995. **4**(6): p. 375-387.
89. Biesheuvel, P.M., M. van der Veen, and W. Norde, *A modified Poisson– Boltzmann model including charge regulation for the adsorption of ionizable polyelectrolytes to charged interfaces, applied to lysozyme adsorption on silica.* The Journal of Physical Chemistry B, 2005. **109**(9): p. 4172-4180.
90. Longo, G.S. and I. Szleifer, *Adsorption and protonation of peptides and proteins in pH responsive gels.* Journal of Physics D: Applied Physics, 2016. **49**(32).
91. Ninham, B.W. and V.A. Parsegian, *Electrostatic potential between surfaces bearing ionizable groups in ionic equilibrium with physiologic saline solution.* Journal of theoretical biology, 1971. **31**(3): p. 405-428.
92. Levin, A. and C. Czeslik, *Interaction of calmodulin with poly(acrylic acid) brushes: Effects of high pressure, pH-value and ligand binding.* Colloids Surf B Biointerfaces, 2018. **171**: p. 478-484.
93. Meissner, J., et al., *Characterization of protein adsorption onto silica nanoparticles: influence of pH and ionic strength.* Colloid Polym Sci, 2015. **293**(11): p. 3381-3391.
94. Kubiak-Ossowska, K., et al., *Lysozyme adsorption at a silica surface using simulation and experiment: effects of pH on protein layer structure.* Physical Chemistry Chemical Physics, 2015. **17**(37): p. 24070-24077.
95. Kubiak-Ossowska, K. and P.A. Mulheran, *Mechanism of hen egg white lysozyme adsorption on a charged solid surface.* Langmuir, 2010. **26**(20): p. 15954-15965.
96. Hildebrand, N., et al., *Adsorption orientation and binding motifs of lysozyme and chymotrypsin on amorphous silica.* The Journal of Physical Chemistry C, 2015. **119**(13): p. 7295-7307.
97. Demaneche, S., et al., *Dissimilar pH-dependent adsorption features of bovine serum albumin and alpha-chymotrypsin on mica probed by AFM.* Colloids Surf B Biointerfaces, 2009. **70**(2): p. 226-31.
98. Höök, F., et al., *Structural changes in hemoglobin during adsorption to solid surfaces: effects of pH, ionic strength, and ligand binding.* Proceedings of the National Academy of Sciences, 1998. **95**(21): p. 12271-12276.
99. Yan, X., et al., *Direct electron transfer of fructose dehydrogenase immobilized on thiol-gold electrodes.* Electrochimica Acta, 2021. **392**: p. 138946.
100. Rabe, M., D. Verdes, and S. Seeger, *Understanding protein adsorption phenomena at solid surfaces.* Adv Colloid Interface Sci, 2011. **162**(1-2): p. 87-106.
101. Wang, C., et al., *Recent developments and applications of the MMPBSA method.* Frontiers in molecular biosciences, 2018. **4**: p. 87.
102. McArdle, T., et al., *Optimizing the mass-specific activity of bilirubin oxidase adlayers through combined electrochemical quartz crystal microbalance and dual polarization interferometry analyses.* ACS Applied Materials & Interfaces, 2015. **7**(45): p. 25270-25280.

103. Sugimoto, Y., et al., *Electrostatic interaction between an enzyme and electrodes in the electric double layer examined in a view of direct electron transfer-type bioelectrocatalysis.* Biosens Bioelectron, 2015. **63**: p. 138-144.
104. Sugimoto, Y., et al., *Role of 2-mercaptoethanol in direct electron transfer-type bioelectrocatalysis of fructose dehydrogenase at Au electrodes.* Electrochimica Acta, 2015. **170**: p. 242-247.
105. Utesch, T., et al., *Effect of the protonation degree of a self-assembled monolayer on the immobilization dynamics of a [NiFe] hydrogenase.* Langmuir, 2013. **29**(2): p. 673-82.
106. Singh, K., et al., *Sources of activity loss in the fuel cell enzyme bilirubin oxidase.* Energy & Environmental Science, 2013. **6**(8).
107. Tagliazucchi, M. and I. Szleifer, *Stimuli-responsive polymers grafted to nanopores and other nano-curved surfaces: structure, chemical equilibrium and transport.* Soft Matter, 2012. **8**(28).
108. Wei, T., M.A. Carignano, and I. Szleifer, *Molecular dynamics simulation of lysozyme adsorption/desorption on hydrophobic surfaces.* The Journal of Physical Chemistry B, 2012. **116**(34): p. 10189-10194.
109. Nap, R., P. Gong, and I. Szleifer, *Weak polyelectrolytes tethered to surfaces: effect of geometry, acid–base equilibrium and electrical permittivity.* Journal of Polymer Science Part B: Polymer Physics, 2006. **44**(18): p. 2638-2662.
110. Moser, C.C., et al., *Nature of biological electron transfer.* Nature, 1992. **355**(6363): p. 796-802.
111. Ricci, A., M. Tagliazucchi, and E.J. Calvo, *Charge regulation in redox active monolayers embedded in proton exchanger surfaces.* Physical Chemistry Chemical Physics, 2012. **14**(28): p. 9988-9995.
112. Benavidez, T.E., et al., *Adsorption of soft and hard proteins onto OTCEs under the influence of an external electric field.* Langmuir, 2015. **31**(8): p. 2455-2462.
113. Baggioli, A., et al., *Atomistic simulation of phase transitions and charge mobility for the organic semiconductor Ph-BTBT-C10.* Chemistry of Materials, 2019. **31**(17): p. 7092-7103.
114. Hexter, S.V., T.F. Esterle, and F.A. Armstrong, *A unified model for surface electrocatalysis based on observations with enzymes.* Physical Chemistry Chemical Physics, 2014. **16**(24): p. 11822-11833.
115. Aragon, S.R., *Recent advances in macromolecular hydrodynamic modeling.* Methods, 2011. **54**(1): p. 101-114.
116. Ciaccafava, A., et al., *Electrochemistry, AFM, and PM-IRRA spectroscopy of immobilized hydrogenase: role of a hydrophobic helix in enzyme orientation for efficient H2 oxidation.* Angew Chem Int Ed Engl, 2012. **51**(4): p. 953-6.
117. Sedenho, G.C., et al., *In situ and operando electrochemistry of redox enzymes.* Current Opinion in Electrochemistry, 2022: p. 101015.

Appendices

This section corresponds to the appendix of the thesis, here are collected some scripts that facilitate the installation and implementation of PyGBe. If well the program is easy to use, these notes and script have the purpose of save time for the user, and preserve the scripts.

Installation notes for PyGBe

The first part corresponds to the instructions to install PyGBe in the operative system, Ubuntu. The releases confirmed where PyGBe works are: 16.04, 18.04, 20.04 and 22.04, however in the last two versions there are problems with the versions of "gcc", that are necessary for the right function of "CUDA". The rule of thumb is to use versions of "gcc" corresponding for the versions of "CUDA" installed. Another problem that could rise at the moment of install CUDA are the graphical drivers.

In this aspect, CUDA use NVIDIA video cards, but not all of them can be used with each version of CUDA. Another problem that could rise at the moment of use CUDA, is with Pycuda, here the problem consist that sometimes Pycuda does not recognize the folder where "CUDA" was installed, and for that reason PyGBe could not work using the graphic processor unit (gpu) of the computer, one way to avoid this problem is to install CUDA first using the APT (Advanced Package Tool) with the command "atp install", doing in this way it is possible to avoid a lot of problems related with the installation of PyGBe.

Finally, the most complicated problem that could rise at the moment of install PyGBe is the installation of the graphical drivers compatible with CUDA. In general, the installer of CUDA has the option of install the driver of the "gpu" automatically. However, it is better to do it with ATP, if this does not work could be necessary to disable the Nouveau drivers that comes with Ubuntu, however this is complicated and there is the possibility of lost the signal in the monitor, if this problem rise, it is possible to revert it connecting to the computer remotely and revert the changes

reinstalling the drivers using the terminal from a second computer. However, the recommendation in this case is simply to get a new graphic card compatible with CUDA.

A video with a description of the process for the installation of PyGBe can be found in the next link:

https://www.youtube.com/watch?v=PQH4l3dDt6E&ab_channel=Scientificprotocols

And the necessary lines to be typed in the terminal of ubuntu for the installation of PyGBe are described next:

```
sudo apt update

nvidia-smi

python –version

bash Anaconda3-2020.02-Linux-x86_64.sh

gcc –version

sudo sh cuda_11.0.1_450.36.06_linux.run --override

sudo apt install swig python3-pip python3-numpy python3-scipy python3-matplotlib
python3-pandas python3-simpy python3-nose python3-pycuda python3-pytools git

reboot

cd $home

mkdir src
cd src

git clone https://github.com/pygbe/pygbe.git

cd pygbe

sudo python3 setup.py install clean

conda create -n pygbe python=3.7 numpy scipy swig matplotlib

source activate pygbe
```

Note: In order to execute PyGBe it is necessary to type in terminal: pygbe + the name of folder

Scripts for run multiple calculations in PyGBe

Due to the repetitive nature of calculate the total energy for many orientations, a script in python was written to do the calculations in these orientations, all the orientations need to be collected inside of a folder.

For the first run the script calculate the result for each orientation, once this is done the script check if all the folders have an output folder with the results If not, the script enter in loop calculating the result for the orientations without the right number of files in the output folder.

This is done in this way because sometimes PyGBe, if well finish the calculation, does not save the result in a file, which carries to missing results. The command lines of the script are written next, together with some notes of its function:

```
'
##################################################################
##################################################
Script that execute PyGBe for all the structures contained in a folder, it is necessary
to provide the path where are the structures in path_output_folder. This script can
resume an interrupted session of calculations, but the calculation was the
interruption happen need to be recalculated again.

python3 Automatic_pygbe_full1.py
##################################################################
##################################################
'


import os
import shutil
import os.path
from os import path
import sys
path_input_folder = "/eos/user/m/mruiz/calculations/calculations_node1/"
#path_input_folder = '/user/m/mruiz/calculations/calculations_node1/'


folders = os.listdir(path_input_folder)
os.chdir(path_input_folder)



counter = 0
```

```
for i in folders:

   os.chdir(path_input_folder+i)
   folders2 = os.listdir(path_input_folder+i)
   print(len(folders2))

   for k in folders2:
      folders3 = os.listdir(path_input_folder+i + "/" + k)
      print(path_input_folder+i + "/" + k)
      condition = path.exists(path_input_folder+i + "/" + k + "/" + "output")


      if condition == True:
         print("There is an output folder already: ", condition)
         pass

      else:
         counter = counter + 1
         print("there is not output folder, running calculation... ")
         print('pygbe ' + path_input_folder+i + "/" + k)
os.system('pygbe ' + path_input_folder+i + "/" + k)

         print('Calculations done: ' + str(counter))
         print('Checking the output files now...')
##########################################################################
##########################################################
"
this part of the script check if all the calculations have finished in the right way, by
counting the number of files
in the output folder. In the current version of PYGBE, (June 2021) the output has four
files

"
##########################################################################
##########################################################

counter2 = 0
for i in folders:

   os.chdir(path_input_folder+i)
   folders2 = os.listdir(path_input_folder+i)

   for k in folders2:
      folders3 = os.listdir(path_input_folder+i + "/" + k)
      print("folders", folders3)
      print(path_input_folder+i + "/" + k + "/" + "output")

      output_files = os.listdir(path_input_folder+i + "/" + k + "/" + "output")
      No_output_files = len(output_files)
      print("No_output_files: ", No_output_files)

      if No_output_files == 4:
         pass
      else:
```

```
        counter2 = counter2 + 1
        print("The number of files is: " + str(No_output_files) + ", deleting output
folder... ")
        shutil.rmtree(path_input_folder + i + "/" + k + "/" + "output")
        print("there is not output folder, running calculation again: ")
        print('pygbe ' + path_input_folder + i + "/" + k)
        os.system('pygbe ' + path_input_folder + i + "/" + k)
counter3 = 0
for i in folders:

  os.chdir(path_input_folder + i)
  folders2 = os.listdir(path_input_folder + i)

  for k in folders4:
    folders5 = os.listdir(path_input_folder + i + "/" + k)
    print("folders", folders5)
    print(path_input_folder + i + "/" + k + "/" + "output")

    output_files = os.listdir(path_input_folder + i + "/" + k + "/" + "output")
    No_output_files = len(output_files)
    print("No_output_files: ", No_output_files)

    if No_output_files == 4:
      pass
    else:
      counter3 = counter3 + 1
      print("The number of files is: " + str(No_output_files) + ", deleting output
folder... ")
      shutil.rmtree(path_input_folder + i + "/" + k + "/" + "output")
      print("there is not output folder, running calculation again: ")
      print('pygbe ' + path_input_folder + i + "/" + k)
      os.system('pygbe ' + path_input_folder + i + "/" + k)

print('Calculations done: ' + str(counter))
print('Calculations done again: ' + str(counter))
```

Scripts to generate vtk files for Paraview

The next script generates a vtk file to visualize the results obtained with PyGBe, one detail is that sometimes there are differences between the number of PHI values calculated by PyGBe and the number of triangles of the mesh of the protein, this happen because the mesh sometimes has tringles with area 0, which is an error. In order to solve the problem, the script recalculates the triangles and creates the vtk file that can be read with Paraview. Inside of the script there are notes indicating what does each part.

```
"
##########################################################################
##########################################################
This script generates the vtk file for the visualization of the results obtained with the
software PyGBe.
It combines the vert, face of the protein to generate a three-dimensional figure made
of triangles and to each triangle is assigned the values of electrostatic potential
calculated by PyGBe stored in the file phi.txt file.
The vtk file produced organizes the information, placing first the vert, then the face
and the end of the phi. This script can create a .vtk file in tandem in a row of folders
where is desired to create the vtk files.
In order to use the script, it is necessary to indicate the directory path of the input
folder of the input
files used by PYGBE to calculate the electrostatic potential, also it is necessary to
have
the same organization of files. Also, it is necessary to indicate where the files vtk will
be saved.

It is used with the next command in the terminal

python3 vtk_generator_stern_gr2.py
charge_electrode  14.159264207765428

##########################################################################
##########################################################
"


import sys
import os
import numpy as np
import shutil

# --- BEGINNING OF INPUT HERE YOU HAVE TO INDICATE THE PATH AND NAME OF
THE FOLDER WITH THE INPUTS OF PYGBE HERE

path_base =
"/media/manuel/2A12535F12532ED7/new_results_minus1_interaction5_fix_rare_ca
```

```
ses/1e3d_5_0.0_salt/1e3d_5_theta_60_phi_273/"
electrode = 'electrode_250x250x10_d02'
electrode_stern = 'electrode_252x252x12_d02'

folder_name = path_base.split('/')[-2]
print(folder_name)
files = os.listdir(path_base)
print(files)


# PHI file
arr2 = os.listdir(path_base + "output")
file_phi = []
for k in arr2:

    if k.endswith("phi.txt"):
        file_phi.append(k)
        # print(k)

path_phi = path_base + "output" + "/" + file_phi[0]
print(file_phi)
print(path_phi)


# PHI0 file
arr3 = os.listdir(path_base)
file_phi0 = []
for k in arr3:

    if k.endswith(".phi0"):
        file_phi0.append(k)
        # print(k)

path_phi0 = path_base + file_phi0[0]
print(file_phi0)
print(path_phi0)


# TOTAL FILES
path_vert = path_base + "geometry" + "/" + "total_vert.vert"
path_face = path_base + "geometry" + "/" + "total_face.face"

# PROTEIN FILES
path_vert_protein = path_base + "geometry" + "/" + folder_name + ".vert"
path_face_protein = path_base + "geometry" + "/" + folder_name + ".face"

# PROTEIN FILES STERN LAYER
path_vert_protein_stern = path_base + "geometry" + "/" + folder_name +
"_stern.vert"
path_face_protein_stern = path_base + "geometry" + "/" + folder_name +
"_stern.face"

# ELECTRODE FILES
path_vert_electrode = path_base + "geometry" + "/" + electrode + ".vert"
```

```
path_face_electrode = path_base + "geometry" + "/" + electrode + ".face"

# ELECTRODE FILES STERN LAYER
path_vert_electrode_stern = path_base + "geometry" + "/" + electrode_stern +
"_stern.vert"
path_face_electrode_stern = path_base + "geometry" + "/" + electrode_stern +
"_stern.face"


# A useful function to compute the area of a triangle.
def triarea(i, j, k, xyz):
    "
    Computes the area of a triangle using Heron's formula
    "
    dij = (xyz[i][0] - xyz[j][0]) ** 2
    dij += (xyz[i][1] - xyz[j][1]) ** 2
    dij += (xyz[i][2] - xyz[j][2]) ** 2
    dij = np.sqrt(dij)
    dik = (xyz[i][0] - xyz[k][0]) ** 2
    dik += (xyz[i][1] - xyz[k][1]) ** 2
    dik += (xyz[i][2] - xyz[k][2]) ** 2
    dik = np.sqrt(dik)
    djk = (xyz[j][0] - xyz[k][0]) ** 2
    djk += (xyz[j][1] - xyz[k][1]) ** 2
    djk += (xyz[j][2] - xyz[k][2]) ** 2
    djk = np.sqrt(djk)
    p = (dij + dik + djk) / 2
    area = np.sqrt(p * (p - dij) * (p - dik) * (p - djk))
    return area
##########################################################################
##########################################
"
VERT DATA TOTAL

Collects all the lines of the vert files of all the surfaces
"
##########################################################################
##########################################
data_vert = []
xyz_vert = []
nverti = []
with open(path_vert, 'r+') as lines:
    n = 0
    for line in lines:
        nv1 = float(line.split()[0])
        nv2 = float(line.split()[1])
        nv3 = float(line.split()[2])
        n += 1
        numbers_line = ('{0:>8.3f} {1:>8.3f} {2:>8.3f}'.format(nv1, nv2, nv3))
        data_vert.append(numbers_line)
        xyz_vert.append([nv1, nv2, nv3])
nverti.append(n)
print("vertexfile - " + path_vert + ": ", n)
long_vert = int(len(data_vert))
```

```
print("long_vert=", long_vert)
##########################################################################
##########################################################
"
FACE DATA TOTAL

In this part of the script are selected the values of the points that forma a triangle
that forms the faces
of the three-dimensional body that represents a protein, in this part four columns are
selected, the first one represents the number of points that conform the triangle, for
that reason the number always is three, and the rest of the columns are the points
that indicate the corners of the triangle, the numeration must start in 0 in order to be
recognized by Paraview, for that reason to the original values of points in the face
files are substrate 1, to assign the values following the format that Paraview can
recognize

"
##########################################################################
##########################################################

data_face = []
nfacei = []
nsum = 0
i = 0
with open(path_face, 'r+') as lines:
    n = 0
    for line in lines:
        nf1 = int(line.split()[0]) - 1 + nsum
        nf2 = int(line.split()[1]) - 1 + nsum
        nf3 = int(line.split()[2]) - 1 + nsum
        area = triarea(nf1, nf2, nf3, xyz_vert)
        if area < 1.0e-10:
            print("small area", nf1, nf2, nf3, area)
        else:
            n += 1
            numbers_line2 = ('{0:>} {1:>8d} {2:>8d} {3:>8d}'.format("3", nf1, nf2, nf3))
            data_face.append(numbers_line2)
nsum += nverti[i]
i += 1
nfacei.append(n)
print("face file - " + path_face + ": ", n)
long_face = int(len(data_face))

##########################################################################
##########################################################
"
DATA VERT PROTEIN
"
##########################################################################
##########################################################

data_vert_prot = []
xyz_vert_prot = []
nverti_prot = []
```

```
with open(path_vert_protein, 'r+') as lines_prot:
    n_prot = 0
    for line_prot in lines_prot:
        nv1_prot = float(line_prot.split()[0])
        nv2_prot = float(line_prot.split()[1])
        nv3_prot = float(line_prot.split()[2])
        n_prot += 1
        numbers_line_prot = ('{0:>8.3f} {1:>8.3f} {2:>8.3f}'.format(nv1_prot, nv2_prot,
nv3_prot))
        data_vert_prot.append(numbers_line_prot)
        xyz_vert_prot.append([nv1_prot, nv2_prot, nv3_prot])
nverti_prot.append(n_prot)
#print("vertex file_prot - " + vf + ": ", n)
long_vert_prot = int(len(data_vert_prot))
print("long_vert_prot =", long_vert_prot)
##########################################################################
##################################################
"
FACE DATA PROTEIN
"
##########################################################################
##################################################

data_face_prot = []
nfacei_prot = []
nsum_prot = 0
i_prot = 0

with open(path_face_protein, 'r+') as lines_prot:
    n_prot = 0
    for line_prot in lines_prot:
        nf1_prot = int(line_prot.split()[0]) - 1 + nsum_prot
        nf2_prot = int(line_prot.split()[1]) - 1 + nsum_prot
        nf3_prot = int(line_prot.split()[2]) - 1 + nsum_prot
        area_prot = triarea(nf1_prot, nf2_prot, nf3_prot, xyz_vert_prot)
        if area_prot < 1.0e-10:
            print("small area", nf1_prot, nf2_prot, nf3_prot, area_prot)
        else:
            n_prot += 1
            numbers_line2_prot = ('{0:>}{1:>8d} {2:>8d} {3:>8d}'.format("3", nf1_prot,
nf2_prot, nf3_prot))
            data_face_prot.append(numbers_line2_prot)
nsum_prot += nverti_prot[i_prot]
i_prot += 1
nfacei_prot.append(n_prot)
#print("face file_prot - " + ff + ": ", n)
long_face_prot = int(len(data_face_prot))
# print("long_face = ", long_face)

##########################################################################
##################################################
"
DATA VERT PROTEIN STERN LAYER
```

```
”
##########################################################################
##########################################################

data_vert_prot_stern = []
xyz_vert_prot_stern = []
nverti_prot_stern = []

with open(path_vert_protein_stern, ‘r+’) as lines_prot_stern:
   n_prot_stern = 0
   for line_prot_stern in lines_prot_stern:
      nv1_prot_stern = float(line_prot_stern.split()[0])
      nv2_prot_stern = float(line_prot_stern.split()[1])
      nv3_prot_stern = float(line_prot_stern.split()[2])
      n_prot_stern += 1
      numbers_line_prot_stern = (’{0:>8.3f}{1:>8.3f} {2:>8.3f}’.format(nv1_prot_stern,
nv2_prot_stern, nv3_prot_stern))
      data_vert_prot_stern.append(numbers_line_prot_stern)
      xyz_vert_prot_stern.append([nv1_prot_stern, nv2_prot_stern, nv3_prot_stern])
nverti_prot_stern.append(n_prot_stern)
# print(”vertex file_prot - “ + vf + “: “, n)
long_vert_prot_stern = int(len(data_vert_prot_stern))
print(”long_vert_prot_stern =”, long_vert_prot_stern)

##########################################################################
##########################################################
”
DATA FACE PROTEIN STERN LAYER
”
##########################################################################
##########################################################

data_face_prot_stern = []
nfacei_prot_stern = []
nsum_prot_stern = 0
i_prot_stern = 0

with open(path_face_protein_stern, ‘r+’) as lines_prot_stern:
   n_prot_stern = 0
   for line_prot_stern in lines_prot_stern:
      nf1_prot_stern = int(line_prot_stern.split()[0]) - 1 + nsum_prot_stern
      nf2_prot_stern = int(line_prot_stern.split()[1]) - 1 + nsum_prot_stern
      nf3_prot_stern = int(line_prot_stern.split()[2]) - 1 + nsum_prot_stern
      area_prot_stern = triarea(nf1_prot_stern, nf2_prot_stern, nf3_prot_stern,
xyz_vert_prot_stern)
      if area_prot_stern < 1.0e-10:
         print(”small area”, nf1_prot_stern, nf2_prot_stern, nf3_prot_stern,
area_prot_stern)
      else:
         n_prot_stern += 1
         numbers_line2_prot_stern = (’{0:>}{1:>8d} {2:>8d} {3:>8d}’.format(”3”,
nf1_prot_stern, nf2_prot_stern, nf3_prot_stern))
         data_face_prot_stern.append(numbers_line2_prot_stern)
nsum_prot_stern += nverti_prot_stern[i_prot_stern]
```

```
i_prot_stern += 1
nfacei_prot_stern.append(n_prot_stern)
# print("face file_prot - " + ff + ": ", n)
long_face_prot_stern = int(len(data_face_prot_stern))
# print("long_face = ", long_face)

##########################################################################
##########################################
"
DATA VERT ELECTRODE
"
##########################################################################
##########################################

data_vert_electrode = []
xyz_vert_electrode = []
nverti_electrode = []

with open(path_vert_electrode, 'r+') as lines_electrode:
    n_electrode = 0
    for line_electrode in lines_electrode:
        nv1_electrode = float(line_electrode.split()[0])
        nv2_electrode = float(line_electrode.split()[1])
        nv3_electrode = float(line_electrode.split()[2])
        n_electrode += 1
        numbers_line_electrode = ('{0:>8.3f} {1:>8.3f} {2:>8.3f}'.format(nv1_electrode,
nv2_electrode, nv3_electrode))
        data_vert_electrode.append(numbers_line_electrode)
        xyz_vert_electrode.append([nv1_electrode, nv2_electrode, nv3_electrode])
nverti_electrode.append(n_electrode)
# print("vertex file_prot - " + vf + ": ", n)
long_vert_electrode = int(len(data_vert_electrode))
print("long_vert_electrode =", long_vert_electrode)

##########################################################################
##########################################
"
FACE DATA ELECTRODE
"
##########################################################################
##########################################

data_face_electrode = []
nfacei_electrode = []
nsum_electrode = 0
i_electrode = 0
area_triangle = []

with open(path_face_electrode, 'r+') as lines_electrode:
    n_electrode = 0
    for line_electrode in lines_electrode:
        nf1_electrode = int(line_electrode.split()[0]) - 1 + nsum_electrode
        nf2_electrode = int(line_electrode.split()[1]) - 1 + nsum_electrode
        nf3_electrode = int(line_electrode.split()[2]) - 1 + nsum_electrode
```

```
        area_electrode = triarea(nf1_electrode, nf2_electrode, nf3_electrode,
xyz_vert_electrode)
        if area_electrode < 1.0e-10:
            print("small area", nf1_electrode, nf2_electrode, nf3_electrode,
area_electrode)
        else:
            n_electrode += 1
            numbers_line2_electrode = ('{0:>} {1:>8d} {2:>8d} {3:>8d}'.format("3",
nf1_electrode, nf2_electrode, nf3_electrode))
            data_face_electrode.append(numbers_line2_electrode)
            if n_electrode < 11: print("n_electrode ", n_electrode -1, "area_electrode0 ",
area_electrode)
            area_triangle.append(area_electrode)
nsum_electrode += nverti_electrode[i_electrode]
i_electrode += 1
nfacei_electrode.append(n_electrode)
# print("face file_prot - " + ff + ": ", n)
long_face_electrode = int(len(data_face_electrode))
# print("long_face = ", long_face)

##########################################################################
##########################################################
"
DATA VERT ELECTRODE STERN LAYER
"
##########################################################################
##########################################################

data_vert_electrode_stern = []
xyz_vert_electrode_stern = []
nverti_electrode_stern = []

with open(path_vert_electrode_stern, 'r+') as lines_electrode_stern:
    n_electrode_stern = 0
    for line_electrode_stern in lines_electrode_stern:
        nv1_electrode_stern = float(line_electrode_stern.split()[0])
        nv2_electrode_stern = float(line_electrode_stern.split()[1])
        nv3_electrode_stern = float(line_electrode_stern.split()[2])
        n_electrode_stern += 1
        numbers_line_electrode_stern = ('{0:>8.3f} {1:>8.3f}
{2:>8.3f}'.format(nv1_electrode_stern, nv2_electrode_stern, nv3_electrode_stern))
        data_vert_electrode_stern.append(numbers_line_electrode_stern)
        xyz_vert_electrode_stern.append([nv1_electrode_stern, nv2_electrode_stern,
nv3_electrode_stern])
nverti_electrode_stern.append(n_electrode_stern)
# print("vertex file_prot - " + vf + ": ", n)
long_vert_electrode_stern = int(len(data_vert_electrode_stern))
print("long_vert_electrode_stern =", long_vert_electrode_stern)

##########################################################################
##########################################################
"
FACE DATA ELECTRODE STERN LAYER
"
```

```
#####################################################################
#################################################

data_face_electrode_stern = []
nfacei_electrode_stern = []
nsum_electrode_stern = 0
i_electrode_stern = 0

with open(path_face_electrode_stern, 'r+') as lines_electrode_stern:
   n_electrode_stern = 0
   for line_electrode_stern in lines_electrode_stern:
      nf1_electrode_stern = int(line_electrode_stern.split()[0]) - 1 +
nsum_electrode_stern
      nf2_electrode_stern = int(line_electrode_stern.split()[1]) - 1 +
nsum_electrode_stern
      nf3_electrode_stern = int(line_electrode_stern.split()[2]) - 1 +
nsum_electrode_stern
      area_electrode_stern = triarea(nf1_electrode_stern, nf2_electrode_stern,
nf3_electrode_stern, xyz_vert_electrode_stern)
      if area_electrode_stern < 1.0e-10:
         print("small area", nf1_electrode_stern, nf2_electrode_stern,
nf3_electrode_stern, area_electrode_stern)
      else:
         n_electrode_stern += 1
         numbers_line2_electrode_stern = (
            '{0:>} {1:>8d} {2:>8d} {3:>8d}'.format("3", nf1_electrode_stern,
nf2_electrode_stern, nf3_electrode_stern))
         data_face_electrode_stern.append(numbers_line2_electrode_stern)
nsum_electrode_stern += nverti_electrode_stern[i_electrode_stern]
i_electrode_stern += 1
nfacei_electrode_stern.append(n_electrode_stern)
# print("face file_prot - " + ff + ": ", n)
long_face_electrode_stern = int(len(data_face_electrode_stern))
# print("long_face = ", long_face)

#####################################################################
#################################################
"
VTK

In this part of the script are collected all the information previously formatted in the
previous sections and write it to a file that obtains the name from the parental
folder, with the headers need them to be recognized by paraview.
The vtk files are write them to the output folder indicated at the beginning of the
script by the user.
"
#####################################################################
#################################################
# write the potential to one file ("*.phi.vtk") and the normal derivative to another file
("*.derphi.vtk").
print("long_vert_prot: ", long_vert_prot)
print("long_face_prot: ", long_face_prot)

print("long_vert_prot_stern: ", long_vert_prot_stern)
```

```
print("long_face_prot_stern: ", long_face_prot_stern)

print("long_vert_electrode: ", long_vert_electrode)
print("long_face_electrode: ", long_face_electrode)

print("long_vert_electrode_stern: ", long_vert_electrode_stern)
print("long_face_electrode_stern: ", long_face_electrode_stern)

total_vert = int(long_vert_prot) + int(long_vert_prot_stern) +
int(long_vert_electrode) + int(long_vert_electrode_stern)
total_face = int(long_face_prot) + int(long_face_prot_stern) +
int(long_face_electrode) + int(long_face_electrode_stern)

print("Total_vert: ", total_vert)
print("Total_face: ", total_face)

##################################################################
##################################################
"
PHI Data
"
##################################################################
##################################################
os.mkdir(path_base + "phi_files")

data_phi_total = []
with open(path_phi, 'r+') as lines:
    for line in lines:
        np1 = float(line.split()[0])
        numbers_line3 = ('{0:.12E}'.format(np1))
        data_phi_total.append(numbers_line3)
nphi = len(data_phi_total)
print("phi_total    =", nphi)


data_phi_protein_stern = []
length_data_phi_protein_stern = len(data_phi_protein_stern)
start_point_protein_stern = 0
end_point_protein_stern = int((len(data_face_prot_stern)))
for f in data_phi_total[start_point_protein_stern:end_point_protein_stern]:
    data_phi_protein_stern.append(f)
print("start_point_protein_stern ", start_point_protein_stern)
print("end_point_protein_stern ", end_point_protein_stern)
print("data_phi_protein_stern ", len(data_phi_protein_stern))
min_phi_protein_stern = min(data_phi_protein_stern)
max_phi_protein_stern = max(data_phi_protein_stern)
with open(path_base+folder_name + "_stern_phi.txt", 'w') as f:
    for item in data_phi_protein_stern:
        f.write("%s\n" % item)
shutil.move(path_base + folder_name + "_stern_phi.txt", path_base + "phi_files")


data_phi_protein = []
start_point_protein = int((len(data_face_prot_stern) * 2))
```

```
end_point_protein = int((len(data_face_prot_stern) * 2) + (len(data_face_prot)))
for item in data_phi_total[start_point_protein:end_point_protein]:
    data_phi_protein.append(item)
print("start_point_protein ", start_point_protein)
print("end_point_protein ", end_point_protein)
print("data_phi_protein ", len(data_phi_protein))
min_phi_protein = min(data_phi_protein)
max_phi_protein = max(data_phi_protein)
with open(path_base + folder_name + "_phi.txt", 'w') as f:
    for item in data_phi_protein:
        f.write("%s\n" % item)
shutil.move(path_base + folder_name + "_phi.txt", path_base + "phi_files")


data_phi_electrode_stern = []
start_point_electrode_stern = int((len(data_face_prot_stern) * 2) +
len(data_face_prot) * 2)
end_point_electrode_stern = int((len(data_face_prot_stern) * 2) +
len(data_face_prot) * 2) + (len(data_face_electrode_stern))
for item in data_phi_total[start_point_electrode_stern:end_point_electrode_stern]:
    data_phi_electrode_stern.append(item)
print("start_point_electrode_stern ", start_point_electrode_stern)
print("end_point_electrode_stern ", end_point_electrode_stern)
print("data_phi_electrode_stern ", len(data_phi_electrode_stern))
min_phi_electrode_stern = min(data_phi_electrode_stern)
max_phi_electrode_stern = max(data_phi_electrode_stern)
with open(path_base + electrode_stern + "_stern_phi.txt", 'w') as f:
    for item in data_phi_electrode_stern:
        f.write("%s\n" % item)
shutil.move(path_base + electrode_stern + "_stern_phi.txt", path_base + "phi_files")


data_phi_electrode = []
with open(path_phi0, 'r+') as lines:
    for line in lines:
        np1 = float(line.split()[0])
        numbers_line3 = ('{0:.12E}'.format(np1))
        data_phi_electrode.append(numbers_line3)
start_point_electrode = 0
end_point_electrode = len(data_phi_electrode)
print("start_point_electrode ", start_point_electrode)
print("end_point_electrode ", end_point_electrode)
print("data_phi_electrode ", len(data_phi_electrode))
min_phi_electrode = min(data_phi_electrode)
max_phi_electrode = max(data_phi_electrode)
with open(path_base + electrode + "_phi.txt", 'w') as f:
    for item in data_phi_electrode:
        f.write("%s\n" % item)
shutil.move(path_base + electrode + "_phi.txt", path_base + "phi_files")

print("len area", len(area_triangle))
print("len data_phi_electrode", len(data_phi_electrode))

print(type(area_triangle))
```

```
print(type(data_phi_electrode))

charge = 0
epsilon = 80
guido = 0
for i in range(len(area_triangle)):
    if i < 10: print(i, area_triangle[i], data_phi_electrode[i])
    #print(type(i), type(charge), type(area[i]), type(data_phi_electrode[i]))
    charge += area_triangle[i]*float(data_phi_electrode[i])
    guido += area_triangle[i]

charge *= -epsilon


print(charge)
#sys.exit("Manual stop")


##########################################################################
########################################
"
VTK PROTEIN STERN
"
##########################################################################
########################################
filename_prot_stern = path_base + folder_name + "_stern.vtk"
with open(path_base + folder_name + "_stern.vtk", 'w') as f:
    f.write("# vtk DataFile Version 3.0\n")
    f.write("GRAPHICAL REPRESENTATION NUDE SURFACES\n")
    f.write("ASCII\n")
    f.write("DATASET POLYDATA\n")
    f.write("POINTS " + "    " + str(long_vert_prot_stern) + " " + "float\n")
    for item in data_vert_prot_stern[0:int(long_vert_prot_stern)]:
        f.write("%s\n" % item)
    polygons_times_4 = str(long_face_prot_stern * 4)
    f.write("POLYGONS " + " " + str(long_face_prot_stern) + " " + polygons_times_4 +
"\n")
    for item in data_face_prot_stern[0:int(long_face_prot_stern)]:
        f.write("%s\n" % item)
    f.write("CELL_DATA " + " " + str(long_face_prot_stern) + " \n")
    f.write("SCALARS PHI float 1\n")
    f.write("LOOKUP_TABLE default\n")
    for item in data_phi_protein_stern:
        f.write("%s\n" % item)
print("Created VTK file: ", filename_prot_stern)

##########################################################################
########################################
"
VTK PROTEIN
"
##########################################################################
########################################
filename_prot = path_base + folder_name + ".vtk"
```

```
with open(path_base+folder_name+".vtk", 'w') as f:
    f.write("# vtk DataFile Version 3.0\n")
    f.write("GRAPHICAL REPRESENTATION NUDE SURFACES\n")
    f.write("ASCII\n")
    f.write("DATASET POLYDATA\n")
    f.write("POINTS" + "    " + str(long_vert_prot) + " " + "float\n")
    for item in data_vert_prot[0:int(long_vert_prot)]:
        f.write("%s\n" % item)
    polygons_times_4 = str(long_face_prot * 4)
    f.write("POLYGONS" + " " + str(long_face_prot) + " " + polygons_times_4 + "\n")
    for item in data_face_prot[0:int(long_face_prot)]:
        f.write("%s\n" % item)
    f.write("CELL_DATA" + " " + str(long_face_prot) + " \n")
    f.write("SCALARS PHI float 1\n")
    f.write("LOOKUP_TABLE default\n")
    for item in data_phi_protein:
        f.write("%s\n" % item)
print("Created VTK file: ", filename_prot)

##########################################################################
#########################################
"
VTK ELECTRODE STERN
"
##########################################################################
#########################################
filename_electrode = path_base + electrode_stern + "_stern.vtk"
with open(path_base+electrode_stern+"_stern.vtk", 'w') as f:
    f.write("# vtk DataFile Version 3.0\n")
    f.write("GRAPHICAL REPRESENTATION NUDE SURFACES\n")
    f.write("ASCII\n")
    f.write("DATASET POLYDATA\n")
    f.write("POINTS" + "    " + str(long_vert_electrode_stern) + " " + "float\n")
    for item in data_vert_electrode_stern[0:int(long_vert_electrode_stern)]:
        f.write("%s\n" % item)
    polygons_times_4_electrode = str(int(long_face_electrode_stern) * 4)
    f.write("POLYGONS" + " " + str(long_face_electrode_stern) + " " +
polygons_times_4_electrode + "\n")
    for item in data_face_electrode_stern[0:int(long_face_electrode_stern)]:
        f.write("%s\n" % item)
    f.write("CELL_DATA" + " " + str(long_face_electrode_stern) + " \n")
    f.write("SCALARS PHI float 1\n")
    f.write("LOOKUP_TABLE default\n")
    for item in data_phi_electrode_stern:
        f.write("%s\n" % item)
print("Created VTK file: ", filename_electrode)

##########################################################################
#########################################
"
VTK ELECTRODE

"
##########################################################################
```

```
#########################################
filename_electrode_stern = path_base + "/" + electrode + ".vtk"
with open(path_base + "/" + electrode + ".vtk", 'w') as f:
    f.write("# vtk DataFile Version 3.0\n")
    f.write("GRAPHICAL REPRESENTATION NUDE SURFACES\n")
    f.write("ASCII\n")
    f.write("DATASET POLYDATA\n")
    f.write("POINTS" + "    " + str(long_vert_electrode) + " " + "float\n")
    for item in data_vert_electrode[0:int(long_vert_electrode)]:
        f.write("%s\n" % item)
    polygons_times_4_electrode = str(int(long_face_electrode) * 4)
    f.write("POLYGONS" + " " + str(long_face_electrode) + " " +
polygons_times_4_electrode + "\n")
    for item in data_face_electrode[0:int(long_face_electrode)]:
        f.write("%s\n" % item)
    f.write("CELL_DATA" + " " + str(long_face_electrode) + " \n")
    f.write("SCALARS PHI float 1\n")
    f.write("LOOKUP_TABLE default\n")
    for item in data_phi_electrode:
        f.write("%s\n" % item)
print("Created VTK file:  ", filename_electrode_stern)


print("start_point_protein_stern ", start_point_protein_stern)
print("end_point_protein_stern ", end_point_protein_stern)
print("start_point_protein ", start_point_protein)
print("end_point_protein ", end_point_protein)
print("start_point_electrode_stern ", start_point_electrode_stern)
print("end_point_electrode_stern ", end_point_electrode_stern)
print("start_point_electrode ", start_point_electrode)
print("end_point_electrode ", end_point_electrode)

with open(path_base + "/" + "summary_vtks" + ".txt", 'w') as f:


f.write("#########################################################
#########################################"  + "\n")
    f.write("Created VTK file:  " + filename_prot_stern + "\n")
    f.write("length_vert_prot_stern: " + str(long_vert_prot_stern) + "\n")
    f.write("length_face_prot_stern: " + str(long_face_prot_stern) + "\n")
    f.write("length_data_phi_protein_stern: " + str(len(data_phi_protein_stern)) +
"\n")
    f.write("start_point_phi_protein_stern: " + str(start_point_protein_stern) + "\n")
    f.write("end_point_phi_protein_stern: " + str(end_point_protein_stern) + "\n")
    f.write("min_data_phi_protein_stern: " + str(min_phi_protein_stern) + "\n")
    f.write("max_data_phi_protein_stern: " + str(max_phi_protein_stern) + "\n")


f.write("#########################################################
#########################################"  + "\n")
    f.write("Created VTK file:  " + filename_prot + "\n")
    f.write("length_vert_prot: " + str(long_vert_prot) + "\n")
    f.write("length_face_prot: " + str(long_face_prot) + "\n")
    f.write("length_data_phi_protein: " + str(len(data_phi_protein)) + "\n")
```

```
    f.write("start_point_phi_protein: " + str(start_point_protein) + "\n")
    f.write("end_point_phi_protein: " + str(end_point_protein) + "\n")
    f.write("min_data_phi_protein: " + str(min_phi_protein) + "\n")
    f.write("max_data_phi_protein: " + str(max_phi_protein) + "\n")


f.write("#################################################################
#########################################" + "\n")
    f.write("Created VTK file: " + filename_electrode_stern + "\n")
    f.write("length_vert_electrode_stern: " + str(long_vert_electrode_stern) + "\n")
    f.write("length_face_electrode_stern: " + str(long_face_electrode_stern) + "\n")
    f.write("length_data_phi_electrode_stern: " + str(len(data_phi_electrode_stern)) +
"\n")
    f.write("start_point_phi_electrode_stern: " + str(start_point_electrode_stern) +
"\n")
    f.write("end_point_phi_electrode_stern: " + str(end_point_electrode_stern) +
"\n")
    f.write("min_data_phi_electrode_stern: " + str(min_phi_electrode_stern) + "\n")
    f.write("max_data_phi_electrode_stern: " + str(max_phi_electrode_stern) + "\n")


f.write("#################################################################
#########################################" + "\n")
    f.write("Created VTK file: " + filename_electrode + "\n")
    f.write("length_vert_electrode: " + str(long_vert_electrode) + "\n")
    f.write("length_face_electrode: " + str(long_face_electrode) + "\n")
    f.write("length_data_phi_electrode: " + str(len(data_phi_electrode)) + "\n")
    f.write("start_point_phi_electrode: " + str(start_point_electrode) + "\n")
    f.write("end_point_phi_electrode: " + str(end_point_electrode) + "\n")
    f.write("min_data_phi_electrode: " + str(min_phi_electrode) + "\n")
    f.write("max_data_phi_electrode: " + str(max_phi_electrode) + "\n")


f.write("#################################################################
#########################################" + "\n")
    f.write("Total_vert: " + str(total_vert) + "\n")
    f.write("Total_face: " + str(total_face) + "\n")
    f.write("Total_phi: " + str(nphi + len(data_phi_electrode)) + "\n")
```

Example of “sbatch” file to run calculations of PyGBe in a server

In order to do a big number of calculations it is necessary to use a server, with a big number of GPUs, this imply that is necessary to write a small list of commands in a bash file that will be used for a cluster management to run PyGBe.

In next is detailed a “sbatch” file to submit a run in sever controlled with the cluster workload manager, “Slurm”. In this file, the double comment deactivates the commands and transforms them in simple text.

The first two lines need to be in the file. They indicate that is a bash file, and it is a file to be readable for “Slurm”. The next lines, starting with #SBATCH are the indications to the server to use the available resources.

The most important lines are: #SBATCH --time=288:00:00 this indicates the time in hours:min:seconds, #SBATCH --nodes=1, the number of nodes used, in the case of PyGBe it only can use one, until the date of publication of this document.

The line #SBATCH -p gpuk indicates the name in the server for the GPU. This information needs to be obtained from the administrator of the server. #SBATCH --gres=gpu:1 the number of GPUs used in the calculation, again in the case of PyGBe only can use one.

The path of where are the folders of the calculations to be done (orientations) need to be indicated in the section of paths

In the section of modules are indicated the programs previously installed in the server, because some of these programs are used for several users of the server, sometimes the programs are already installed, and is only necessary to load the program, in the case of PyGBe

it needs the modules of anaconda and CUDA.

In the section of job steps are indicated the flow of actions necessary to run PyGBe, once that the resources have been assigned, the paths indicated and the modules loaded. It is necessary to indicate the actions for PyGBe first it is necessary to activate the gpu and then run the script of python that runs the calculations of multiple orientations in PyGBe. The last two lines of the bash file deactivate the resources used from the server and remove the temporary files generated during the run of PyGBe.

A final note is that if well, to do calculations in a server accelerate the obtention of the results, in real life the server always is used for 5 or more users which makes slower the obtention of the results.
Next are the lines for the sbatch file:

```
#!/usr/bin/bash
## Shebang
## sbatch for run Automatic_pygbe_full1.py

## Resource Request

#SBATCH --job-name=Pygbe1
#SBATCH --time=288:00:00
#SBATCH --nodes=1
#SBATCH --ntasks-per-node=1
#SBATCH --mail-user=mruiz@usm.cl
#SBATCH --mail-type=BEGIN,END,FAIL
#SBATCH -o pygbe-%j
#SBATCH --mem=1024M
#SBATCH -p gpuk
#SBATCH --gres=gpu:1


## Job paths

DATADIR=/user/m/mruiz/PycharmProjects/rotation_hydrogenase
SCRATCH=/user/m/mruiz/scratch
export PATH=$PATH:/user/m/mruiz/PycharmProjects/rotation_hydrogenase
mkdir -p $SCRATCH
cd $DATADIR


## Job modules

module purge
```

```
use anaconda3
use cuda10

## Job Steps

source activate gpu

python Automatic_pygbe_full1.py

source deactivate
rm -rf $SCRATCH
```

Memory photos

Figure 30. *Manuel Ruiz in front of the main building of Politecnico in Piazza Leonardo da Vinci, Milano, (December 2020).*

Figure 31*. Professors Guido Raos (left) and Christopher Cooper right).*

In front of a polyethylene model in the Department of Chemistry, Materials and Chemical Engineering "Giulio Natta", Politecnico di Milano, (May 2023).